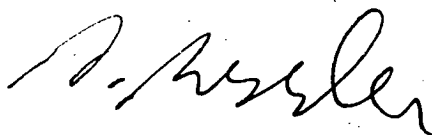Chaos in KdV-like equations

by

J. Roessler, Dipl.Phys., PhD

Physics Department

submitted in fulfillment of the requirements for the degree of

Doctor of Philosophy

University of Tasmania, August, 1990

This thesis contains no material which has been accepted for the award of any other higher degree or graduate diploma in any tertiary institution and that, to the best of the candidate's knowledge and belief, the thesis contains no material previously published or written by another person, except when due reference is made in the text of the thesis.

(J. Roessler)

Abstract. The correspondence between soliton solutions of nonlinear partial differential equations and homoclinic orbits in appropriately chosen phase spaces of these equations is well-known. Perturbations of homoclinic orbits can be studied by use of the Melnikov technique; this focusses on the splitting of such orbits into stable and unstable invariant manifolds and explains the emergence of chaotic phenomena via Smale horseshoes.

In this thesis the Melnikov method is applied to the homoclinic orbits corresponding to solitons of the Korteweg-de Vries (KdV) and modified Korteweg-de Vries (MKdV) equations. These equations are reduced to third order ordinary differential equations by a travelling wave ansatz, defining a three-dimensional phase space of the equivalent systems of three first order equations. The geometry of periodic and homoclinic orbits and their structural changes under perturbations is investigated. It turns out that the three-dimensional phase spaces foliate into a continuous family of invariant two-dimensional subspaces. By integrating the equations to second order the analysis by Melnikov's method is restricted to these subspaces and is considerably simplified. The Melnikov integrals stemming from the periodic and dissipative part of the perturbations, determining the onset of chaos, are then evaluated for the reduced KdV and MKdV systems. They are used to calculate the critical ratios between perturbation amplitude and dissipation coefficient at which tangency between stable and unstable manifolds occur. At these critical ratios the transition/bifurcation from regular to chaotic behaviour occurs. It is observed that the Melnikov function for the periodic perturbation of the MKdV case vanishes for certain

perturbation frequencies and parameter values, as confirmed by numerical work. The apparent discrepancy between structurally unstable homoclinic orbits and stable solitons is discussed and it is shown that solitons can persist despite the splitting of their corresponding homoclinic orbits under perturbation. Finally, subharmonics and resonance for the periodic solutions under perturbations are investigated using fourth order averaging techniques applied over the solution periods, which reveals a period doubling bifurcation in the subharmonics.

Table of contents

6

1. Introduction

Although chaotic phenomena such as turbulence or fluctuations in ecological populations, stock market, weather, etc. have been known for decades, if not centuries, satisfactory mathematical modelling of dynamical systems and the techniques for analysing them are rather recent. However, there are two principal causes for the rather dramatic increase of successful studies into chaos. One is the influx of methods and results from fields of pure mathematics such as topology, functional analysis and operator theory into the applied sector, mainly differential equations. The other is the application of numerical techniques and iterative methods in conjunction with electronic data processing or machine simulation of analytic models. The combination of these two is responsible for the drastic surge in knowledge and improved understanding of chaos in the last two decades.

1.1 The definition of chaos and related concepts

Just as mathematics, the analysis of chaos itself can be divided into two categories. The study of maps and the structure of the sets they generate in terms of fractals and strange attractors can be considered pure, whereas the study of chaotic behaviour in differential equations is more application-oriented. Before introducing the techniques and problems of the study of chaos in differential equations it is appropriate to consider the various definitions of chaos as they can be found in the literature.

The first mathematical definition of chaos was developed for one-dimensional maps by Li and Yorke [1]. It is closely associated with their discovery that period three implies chaos and is usually presented as a theorem. Their definition can be considered relevant

7

even in the present context of differential equations, as most other definitions are extensions of the Li-Yorke definition.

Theorem by Li and Yorke. Let J be an interval and F: J → J be continuous. Suppose there is a point a ε J that satisfies either

$$F^3(a) \leqslant a < F(a) < F^2(a)$$

or

$$F^3(a) \geqslant a > F(a) > F^2(a)$$

Then (1) For every integer k>0 there is a point in J having period k.

(2) J has an uncountable subset S (called the scrambled set) that contains no periodic points and satisfies the following conditions:

For each p, q distinct in S we have

$$\limsup_{n \to \infty} |F^n(p) - F^n(q)| > 0$$

and

$$\liminf_{n \to \infty} |F^n(p) - F^n(q)| = 0 .$$

For each p ε S and each periodic q ε J we have

$$\limsup_{n \to \infty} |F^n(p) - F^n(q)| > 0 .$$

Marotto [2] extended this theorem to n dimensions and his work in turn has been generalized further by Shiraiwa and Kurata [3]. The crucial element in the above theorem is the presence of subsequences in the mapping sequences F^n which lead to a nonzero separation of two arbitrarily close points p and q

in the limit of an infinite number of iterations. This can be interpreted as sensitive dependence on initial conditions, which is, in one form or another, the key ingredient in every chaos definition as well as in the definitions of subsets in mathematical spaces in which dynamical systems exhibit chaos, or strange attractors.

The concept of sensitive dependence on initial conditions is by no means a new one. In fact, occurrences of the phenomenon have been reported as far back as Adam and Eve. Who could have forseen the profound consequences of a naive little pleasure like eating some fruit (e.g. like an apple). For further details see reference [4].

The other important condition for chaos is the existence of "nonperiodicity". Ott [5], for instance, proposes to define a map as chaotic if it has sensitive dependence on initial conditions, is nonperiodic and has a vanishing average correlation function. The correlation is defined between two points in the iteration sequence such that if the number of iterations between the two points is taken to the infinite limit, the average of the correlation function vanishes.

The study of chaos in differential equations requires a definition of chaos in abstract spaces such as function spaces. Auslander and Yorke [6] propose the following definition.

> <u>Definition of chaos by Auslander and Yorke</u>. If X is a compact metric space and τ a continuous surjection from X to itself then (X, τ) is defined to be a compact system. The point $x \in X$ is said to be stable if for each $\varepsilon > 0$ there is a $\delta > 0$ such that $d(\tau^n(x), \tau^n(y)) < \varepsilon$ for each y with $d(x,y) < \delta$ and each $n \in N$. The compact system (X, τ) is

defined to be chaotic if no point $x \in X$ is stable and if there is some $y \in X$ whose orbit is dense in X.

Clearly, the absence of stability implied in the definition can again be translated into sensitive dependence on initial conditions. Although the chaos definitions[7,8] discussed above are based on discrete maps they are useful for differential evolution equations as well, since these equations can be considered as generators of semigroups with discrete subgroups. In practical applications, this means discrete timesteps on the solutions.
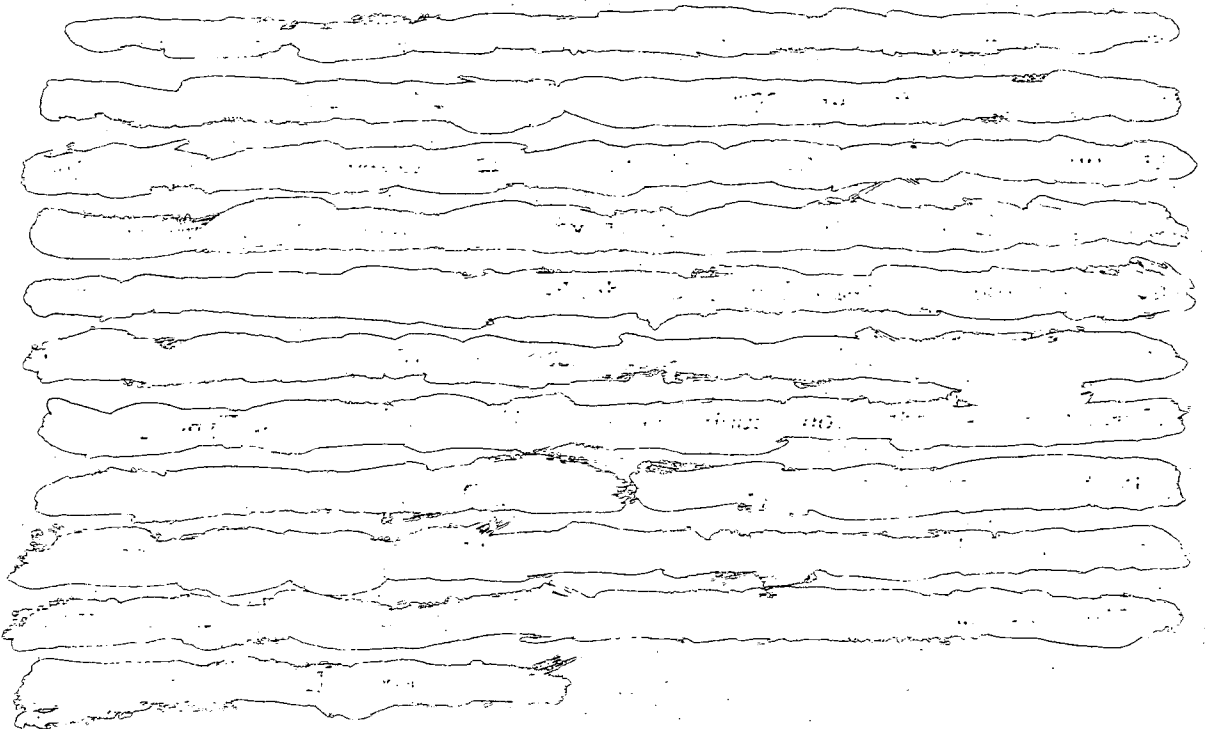
1.2 Chaos in differential equations

Beginning with Poincare in 1880 [9] there has been a continuous evolution of the mathematics underlying the phenomena that are now described as chaotic. Amongst the many contributions to this development the work of Duffing in 1918 [10] about mechanical forced oscillations and van der Pol in 1927 [11] about electrical forced oscillations could be considered poioneering. On the other hand Ott

[5] concludes on the basis of the existing literature that it can be surmised that "...*virtually all the activity in this field (at least when restricted to problems in the physical sciences) has occurred since 1975. The notable exceptions to this statement are the papers of Lorenz (1963) and of Ruelle and Takens (1971)*." Both papers are concerned with systems containing no explicit time dependence, that is, the systems are *autonomous*. Lorenz [12] (see also Sparrow [13]) investigated machine solutions of a three dimensional system of nonlinear ordinary differential equations (ODEs) which was derived by spectral ansatz frcm a partial differential equation (PDE) describing the evolution of Benard instability: the instability that results when a fluid layer is heated from below. He was able to establish the existence of chaos in particular regions of the phase space with an intricate geometric structure.

The work of Takens and Ruelle [14] is an early example of using results of pure mathematics such as topology to study solution structures of PDEs such as the Navier-Stokes equations. Their mechanism for the onset of turbulence is basically a sequence of three Hopf bifurcations which generate a three-torus in phase space. They further show structural instability of the vector fields which generate solution curves on the suface of this torus. This is done by defining a Poincare map based on the period of the third Hopf bifucation. The phase space of this Poincare map contains the torus relating to the two initial Hopf bifurcations. They further showed that in a C^2-neighbourhood of this Poincare map there exist horseshoe diffeomorphisms. These diffeomorphisms were discovered by Smale [15] who investigated most of their properties such as Cantor set structure, hyperbolicity and the resulting structural stability, as

well orbits of all periods and a nonperiodic dense orbit. These properties cause sensitive dependence on initial conditions. As a consequence, small perturbations on the solution generating vector fields will produce structural change into vector fields which generate horseshoe diffeomorphisms, with the ensuing chaotic behaviour.

It is important to realize that this mechanism invalidates the type of mechanism proposed by Landau and Lifshitz [16]. Their idea was that turbulent behaviour produces an infinite number of periods in superposition. Such a solution cannot develop as the superposition of three periods already causes structurally unstable solutions.

Takens and Ruelle also consider the possibility of repeated double-looping of the two-torus by a map in the neighbourhood of the Poincare map and thereby generating a sequence of Smale-Williams solenoids. This is related to period doubling in three dimensions and thereby creates a link to the mechanism of chaos by period doubling as developed by Feigenbaum [17,18]. Before discussing this alternative mechanism, it is appropriate to take a view of the problems arising in connection with the application of the results of Takens and Ruelle to specific differential equations.

The main problem for a given autonomous system $dx/dt = X(x)$ is the determination of the eigenvalues of the operator X in the evolution equation and their critical points where the Hopf bifurcations occur. For a given ODE system this is simply done by linearizing the system about the stationary solution and calculating the eigenvalues of the Jacobian. A Hopf bifurcation or transition to a periodic solution occurs when a complex conjugate pair of eigenvalues crosses the imaginary axis, that is, when their real part changes sign under

12

variation of the bifurcation parameter. Once this occurs an analytic approximation to the periodic solution can be constructed. The problem starts with the second Hopf bifurcation, which does not take place in the space spanned by the dependent variables of the ODE system but in the function space containing the periodic solution of the first Hopf bifurcation. As a consequence, it is rather difficult if not impossible to construct an analytic approximation to this new doubly periodic solution. (It has been brought to the author's attention that Fowler et. al. [19] give an example of a system where such an approximation can be constructed.)

For PDEs the problem arises with the first bifurcation already, since the place of the Jacobian in the ODE case is now taken by a differential operator defined in the solution space of the PDE. The determination of eigenvalues now requires spectral theory and an analytic computation of eigenvalues is a nontrivial problem for even the most simple differential operators such as the Laplacean.

Further work on chaotic solutions of first order PDEs has been done by Brunovsky [20], Lasota [21] and Wolfe and Morris [22]. Brunovsky and Lasota consider an equation with one space-variable and a form which permits effective use of the method of characteristics. This allows them to derive a set of conditions for the equation and its boundaries which causes solutions to be chaotic according to the definition of Auslander and Yorke given in section 1.1. Wolfe and Morris generalize these results to arbitrary dimensions of the space variable and the dependent variable. As in the case of the work of Takens and Ruelle, applications of these results to specific equations are still missing at this time, since the conditions on the equations as well as on the boundaries are rather restrictive.

As opposed to the models for chaos described so far, which focus mainly on PDEs and which encounter substantial technical difficulties in their direct applications, the mechanism based on period doubling has been verified in various dynamical systems in general and ODEs in particular such as the Lorenz equations, the Duffing model and the forced oscillator with friction. However, it should be emphasized at this point that the Duffing and Lorenz equations are spectral reductions of PDEs. A short discussion of the various reduction techniques of PDEs to ODEs and their present significance in chaos modelling is therefore appropriate.

1.2.1 Reduction of PDEs to ODEs

We give a list of the four most frequently used reduction methods, not necessarily in order of importance.

1. Reduction by spectral ansatz. Although this technique is an approximative Galerkin method, it has shown to preserve the chaotics of the underlying PDE models and reflect them realistically in the behaviour of the ODE system. It consists of formally expanding the solution into a Fourier series with respect to the spatial variable and truncating after a finite number of terms. The time dependent Fourier coefficients are the new dependent variables in the resulting ODE system, whose dimension is equal to the order of truncation. The most prominent example is the Lorenz system, which has been briefly discussed at the beginning. Its truncation is of third order with two temperature Fourier modes and one velocity Fourier mode. The other well-known example is just as important and reduces the integro-differential equation of the elastodynamic beam to the Duffing system by a one-mode truncation with respect to the

14

deflection of the beam from the stable equilibrium. For details see Tseng and Dugundji [23], Moon and Holmes [24], Holmes [25], Moon [26], Marsden and Holmes [27], Greenspan and Holmes [28], and Guckenheimer and Holmes [29].

2. Approximation by finite differences or finite elements.

The finite difference method approximates the continuous spatial domain of the PDE by a finite selection of discrete points such that the temporal evolution of the unknown variable, such as e. g. velocity in the case of the Navier-Stokes equation, is monitored at these points or sites. In this case the solution ansatz consists of a finite sum taken over the set of these selected points. The individual terms in this sum are products consisting of unknown time dependent functions multiplied with the initial values of the unknown variable at the selected points. The time evolution at one of these selected points is therefore described by an ODE. The number of ODEs equals the number of selected points and the coupling between ODEs of neighbouring points is naturally introduced by the finite difference approximations of the spatial differential operators.

The finite element method is basically like a finite difference method except that the selected points are replaced by weight functions with finite support and overlap with neighbouring weight functions to provide coupling. This is a Galerkin method as well since it reduces the weight functions to coefficients in the resulting ODE system by taking scalar products of them with an appropriate set of test functions, usually identical to the weight functions.

These two methods are ready made for machine calculations as the number of ODEs can be substantial. Their significance for chaos studies is therefore in the numerical analysis of turbulence in atmospheric physics and fluid dynamics. For detailed discussions and applications of these methods see e.g. Fletcher [30,31] and Temam [32].

3. Similarity solutions.

The majority of nonlinear evolution equations are invariant under scaling transformations of the type $(x,t,u) \rightarrow (\alpha^a x, \alpha^b t, \alpha^c u)$. Here, x, t, u are independent space and time variable and dependent variable. α, a, b, c are real scalars. Invariants of this transformation are of the type $y_1 = x^{1/a} t^{-1/b}$, $v_1 = u^{1/c} t^{-1/b}$, $y_2 = x^{-1/a} t^{1/b}$, $v_2 = u^{-1/c} t^{1/b}$. Substituting a pair of these invariants into the equation will cause t to appear in each term of the equation to the same power and therefore factor out, leaving a nonlinear and nonautonomous ODE with y_i and v_i (i=1,2) as independent and dependent variable respectively. This equation is, in the case of the Burgers, KdV, and MKdV, a generalized Riccati equation with solutions like Hermite polynomials or Painleve transcendents. To date there is no mechanism for chaos that seems to be applicable to this type of equation or solutions thereof. For details see e.g. Olver [33].

4. Travelling wave ansatz.

Introducing the variable $y=x-ct$ in the PDE leads to an ODE with the independent variable y. The solution is therefore a wave of fixed shape travelling with speed c. This type of ansatz leads to the well-known cnoidal waves for the KdV and MKdV equation and provides an easy way to obtain soliton solutions.

16

For further discussions see e.g. Whitham [34]. This is also the approach used in the present context to establish the connection between saddle connections and solitons.

1.2.2 The period doubling mechanism

Compared to the previous models the period doubling mechanism holds two significant advantages; firstly it provides a simpler analysis, and secondly it is applicable to both dissipative and area-preserving or Hamiltonian systems. The Hopf bifurcation, and thereby the Takens-Ruelle mechanism, is limited to dissipative systems. This limitation is shared by the models developed by Brunovsky, Lasota, Morris and Wolfe since some of the conditions imposed on it are equivalent to dissipation.

The phenomenon of period doubling was quantified by Feigenbaum [17,18] in his investigations of one-dimensional unimodal maps. In our context the period doubling map is a Poincare map of at least two dimensions depending on a bifurcation parameter. Our starting assumptions are an at least three-dimensional dynamical system with periodic behaviour, which presents itself as a fixed point of the Poincare map. This Poincare map undergoes a "pitchfork" bifurcation as the parameter reaches a critical value. This first pitchfork bifurcation transfers stability from the stable fixed point to an orbit with period two. In terms of analysis, this happens when an eigenvalue of the linearized Poincare map leaves the unit circle in the complex plane by crossing through −1. In geometrical terms the orbit representing the original periodic solution splits in such a way that it can be embedded on a Mobius strip transversal to the plane of the Poincare map. This leaves two penetration points on this Poincare

17

plane which represent an orbit of period two. An infinite number of subsequent pitchfork or period doubling bifurcations corresponds to a sequence of critical values of the bifurcation parameter with an accumulation point. The period of subsequent solutions increases therefore in powers of two, and grows to an infinite period once the bifurcation parameter reaches the accumulation point. This nonperiodic orbit is a stable and dense attractor.

As Eckmann [35] notes, this attractor has no sensitive dependence on initial conditions; chaotic behaviour can be attributed to denseness and aperiodicity. On the other hand, however, attention should be drawn to the work of Greenspan and Holmes [28], which demonstrate sensitive dependence on initial conditions for period doubling via pitchfork bifurcations. They use averaging methods to study Poincare maps in resonant and subharmonic systems which arise through superposition of two frequencies; one is the system frequency and the other that of periodic external forcing. The method of analysis employed by Greenspan and Holmes goes back to Melnikov [36]. This method has found widespread use in the study of chaotic dynamical systems and is used in this thesis. Before introducing it, some of the geometry and associated dynamics has to be considered. We also draw attention to the descriptions of the subject by Wiggins [37], Holmes and Marsden [27], and in [29].

1.2.3 Saddle connections and perturbations

In the following introduction to perturbed saddle connections we focus on the homoclinic orbits. As noted by Wiggins [37], the study of such orbits connected to a saddle goes back to Poincare [38] in his work on the three body problem, where he also coined the term

18

"homoclinic". Generalizations of the homoclinic orbit are "heteroclinic" orbits, that is, orbits connecting two different saddles, and heteroclinic cycles, which is a set of heteroclinic orbits with their saddles connected to a closed cycle. The following description extends easily to these generalizations.

a) Autonomous perturbations

We assume a planar autonomous and area preserving dynamical system with two fixed points; one saddle and one centre, as shown in figure 2b. The phase portrait therefore must contain a homoclinic orbit connecting the saddle to itself and enclosing the centre. This homoclinic orbit or saddle connection can be understood as half of the saddle's stable and unstable manifold represented by an identical curve in phase space. If the system is now subjected to a small autonomous perturbation which is a function of the dependent variables, the position of the fixed points will shift slightly and the eigenvalues determining their type will be slightly perturbed. The saddle is determined by a pair of real eigenvalues of opposite sign, and if the perturbation is small enough this situation and therefore the saddle will remain. The centre corresponds to a pair of imaginary eigenvalues of opposite sign, sitting on the imaginary axis symmetrically with respect to the origin. Almost every perturbation of the type introduced above will shift them not only parallel to the imaginary axis, but also transverse to it. That means these eigenvalues become complex conjugate and the centre turns into a sink for negative real part or negative perturbation, and into a source if the real part or perturbation is positive. Consequently, the set of closed orbits concentric about the original center break up and turn

into spirals. Since the homoclinic orbit is an element of this set, it is subjected to this breakup as well; in other words, stable and unstable manifold split. In case of a sink the unstable manifold must spiral inward and in case of a source the spirals are directed outwards accordingly. This change or break in symmetry from closed orbits to spirals and from homoclinic orbit into separated stable and unstable manifold is a prime example of structural instability.

b) Nonautonomous periodic perturbations

We assume the same dynamical system and phase portrait as in a), except that it is now subjected to a small time periodic perturbation. As a consequence, the perturbed system will be nonautonomous and its phase portrait will vary periodically with time. To take advantage of this periodicity we define a Poincare map which describes the evolution of the system in time intervals equal to the period of the perturbation. This way we retain a time independent phase portrait, although it is the one of the Poincare map and not of the original perturbed system. If the perturbation is small enough this phase portrait will be similar to the perturbed one in a) – the saddle and centre will relocate slightly. The centre, however, will retain its stability type and the homoclinic orbit will split into stable and unstable manifold which will intersect transversally at a countably infinite number of points.

Another essential difference compared to a) is the behaviour of the concentric and periodic orbits. They will undergo phase locking or resonance as will be studied in detail in section 7. One should note at this point that, in contrast to the other system reactions, the transversal intersection of manifolds and the phase locking cannot be

concluded directly from the geometry of the unperturbed phase space and the type of perturbations imposed on it. They appear of course in numerical simulations and the phenomenon of phase locking makes sense on the basis of physical arguments and is familiar in engineering applications. However, it is the application of Melnikov analysis which demonstrates the appearance of transversal intersections and phase locking by use of mathematical perturbation techniques.

To develop an understanding for the emergence of chaos it is sufficient to assume the presence of transversely intersecting manifolds and study their dynamics as the perturbed system evolves in time as will be done in the next section.

1.2.4 Dynamics of the Poincare map

Suppose the perturbed and intersecting manifolds in the phase space of the Poincare map appear as in figure 1a. This type of picture is a consequence of uniqueness of solutions and the hyperbolic deformation near the saddle point. Uniqueness of solutions implies that a point on an invariant manifold cannot leave the manifold under the map associated with it, which explains the attribute "invariant". An intersection is a point shared by both manifolds and therefore cannot leave either of them under the Poincare map. Since the saddle is an accumulation point for the Poincare map or its inverse, it takes (in the limit) an infinite number of intersections for a particular intersection to be mapped forward or backward into the saddle. A generalization of this effect to sections of the manifolds is known as the λ-Lemma (see [28,29]).

We now monitor the evolution of the rectangle $P\circ$ in figure 1b, (which is, for explanatory purposes, an idealization of figure 1a)

21

under the dynamics of the Poincare map P. After vertical stretching and bending in the process of a number of Poincare iterations (three in figure 1b), P^0 will have completed one cycle and returned to its approximate starting position, however in the shape of a horseshoe, denoted by P^3. This cycle is clearly the first iteration of Smale's horseshoe diffeomorphism [15] as already mentioned in connection with the Takens-Ruelle mechanism and subsequent iterations or cycles will reveal all the dynamic and chaotic properties of the Smale horseshoe.

1.2.5 Melnikov's method

Given a particular dynamic system and perturbation as described above, the question arises if and under what conditions will it show transverse intersections of the perturbed manifolds. The obvious approach is to construct a distance function between the perturbed manifolds, and this is precisely what Melnikov [36] achieved by using perturbation methods. Although his method determines this distance to a first order approximation in a power expansion only, his results agree surprisingly well to numerical calculations. An outline of the different steps in Melnikov's construction is given below. For mathematical details see [28,29]. *They are elaborated upon later.*

1. Expand the solutions lying on the two perturbed manifolds formally in powers of a parameter representing the size of the perturbation, e.g. the amplitude.

2. Derive a first order variational equation by substituting the solution expansions of step one into the original perturbed system and truncating after the linear term.

22

3. Define a first order distance function by taking the distance between the the first order terms of the two expanded solutions in step one.

4. Project this distance onto a line perpendicular to the unperturbed homoclinic orbit at a point in time equivalent to the initial time in the solutions of step one. The projection can be performed by employing a wedge product, which is a vector product reduced to the two dimensions of the phase plane.

The projected distance of step four cannot be calculated in practical terms as it contains the first order terms of the solution expansions introduced in step one; these solutions and their expansions are not known analytically. This problem can be resolved as follows:

5. Take the time derivative on the projected distance function of step four. Note that this is done with respect to the current time and not the initial time of the solutions involved.

6. Eliminate the time derivatives of the first order solution expansions arising in the expression of step five. This is done by substituting the variational equation of step two and results in a linear evolution equation for the first order approximation of the projected distance function of step four.

7. Integrate the evolution equation of step six from $-\infty$ to $+\infty$. The integrand in the resulting integral contains the initial time of the solutions involved. This is the time at which the integral approximates the distance between the manifolds.

The distance formula resulting from the above procedure is an integral with respect to time over the wedge product between the unperturbed solution and the perturbation. Also note that the outlined derivation does not depend on a particular type of perturbation; it can be dissipative as described in 1.2 a) or periodic as in 1.2 b), or a combination of the two. Since this involves perturbation parameters such as the amplitude of the periodic perturbation and the damping coefficient of the friction perturbation, it provides a means for finding critical values at which the distance function disappears; therefore a comparison to machine simulations becomes possible. Technical details will be discussed in section 6. It is important to note that Melnikov's method can be extended to dissipative systems, which adds an extra term to the integrand of the distance formula. For details, see Holmes [39] and Salam [40]. The Melnikov technique has also been applied by Lima and Pettini [41] to model the suppression of chaos by external forcing in the Duffing–Holmes oscillator. Recently the distance approximation for Hamiltonian systems has been extended to second order by Liu and Gu [42]. However, their applications focus on subharmonics and ultrasubharmonics of the perturbed pendulum.

In summary, saddle connections are linked to chaos via perturbations, structural instability, and Smale horseshoes. On the other hand, homoclinic and heteroclinic saddle connections correspond to solitons and shock wave solutions respectively in nonlinear evolution PDEs, as illustrated by Jeffrey and Kakutani [43]. It is therefore natural to subject these solution types to perturbations and investigate their reaction. We now give an introduction to solitons

24

in connection with the KdV and MKdV equation, as they are prime examples for soliton solutions and have found widespread applications.

1.3   Solitons and cnoidal waves

According to Drazin [44,p.8], solitons are "not precisely defined". However, we can adopt his description as a working definition:

A **soliton** is any solution of a nonlinear equation or system which

1) represents a wave of permanent form;

2) is localized, decaying or becoming constant at infinity;

3) may interact strongly with other solitons so that after the interaction it retains its form, almost as if the principle of superposition were valid.

In the present study the properties 1) and 2) are of particular interest, as these correspond to a saddle connection in an appropriate phase space. Solitons with different values at negative and positive infinity are sometimes referred to shock waves in the literature. As will be shown later, they relate to heteroclinic saddle connections, whereas solitons with identical values at negative and positive infinity relate to homoclinic orbits.

Solutions which are periodic wave trains of infinite length are called cnoidal waves since they can be represented by Jacobi's elliptic cn function. In the limiting case of an infinitely long period they degenerate into solitons.

1.3.1 Stability of solitons and cnoidal waves

Liapunov stability of solitons was shown by Jeffrey and Kakutani [43] for the KdV equation in particular and by Benjamin [45] in general. Their methods consist of adding a perturbation to the soliton solution and showing that this new state must relax into soliton state. We give an outline of Benjamin's method as it is the more general one.

Assuming the soliton and its second derivative to vanish in the infinite spatial limits, he proved, using a Lagrangean variational formulation, that the Hamiltonian of a soliton solution represents a local energy minimum within a neighbourhood (in solution space) of the soliton containing non-soliton solutions. Since the soliton soutions of a given system form a continuous set parameterized by the wave speed, any small enough perturbation out of this set will return the system into the soliton set, but not necessarily to the soliton with the wave speed before perturbation. Benjamin [46] also proved Lyapunov stability of cnoidal solutions with respect to perturbations of the same period by the variational method. His result was extended by Drazin [47] to Lyapunov stability of KdV solitons with respect to an arbitrary frequency by use of Floquet theory.

Considering the earlier mentioned fact that solitons and cnoidal waves correspond to saddle connections and closed orbits, respectively, which are known to be structurally unstable, this almost seems to be a contradiction. It is therefore necessary to elaborate on this problem and demonstrate the compatiblilty of the two concepts under the various conditions.

First we note that stability of a particular set of solutions does not only depend on their functional form, but much more on the character of the underlying system. Benjamin and Drazin use the original PDE KdV equation for their variational analysis, and permit variation in the wave speed. This means, that a perturbation can affect the wave speed and shape of a soliton or cnoidal wave, but it cannot change them into other solution types. On the other hand, they are restricted to solitons vanishing at the spatial infinities. The concept of structural instability, however, relates to KdV reduced to two first order ODEs by travelling wave ansatz and integration. As a consequence, the wave speed is a fixed parameter within the ODE system.

Secondly, it is important to distinguish the types of perturbation. Benjamin as well as Jeffrey and Kakutani add their perturbations to the soliton solutions and do not specify a particular type of perturbation, which means that no specific time evolution of the perturbation must be allowed. In the case of KdV, reduced to an ODE system, a time periodic forcing perturbation plus dissipation is added to the system. These type of perturbations invariably force oscillation and damping onto the unperturbed solution, which means that a solution type without these characteristics will change.

1.3.2. The Melnikov technique and solitons of the KdV and MKdV equation.

As already mentioned, Jeffrey and Kakutani [43] have shown that soliton solutions of the KdV and MKdV equation are associated with homoclinic orbits in phase space. This association has been further

27

developed by Holmes and Marsden [27] as well as by Birnir [48]. Since the main application of the Melnikov method is to the splitting of the homoclinic orbit into stable and unstable manifolds due to perturbation of the nonlinear differential equation, we have in this work used the method to study the effect of periodic and dissipative perturbations on the equation,

$$u_t + u_x u^m + u_{xxx} = 0 .$$ (1.1)

For m=1 this is the KdV equation and for m=2 it is the MKdV equation; from now on we label them collectively as the (M)KdV equation. To be more precise, we have extended equation (1.1) to the (M)KdV-Burgers equation by allowing for a dissipation term proportional to u_{xx} and by adding an external force term that is periodic in space and time.

We shall in fact only be studying the "reduced (M)KdV equation" which arises when a travelling wave ansatz is made:

$$u(x,t) = u(x-ct) \equiv u(y) ,$$ (1.2)

where c is the wave speed. In this way we are left with the reduced third order ordinary differential equation (ODE),

$$u_{yyy} + u_y u^m - cu_y = 0 .$$ (1.3)

As explained by Olver [33], the most general periodic solution to this equation for m=1 after two integrations reads

$$u(y) = A \; cn^2(\omega y + \delta) + M ,$$ (1.4)

where the constants A, ω and M are actually interrelated and cn is the standard Jacobian elliptic function. It is called [33,44] the cnoidal wave solution. In the limit where the homoclinic orbit is approached

and the elliptic modulus $k \to 1$, the solution (1.4) degenerates to the form

$$u(y) = 3 \, sech^2(y/2 + \delta) \, , \qquad\qquad (1.5)$$

which is the soliton or **solitary wave** solution.

A generalization of this soliton to $m \ll 1$ is shown in [44] to be

$$u(y) = 3 \, sech^{2/m}(y/D + \delta) \, , \qquad\qquad (1.6)$$

$$D = \sqrt{[2(m+1)(m+2)/3^m]}/m \, .$$

In order to motivate this study, we shall review in section 2 some of the applications of the (M)KdV equation to fluid waves and plasma physics, introduce dissipation in this context (thus going to the (M)KdV-Burgers equation) and include periodic wave perturbations. It is also appropriate to introduce other PDEs which reduce under the ansatz (1.2) to the form (1.3). Examples are the Boussinesq equations, the BBM equations, and model equations for waves in elastic media. In section 3 we apply a travelling wave ansatz to the (M)KdV-Burgers equation and the other equations introduced in section 3 under periodic forcing and analyse the phase portrait associated with the cnoidal and soliton solutions for a generalised (M)KdV equation

$$u_t + au_x u^m + bu_{xxx} = 0 \quad . \qquad\qquad (1.7)$$

Sections 4 and 5 analyse the wave solutions of the reduced (M)KdV equation and their geometry in the phase space. The Melnikov method is reviewed in section 6 and the Melnikov integrals as well as tangencies of manifolds and bifurcation curves are calculated. This section is guided by the well-known application of the Melnikov theory

to the Duffing system by Greenspan and Holmes [28] or Guckenheimer and Holmes [29]. In section 7 the dynamics of resonance and subharmonics are studied. Section 8 presents the numerical work such as the plots of the manifolds in the phase portraits and compares the computations to the calculations of section 6. A summary and interpretation of results is given in section 9.
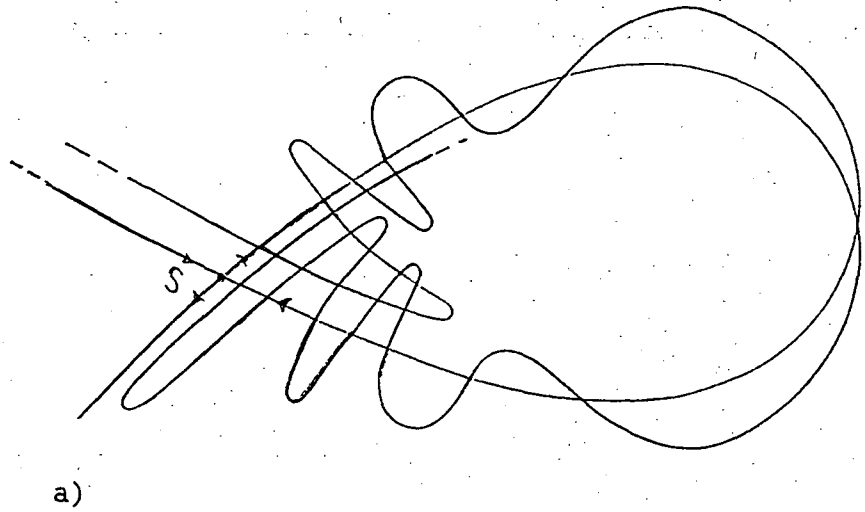
a)
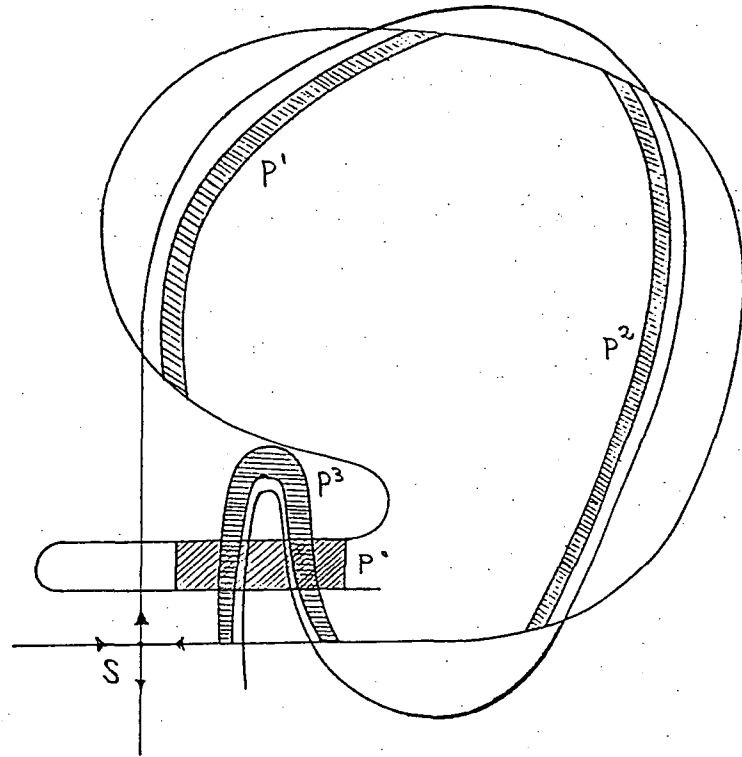
b)

Figure 1. (a) Intersecting invariant manifolds connected to a saddle s. (b) Idealization of (a); the rectangle P^o undergoes three Poincare iterations and returns to its original position deformed into a horseshoe P^3.

2. The (M)KdV equation in fluids, plasma and lattices, and related equations

Most of the numerous publications on the (M)KdV equation in the last two decades have concentrated on properties of the equation itself such as conservation laws, inverse scattering theory, group structures and transformations between solutions. In the present context it is necessary to review some of the physical background to the MKdV equation so as to provide some framework for the type of perturbations that are introduced which then permit analysis via Melnikov's theory. It is also useful to look at equations which are related to the MKdV equation in the sense that a travelling wave ansatz reduces them to the same ODE as it does the (M)KdV equation. Our examples in this context are the Boussinesq equations, the BBM or Peregrine equation and a nonlinear equation for dispersive waves in elastic media. Furthermore, we note that an exponential wave ansatz reduces the cubic Schroedinger equation to equation types equivalent to the (M)KdV equations reduced by travelling waves. We now present a catalogue of cases where the (M)KdV equations or some variant of it emerges.

2.1   Shallow water waves

The general KdV equation

$$u_t + a\, u_x u + b\, u_{xxx} = 0 \qquad\qquad (2.1)$$

was originally derived by Korteweg and de Vries in 1895 [49] to describe gravity waves on a layer of an inviscid, incompressible fluid of finite depth undergoing irrotational motion. In this context equation (2.1) has two applications:

1. It describes the evolution of the height perturbation h_1

$$h_1(x,t) = h(x,t) - h_0, \qquad (2.2)$$

where h_0 is the height of the unperturbed layer and $h(x,t)$, the height of the perturbed layer, plays the role of u in (2.1).

2. It describes the evolution of the horizontal component of the perturbation velocity. Including the influence of viscosity adds a dissipation term $-\nu u_{xx}$ to equation (2.1) and thereby leads to the KdV-Burgers equation

$$u_t + a\, u_{xx} + b\, u_{xxx} - \nu\, u_{xx} = 0. \qquad (2.3)$$

An external forcing term in form of a horizontal acceleration u_p periodic in space and time;

$$u_p(x,t) = \alpha \cos(\omega x - \omega_p t) \qquad (2.4)$$

provides a periodic perturbation to equation (2.3). The dissipation term $-\nu u_{xx}$ and the periodic perturbation (2.4) will, after further reduction, allow the application of Melnikov's theory.

2.2 Waves in liquid-filled elastic tubes

It was shown by Johnson [50] that the propagation of waves in a viscous fluid contained in an elastic tube can be described by the KdV-Burgers equation

$$h_t + h_x h + h_{xxx} - \delta\, h_{xx} = 0 , \qquad (2.5)$$

with x as radial coordinate and $h(x,t)$ a quantity proportional to

the radial perturbation of the tube wall. An external perturbation of the type (2.4), namely

$$h_p(x,t) = \alpha \cos(\omega x - \omega_p t), \qquad\qquad (2.6)$$

can again be added to (2.5) by introducing an external pressure vibrating periodically in x and t.

2.3 Magneto-acoustic waves in plasma

Kawahara [51] showed that the equations describing a magneto-acoustic wave in plasma under the effect of ion-electron collisions can be reduced to a KdV-Burgers equation. In this case the dependent variable is a first-order perturbation of the plasma velocity and ion-electron collisions are responsible for the dissipation term. External forcing can be imposed by fluctuating electromagnetic fields with time and space dependence as in (2.4) or (2.6).

2.4 Alfven waves in plasma

Alfven waves have also been studied by Kawahara. In a review of his analysis in [51] the following equation is derived:

$$\partial f/\partial t + f^2\, \partial f/\partial x = V_o \mu\, \partial^3 f/\partial x^3 . \qquad\qquad (2.7)$$

This is of course the MKdV equation and the dependent variable f is proportional either to the density or velocity fluctuations due to dispersion of the plasma. The wave solutions of (2.7) are the Alfven waves, μ is a constant and V_o is the phase velocity of an idealized (i.e. nondispersive) Alfven wave. External forcing of the

type explained for magneto-acoustic waves in section 2.3 provides periodic perturbations.

2.5   Lattice waves

By lattice we mean here the atomic structure of solids and the vibrations of the atoms is usually described by so-called lattice waves. We consider the one-dimensional model consisting of a number of particles each of mass m connected to its two neighbours by two springs. Instead of a spring force proportional to the equilibrium displacement y, say, of the individual particle, Zabusky [52] considered the nonlinear dependence between spring force F and y:

$$F = \kappa(y + \alpha \, y^{p+1}) \, , \qquad\qquad (2.8)$$

with κ, α, p being constants. It is shown in [52] that the dynamics of a one-dimensional lattice with a spring force of type (2.8) can in the continuous limit be reduced to the equation

$$\partial u/\partial t + u^p \, \partial u/\partial x + \mu \, \partial^3 u/\partial x^3 = 0 \, , \qquad\qquad (2.9)$$

with $u = \partial y/\partial x$ and μ a constant depending on α and   p. Perturbations in the form of mechanical vibrations presented in the form (2.4) can be considered for periodic forcing.

2.6   The Boussinesq equations

More than twenty years before Korteweg and de Vries, Boussinesq [53] derived the equation

$$u_{tt} = bu_{xxxx} + eu_{xx} + a(u^2)_{xx} \qquad\qquad (2.10)$$

35

from potential theory as a model equation for the dynamics of shallow water waves, as elaborated upon by Ursell [54]. u is the vertical amplitude of the waves and a and e are positive coefficients depending on the thickness of the water layer. The coefficient b depends on the layer thickness as well and is negative for the "good" and positive for the "bad" Boussinesq equation. To study the propagation and dispersion of lattice waves as described in section 2.5, Zabusky [52] considered, besides equation (2.9), under assumption (2.8) the equation

$$y_{tt} = -(e + ay_x)y_{xx} - by_{xxxx} .$$ (2.11)

Here, y is the lattice displacement and a, b, e are positive coefficients depending on the resonant frequency, the distance between lattice nodes, the coefficient α of (2.8) and the wave speed in the limit $\alpha \to 0$. This can be considered as a potential form or first integral of the bad Boussinesq equation as it reduces to equation (2.10) with b positive if differentiated with respect to x and the substitution $y_x = u$ is made.

As noted by Manoranjan et.al. [55] the two Boussinesq equations have received little attention compared to other soliton producing equations such as (M)KdV, Burgers, sinh-Gordon, and sine-Gordon. One reason for this is the second time derivative on the dependent variable, causing a higher degree of technical difficulty in their analysis. Some of the mathematical properties of the bad Boussinesq equation have been studied by Hirota [56] whereas some of the mathematics of the good Boussinesq equation have been covered in [55], and by McKean [57]. Perturbations of the form (2.4) can model

mechanical vibrations as well as a periodic structure of the solid
bottom of a fluid layer.

2.7   The BBM (Benjamin/Bona/Mahoney) equation

As an alternative and improvement to the KdV equation, Benjamin, Bona
and Mahoney [58] proposed

$$u_t + eu_x + au_x u + gu_{xxt} = 0 \qquad\qquad (2.12)$$

as a model equation for the propagation of long waves in shallow
water. This equation was also used by Peregrine [59] to model the
evolution of an undular bore in a shallow water channel and is
therefore sometimes called the regularized long-wave (RLW) equation or
Peregrine equation. The dependent variable u is, as in the case of
KdV, the fluctuation of the horizontal velocity component or the wave
height and the coefficients a, e, g depend on the layer thickness.
It is elaborated in [58] (section 3, p.63) that the addition of a
forcing term f(x,t) to (2.12) provides an important generalization.
In the present context this term would of course again have the form
and interpretation of (2.4). Moreover, (2.12) could be extended to
cover dissipative effects as well by adding the viscosity term νu_{xx}
as in the case of the KdV-Burgers equation in section 2.1.

2.8   Nonlinear dispersive waves in elastic media

Toda [60] derived the equation

$$u_{tt} = au_x u_{xx} + bu_{xxxx} + eu_{xx} \qquad\qquad (2.13)$$

as the continuum limit of an equation of motion for an infinite chain
of particles connected by springs of nonlinear spring constant. It is

therefore used to model wave propagation in an anharmonic lattice or in elastic solids respectively (see Grindlay and Opie [61]). The dependent variable u is in this case the wave deflection and an additional term of the type νu_{xxx} induces dissipation.

It is shown in [60] that the asymptotic transformation

$$\xi = a/\sqrt{e} \ (x - \sqrt{e} \ t), \quad \tau = a^3 t, \quad \delta = b^2/(\sqrt{2} \ e),$$
$$u = 2\sqrt{e} \ z(\xi, \tau), \quad v = \partial z/\partial \xi \tag{2.14}$$

reduces (2.13) to the KdV equation

$$\partial v/\partial \tau + v \ \partial v/\partial \xi + \delta^2 \partial^3 v/\partial \xi^3 = 0. \tag{2.15}$$

2.9 The cubic Schroedinger equation

The equation

$$iu_t + \mu u_{xx} + \nu |u|^2 u = 0 \tag{2.16}$$

is known as the nonlinear or cubic Schroedinger equation and is of central importance for wave propagation in optic fibres (for an extensive survey see Kumar [62]). Drazin [44] shows that the ansatz

$$u = r(y)\exp\{i(\theta(y) + nt)\}, \quad y = x - ct \tag{2.17}$$

leads to differential equations for phase $\theta(y)$ and squared amplitude $s(y) = r^2(y)$:

$$\theta_y = (c + A/s), \quad \nu s_y^2 = -2[s^3 - 2\mu(n - c^2/4)s^2 - Bs + A^2/2]. \tag{2.18}$$

A and B are integration constants and it is clear that the second equation in (2.18) originates from the equation

$$\nu s_{yy} = -3s^2 + \mu(4n - c^2)s + B \tag{2.19}$$

38

by integration. On the other hand, Whitham [63] uses the alternate ansatz

$$u = r(y)\exp\{i(cx/2-\omega t)\}, \quad y = x - ct \qquad (2.20)$$

in (2.16) to derive the equation

$$\nu r_{yy} = (c^2/4-\omega)r + \nu r^3. \qquad (2.21)$$

The equations (2.21) and (2.19) for amplitude and amplitude squared respectively are equivalent to the first integrals of the KdV and MKdV equations reduced by travelling wave ansatz, as will be shown in section 3.2.

3. Travelling wave reductions

Before we perform the reductions on the equations introduced in section 2, we explain the effect of scale transformations on system coordinates. Periodic and dissipative perturbations are only included in the reductions of (M)KdV. To extend Boussinesq and BBM reductions to perturbed systems, we can simply add the dissipative and periodic perturbations as discussed previously.

3.1   Scale transformations

In a large number of systems, including the examples above, it is possible to make the following approximation [43] in the dispersion relation for the frequency Ω:

$$\Omega(k) = c_0 k + c_1 k^3 + \dots \ . \tag{3.1}$$

This is a necessary but not sufficient condition for the reduction of the original systems to the (M)KdV or (M)KdV-Burgers equation. The dispersion relation (3.1) leads to a phase velocity V_p of the form

$$V_p = \Omega/k = c_0 + c_1 k^2 + \dots \ . \tag{3.2}$$

This reveals the coefficient c_0 as the long wavelength limit of the phase velocity.

Let x_0 and t_0 stand for the original space and time variables. By introducing a scale transformation

$$x = k^n(x_0 - c_0 t_0), \quad t = k^{n+2} t_0 \ , \tag{3.3}$$

(which is used throughout for dispersive systems) it is possible to

retain a travelling wave ansatz with phase velocity c on the new coordinates x, t :

$$y = x - ct = k^n(x_0 - V_1 t_0), \quad V_1 = c_0 + ck^2 \qquad (3.4)$$

with a new phase velocity V_1. Comparing V_1 with the expansion (3.2) we observe that c corresponds to the coefficient c_1 so

$$V_p \sim V_1 \qquad \text{for} \quad k < 1. \qquad (3.5)$$

That is, due to the expansion (3.2) and the transformation (3.3), any additional travelling wave ansatz (3.4) leaves the phase velocity V_p (or its approximation c_0) 'almost invariant' for k small enough. Moreover we note that the space coordinate x in any KdV type equation is moving with velocity c_0 with respect to the stationary coordinate x_0. The applications in sections 2.1 to 2.4 listed above use the power $n=1$ in (3.3) whereas the MKdV equation (2.9) for lattice waves in section 2.5 can be derived for $n=0$.

3.2   Reduction of KdV and MKdV

We begin with the equation

$$-u_t + a\, u^m u_x + b\, u_{xxx} + \delta\, u_{xx} + \alpha \cos(\omega x - \omega_p t) = 0. \qquad (3.6)$$

This is for $m=1$ a KdV-Burgers equation and for $m=2$ a MKdV-Burgers equation extended by an external periodic forcing term.

A travelling wave ansatz

$$y = x - ct, \quad c = \omega_p/\omega \qquad (3.7)$$

reduces equation (3.6) to

$$c\, u_y + a\, u^m u_y + b\, u_{yyy} + \delta\, u_{yy} + \alpha \cos(\omega y) = 0. \qquad (3.8)$$

Redefining units of x and t, the wave speed c can be normalized to unity without loss of generality. Adopting this convention from now on and integrating equation (3.8) gives

$$u + a\, u^{m+1}/m+1 + b\, u_{yy} + \delta\, u_y + \alpha \sin(\omega y)/\omega = k_1, \qquad (3.9)$$

with k_1 as integration constant. This equation is our main object of analysis. From now on we will study the two different cases m=1 (KdV) and m=2 (MKdV) separately. The first step is to find analytic solutions of (3.9) for vanishing dissipative and periodic forcing terms ($\alpha = \delta = 0$). These solutions are of course the travelling wave solutions of the KdV or MKdV equation and after reintroducing small dissipative and periodic forcing terms ($1 > \alpha$, $\delta > 0$) as perturbations, we have the conditions necessary for Melnikov's method.

3.3 The reduced Boussinesq equation

Following Manoranjan et.al. [55] we rewrite the Boussinesq equation (2.10) as the first order (in time) system

$$\begin{aligned} w_t &= bu_{xxx} + eu_x + a(u^2)_x \,, \\ u_t &= w_x \,. \end{aligned} \qquad (3.10)$$

The ansatz $y = x - ct$ reduces (3.10) to

$$\begin{aligned} -cw_y &= bu_{yyy} + eu_y + a(u^2)_y \,, \\ -cu_y &= w_y \,. \end{aligned} \qquad (3.11)$$

Eliminating w_y and integrating leads to

$$u + bu_{yy} + au^2/2 = k_1 \,, \qquad (3.12)$$

where we have set $c^2 + e = -1$ in order to obtain a form equivalent to (3.9) with $\alpha = \delta = 0$.

3.4 The reduced BBM equation

The wave ansatz $y = x - ct$ reduces the BBM equation (2.12) to

$$(c + e)u_y + au_y u + gcu_{yyy} = 0 . \qquad (3.13)$$

An integration gives

$$(c + e)u + au^2/2 + gcu_{yy} = k_1 . \qquad (3.14)$$

Setting

$$c + e = 1, \quad g(e - 1) = b \qquad (3.15)$$

gives (3.14) in a form equivalent to (3.12).

3.5 The reduced elastic media wave equation

Under the wave ansatz the equation (2.11) introduced in section 2.6 reduces to

$$-c^2 u_{yy} = au_y u_{yy} + bu_{yyyy} + eu_{yy} . \qquad (3.16)$$

Integrating and substituting $v = u_y$ leads to

$$bv_{yy} + (a/2) v^2 + (e + c^2) v = k_1 . \qquad (3.17)$$

The substitution

$$c^2 + e = 1 \qquad (3.18)$$

changes (3.17) into the form (3.12).

4. Wave solutions of the KdV equation and their geometry

Here we derive the wave solutions for the KdV equation and analyze their geometry in both the three-dimensional and the reduced two-dimensional phase space of the ODE systems resulting from the wave reduction.

4.1 Cnoidal and soliton solutions of the KdV equation

The "unperturbed" equation

$$u + a u^2/2 + b u_{yy} = k_1, \qquad (4.1)$$

is obtained from (3.9) by setting $\alpha = \delta = 0$ and $m = 1$. Multiplying it by u_y, integrating and regrouping terms, leads to

$$u_y = \sqrt{[u^3 + 3u^2/a + 6k_1 u/a + 6k_2/a]} \sqrt{(a/3b)} \qquad (4.2)$$
$$= \sqrt{[(u-r_1)(u-r_2)(r_3-u)]} \sqrt{(a/3b)}.$$

The method of quadratures gives an elliptic integral (see e.g. Byrd and Friedman, [64], #236.00, p.79) and consequently the cnoidal wave solution

$$u(y) = A \, cn^2[\lambda(y-y_0),k] + r_2 \qquad (4.3)$$

of the reduced KdV equation

$$u_y + a u_y u + b u_{yyy} = 0. \qquad (4.4)$$

The abbreviations in (4.3) are as follows:

$$A = r_3 - r_2, \qquad \lambda = \sqrt{[a(r_3-r_1)/3b]}/2,$$

y_0 = arbitrary phase shift,

$$k = \sqrt{[(r_3-r_2)/(r_3-r_1)]} = \text{elliptic modulus}, \qquad (4.5)$$

In the limit $k \to 1$ the solution (4.3) reduces to

$$u(y) \to A \, \text{sech}^2[\lambda(y-y_o)] + r_2, \tag{4.6}$$

which is the soliton solution of the KdV equation. We further note in this limit

$$r_1 = r_2, \qquad r_3 = 3/a - 2r_1$$
$$k_1 = ar_1^2/2 - r_1, \quad k_2 = r_1^2/2 - ar_1^3/3. \tag{4.7}$$

These relations are easily derived by matching powers of u in $(u-r_1)^2(r_3-u)$ with those in the RHS polynomial of (4.2).

4.2   The phase space of the reduced KdV equation

In order to investigate the phase space of equation (4.4), within which the solutions (4.3) and (4.6) prevail, we represent equation (4.4) as a three-dimensional system of first order equations:

$$u_y = u_1$$
$$u_{1y} = u_2 \tag{4.8}$$
$$u_{2y} = (1 - au)u_1/b.$$

Clearly, the complete set of fixed points (u_s, u_{1s}, u_{2s}) of this system is the entire u-axis in the phase space spanned by u, u_1, u_2. Moreover, it is trivial to verify that the system (4.8) linearized about any of these fixed points has at least one eigenvalue equal to zero (all three eigenvalues are zero for $au_s=1$); the fixed points become degenerate. This means that the problem of degenerate fixed points for the (unreduced) KdV equation as noted by Birnir [48] carries over to the reduced version (4.4) or (4.8) respectively.

45

The situation changes, however, with the two-dimensional system arising from (4.1) integrated once more,

$$u_y = u_1$$

$$u_{1y} = (k_1 + u + au^2/2)/b \quad .$$

(4.9)

Its fixed points (u_s, u_{1s}) in u-u_1 space are

$$u_{1s} = 0, \qquad u_{s+} = (1 \pm \sqrt{[1 + 2ak_1]})/a$$

(4.10)

with eigenvalues

$$\lambda_+ = \pm \sqrt{[(1 - au_{s+})/b]} = \pm \sqrt{[\pm \sqrt{(1 + 2ak_1)}/b]} \quad .$$

(4.11)

Depending on the integration constant k_1, three topologically distinct cases are possible for the phase portrait:

case 1: $k_1 < -1/2a$.

(4.12)

(4.10) shows that there are no real zeros for u_{s+} and thus no fixed points for the system (4.9); see Figure 2a).

case 2: $k_1 > -1/2a$.

(4.13)

(4.10) and (4.11) produce a saddle at $(u_{s-}, 0)$ and a centre at $(u_{s+}, 0)$; see Figure 2b). According to (4.10) the distance d between them is

$$d = 2\sqrt{[1 + 2ak_1]}/a.$$

(4.14)

case 3: $k_1 = -1/2a$.

(4.15)

The distance d between saddle and center is zero and so is the eigenvalue λ. This corresponds to a doubly degenerate Hamiltonian bifurcation in Greenspan's and Holmes' [28] terminology. The position of this degenerate fixed point is $1/a$; see Figure 2c).

46

The phase diagram for the original 3-dimensional system (4.8) can now easily be constructed. Add the dimension $u_2 = u_{yy}$ to the two-dimensional phase diagram of the system (4.9). Then in any section parallel to the u-u_2 plane there is a family of parabolas defined by (4.1) and continuously parameterized by k_1. Each one of these parabolas defines a surface P parallel to the $u_1 (=u_y)$-axis in u-u_1-u_2 space. Every such surface contains a phase portrait topologically equivalent to one of the three possible cases described by (4.12), (4.13), (4.15). The specification of these three cases is:

case 1. The surface P is bounded away from the u-axis.

case 2. The surface P is penetrated by the u-axis at the saddle and centre of the phase portrait contained on P.

case 3. The surface P touches the u-axis exactly where saddle and centre of the phase portrait on P merge.

Figure 3 elucidates this geometry.

4.3   Analytic solutions and the phase portrait

We briefly comment on the three configurations above and on their connection to the analytic solutions mentioned in section 4.1. The vital quantity is the polynomial on the RHS of (4.2) with roots r_1, r_2, r_3.

case 1: The polynomial has one real and two complex conjugate roots.

case 2:   The three roots are real, which corresponds to the cnoidal
         and soliton solutions.   It is clear that the cnoidal
         solutions (4.3) define the family of closed orbits,
         concentric to the center $(u_{s+},0)$ and parameterized by
         the elliptic modulus   k   (see (4.5)), whereas the
         homoclinic orbit connected to the saddle $(u_{s-},0)$ and
         enclosing the concentric orbits provides the soliton
         solution (4.6).

case 3:   The three real roots coalesce at u=1/a. Centre and saddle
         meet there.

4.3   Antisoliton solutions

Following Manoranjan et.al. [55] we refer to the solutions
corresponding to the stable and unstable parts of the invariant
manifolds opposite to the homoclinic orbit as antisoliton solutions.
Assuming the homoclinic orbit to the right of the saddle as in section
4.1, the condition for antisoliton solutions reads

$$u(y) \leqslant r_1 . \tag{4.16}$$
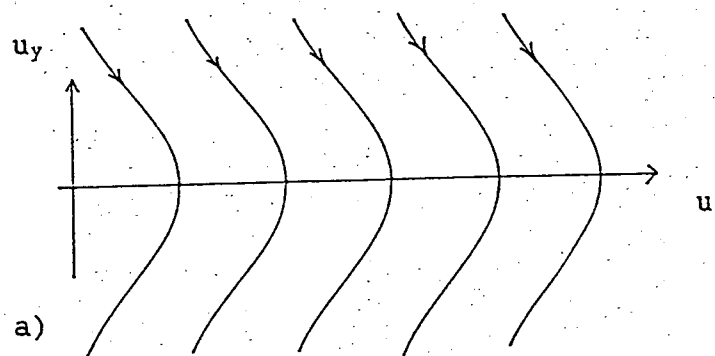
Solving equation (4.1) as in section 4.1, but under the condition
(4.16) and use of [64], p.68, #231.00, gives the solution

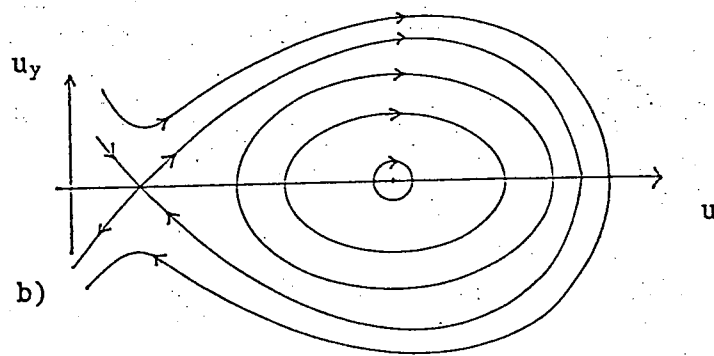$$u(y) = - A \, sn^{-2}[\lambda(y-y_0)] + r_1 , \tag{4.17}$$

with A, λ and k as in (4.5). It reduces in the limit $r_1=r_2$ or k=1, respectively, to the antisoliton solution

$$u(y) = - A \operatorname{cosech}^2[\lambda(y-y_0)] + r_1 , \qquad (4.18)$$

or a double pole at $y=y_0$. Antisolitons are of interest as they interact strongly with solitons under perturbation.
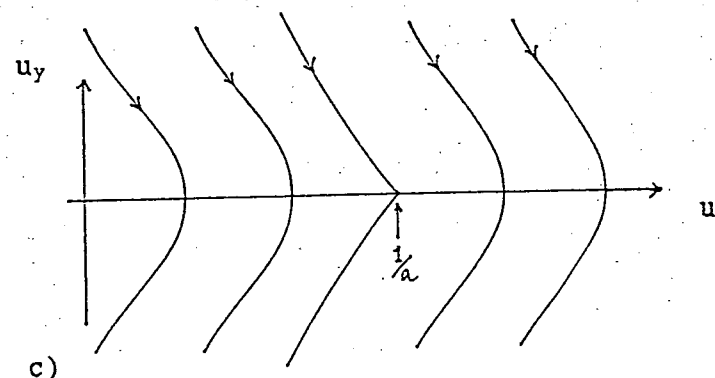
Figure 2.   Phase portrait of the system (4.9).   Cases:

(a) $k_1 < -1/2a$,   (b) $k_1 > -1/2a$,   (c) $k_1 = -1/2a$
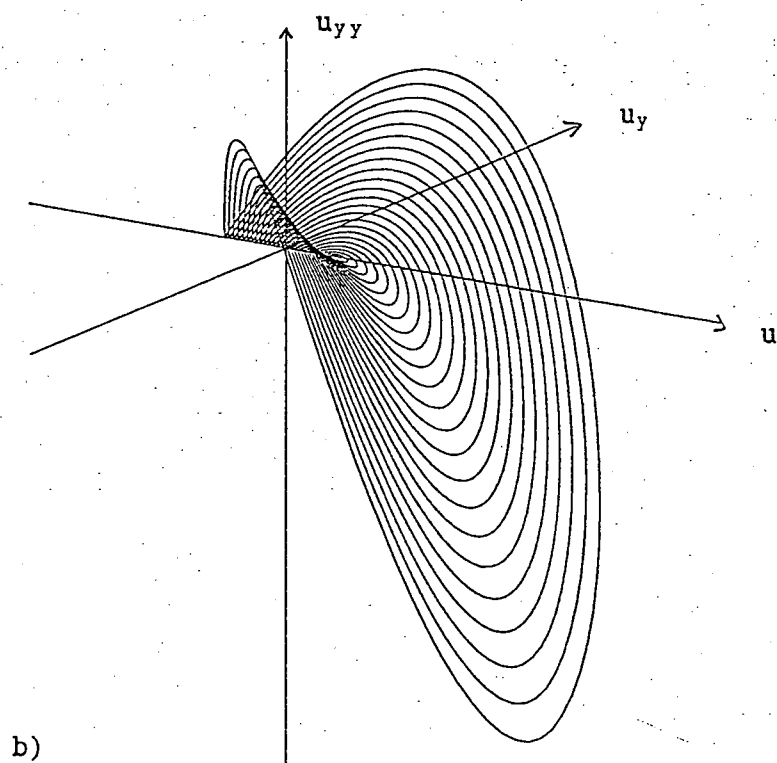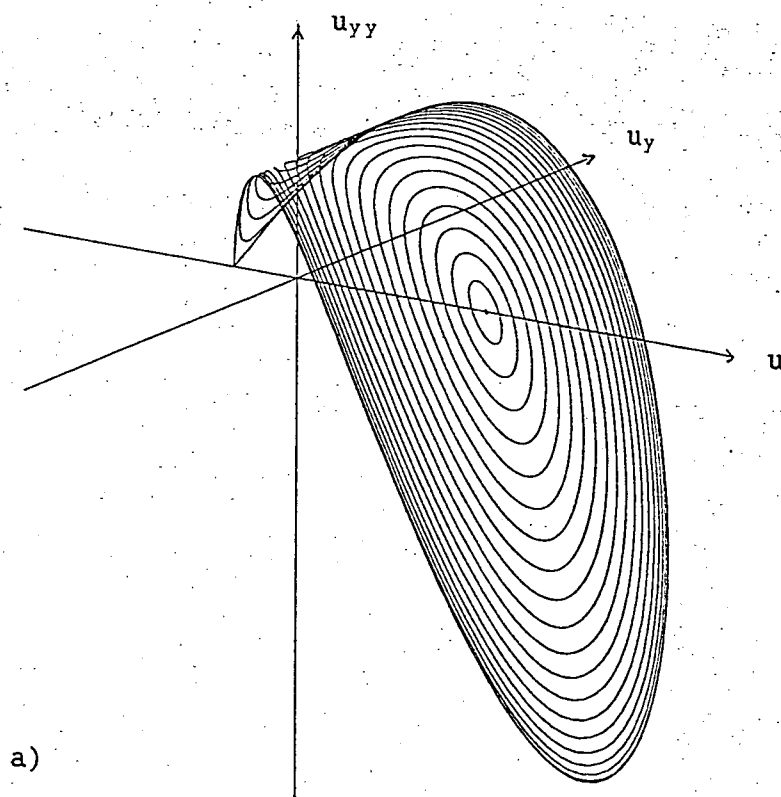
Figure 3. (a) A family of periodic orbits on a parabolically curved invariant surface in the phase space of system (4.8) enclosed by a homoclinic orbit. (b) Set of homoclinic orbits in the phase space of system (4.8).

5. Wave solutions of the MKdV equation and their geometry

Our method of analysis of these solutions is similar to that of section 4. It turns out that in the phase portrait of the reduced MKdV equation permits considerable more variety than the one of the KdV equation. This variety is controlled by the coefficients of the MKdV equation and manifests itself in the geometry of fixed points and saddle connections. Hence we place more emphasis on the homoclinic and heteroclinic saddle connections corresponding to solitons and shock waves. This way the difference between the different phase portraits possible and their dependence on the MKdV coefficients is emphasized. The similarity of the reduced MKdV equation to the Duffing oscillator with weak feedback control, as studied by Wiggins and Holmes [65], is worth mentioning, as the unperturbed system of their oscillator can be considered a special case of the following analysis. A comparison to the study by Wiggins and Holmes is presented in section 5.7.

5.1   Saddle connections

As in the case of the KdV equation we begin with the equation (3.9). We set $\alpha=\delta=0$ and $m=2$ and obtain the equation:

$$u + a\, u^3/3 + b\, u_{yy} = k_1, \tag{5.1}$$

Multiplying it by u_y, integrating and regrouping terms, leads to

$$u_y = \sqrt{[-u^4 - 6u^2/a + 12k_1 u/a + 12k_2/a]}\,\sqrt{(a/6b)} \tag{5.2}$$

$$= \sqrt{[(u-r_1)(r_2-u)(r_3-u)(r_4-u)]}\,\sqrt{(a/6b)},$$

with the convention $r_1 < r_2 < r_3 < r_4$. We obtain real solutions u such that

$$r_1 \leqslant u \leqslant r_2 < r_3 \leqslant u \leqslant r_4 \quad \text{for} \quad a, b < 0. \qquad (5.2')$$

By adjusting the integration constant k_2 we can obtain $r_2 = r_3$ which will show up in the space spanned by u_y and u as a figure eight phase portrait, i.e. two homoclinic loops connected to one saddle. Figure 4a illustrates this case for various values of k_1. The role of this integration constant will be studied in detail in sections 5.6 and 5.7. We will abbreviate this figure eight case as (f8).

Alternatively, we can change the signs in the roots of (5.2) such that

$$u_y = \sqrt{[u^4 + 6u^2/a - 12k_1 u/a - 12k_2/a]}\sqrt{(-a/6b)} \qquad (5.3)$$

$$= \sqrt{[(u-r_1)(u-r_2)(r_3-u)(r_4-u)]}\sqrt{(-a/6b)}.$$

Now, real solutions are obtained for

$$r_1 < r_2 \leqslant u \leqslant r_3 < r_4 \quad \text{with} \quad a < 0 < b. \qquad (5.2')$$

Again by adjusting k_2 so that $r_1 = r_2$ (or $r_3 = r_4$ resp.) we obtain in $u_y - u$ space two saddles and one homoclinic orbit. This geometry, which we abbreviate as (2s), is shown in Figures 4b for various values of k_1.

The two cases described above are the only ones exhibiting saddle connections. We study the case (f8) shown in Figure 4a first.

5.1.1 The figure eight (f8) phase portrait

Applying the method of quadratures to (5.2) gives an implicit representation of the solution u(y):

$$\sqrt{[a/(6b)]}(y-y_o) = \int_{u}^{u_o} du/\sqrt{[-u^4 - 6u^2/a + 12k_1 u/a + 12k_2/a]}$$

$$= \int_{u}^{u_c} du/\sqrt{[(u-r_1)(r_2-u)(r_3-u)(r_4-u)]}. \qquad (5.4)$$

In order to find the solution relating to the *left* homoclinic orbit we note the condition for this solution u with respect to the roots r_1, r_2, r_3, r_4 to be

$$r_1 \ll u < r_2 = r_3 < r_4 . \qquad (5.5)$$

It is clear that r_2 or r_3 is now identical with the saddle position on the u-axis of the $u-u_y$ phase plane. The integral in (5.4) now becomes

$$\sqrt{[a/(6b)]}(y-y_o) = \int_{r_1}^{u} du/\sqrt{[(u-r_1)(r_4-u)]}(r_2-u). \qquad (5.4)$$

The substitution $v = 1/(u-r_2)$ (see [66], p.89,#2.281) gives

$$\sqrt{[a/(6b)]}(y-y_o) = \int_{v_c}^{v} dv/\sqrt{[-1 + Bv + Cv^2]}, \qquad (5.5)$$

$$B = r_1+r_4-2r_2, \quad C = (r_1-r_2)(r_2-r_4) > 0, \quad v_c = 1/(r_1-r_2).$$

This can be readily integrated (see [66], p.81, #2.261):

54

$$\sqrt{[a/(6b)]}(y-y_o) = \{\ln(2\sqrt{[CR(v)]}+2Cv+B) - \ln(2\sqrt{[CR(v_o)]}+2Cv_o+B)\}/\sqrt{C},$$

$$R = -1 + Bv + Cv^2. \tag{5.6}$$

Resubstituting B, R, v_o, v, we can solve for u and obtain after some basic manipulations:

$$u(y) = C/\{(r_1+r_2)\cosh((y-y_o)\sqrt{(Ca/6b)}) + 2r_2\} + r_2. \tag{5.7}$$

The roots r_1 and r_4 can be expressed in terms of the coefficients a, b and r_2 by matching powers of u between the two representations in (5.2) and solving the resulting algebraic system for r_1 and r_4. Although the system is overdetermined, r_1 and r_4 have the unique solutions

$$r_1 = -r_2 -\sqrt{[-(2r_2{}^2+ 6/a)]}, \quad r_4 = -r_2 +\sqrt{[-(2r_2{}^2+ 6/a)]}. \tag{5.8}$$

The derivation of the *right* homoclinic orbit is identical -- except that the roots r_4 and r_1 are interchanged.

5.1.2 The two saddles (2s) phase portrait

The method of the (2s) analysis is of course the same as for (f8). The condition on the roots and solution for the homoclinic orbit connected to the *left* saddle (see figure 4b) is now

$$r_1 = r_2 < u \ll r_3 < r_4 , \tag{5.9}$$

with r_1 or r_2 being the saddle position on the u-axis in the $u-u_y$ diagram. Using as starting point equation (5.3) and following the analysis of (f8) we obtain as (2s)-counterpart to the (f8)-solution (5.7),

$$u(y) = C/\{(r_1+r_3)\cosh((y-y_0)\surd[-Ca/(6b)]) + 2r_1\} + r_1, \quad (5.10)$$

$$C = (r_3-r_1)(r_4-r_1) > 0,$$

$$r_3 = -r_1 - \surd[-(2r_1^2 + 6/a)], \quad r_4 = -r_1 + \surd[-(2r_1^2 + 6/a)]. \quad (5.11)$$

The replacements $r_1 \to r_4$, $r_3 \to r_2$ give us the solution for the homoclinic orbit connected to the *right* saddle.

5.2 Homoclinic orbits (f8) and (2s) combined

By substituting the roots (5.8) and 5.11) into the corresponding solutions (5.7) and (5.10), we can express the homoclinic orbit solutions of (f8) and (2s) in a combined form:

$$u(y) = C/\{A \cosh(E(y-y_0)) + 2r_s\} + r_s, \quad (5.12)$$

$$A = A_\pm = \pm\surd[-2(r_s^2 + 3/a)], \quad C = -6(r_s^2 + 1/a),$$

$$E = E_\pm = \pm\surd[-a/b(r_s^2 + 1/a)],$$

r_s = position of saddle on u-axis.

(f8): $a, b < 0$, $0 < r_s^2 < -1/a$,

A_-: *left* loop, A_+: *right* loop.

(2s): $a < 0 < b$, $-1/a < r_s^2 < -3/a$,

A_-: loop on *left* saddle, A_+: loop on *right* saddle,

r_s negative r_s positive

5.3 Heteroclinic orbits and other limit cases

We first look at the limiting case $r_s = \pm\surd[-1/a]$. It is easy to see that for (f8) either the right (+) or left (−) loop shrinks to a point. The "surviving" loop, however, is still given by solution

(5.12). For (2s) the loop on the right (+) or left (-) saddle shrinks to a point.

The heteroclinic limit for (2s) appears when $r_s = \pm\sqrt{[-3/a]}$. The two saddles at $u = +\sqrt{[-3/a]}$ and $u = -\sqrt{[-3/a]}$ are connected by two heteroclinic orbits (see figure 5b). Symmetry to u- and u_y-axis and elliptic fixed point in the origin is evident. Taking this heteroclinic limit of the above solution (5.12) gives only the two fixed point solutions $u = \pm\sqrt{[-3/a]}$ corresponding to the two saddles. To determine the solutions corresponding to the two heteroclinic orbits, we note that the conditions for these solutions u and the roots of the polynomial in (5.3) are $k_1 = 0$ due to symmetry and

$$-\sqrt{[-3/a]} = r_1 = r_2 < u(y) < r_3 = r_4 = +\sqrt{[-3/a]}. \qquad (5.13)$$

These conditions reduce (5.3) to

$$\pm\sqrt{[-a/(6b)]}(y - y_0) = \int_0^u du/(r_s{}^2 - u^2), \qquad (5.14)$$

with the solution

$$u(y) = \pm\sqrt{[-3/a]}\ \tanh(\pm(y - y_0)/\sqrt{[2b]}). \qquad (5.15)$$

5.4   Periodic solutions

The derivation of the periodic solutions is the same as for the homoclinic or heteroclinic solutions, except that the conditions on the solutions and polynomial roots lead to elliptic integrals. We therefore just list these conditions and the corresponding elliptic

integrals, referring to [64], and then present the solutions in combined forms.

Conditions between roots r_1, r_2, r_3, r_4, and solutions u:

(f8) - inside *right* loop:

$r_1 < r_2 < r_3 < u \ll r_4$,   [64], p.120, #256.

(f8) - inside *left* loop:

$r_1 \ll u < r_2 < r_3 < r_4$,   [64], p.103, #252.

(f8) - outside loops:

$r_1 \ll u \ll r_4$, r_2, r_3 complex conj.,   [64], p.133, #259.

(2s) - inside loop on *right* saddle:

$r_1 < r_2 \ll u < r_3 < r_4$,   [64], p.116, #255.

(2s) - inside loop on *left* saddle:

$r_1 < r_2 < u \ll r_3 < r_4$,   [64], p.112, #254.

(2s) - between heteroclinic saddle connections:

$r_1 < r_2 \ll u \ll r_3 < r_4$, $r_1 = -r_4$, $r_2 = -r_3$, [64], p.116, #255.

Periodic solutions inside the homoclinic loops:

$$u(y) = (r_d - r_c)/(\alpha_s^2 sn^2\{Q_s(y - y_o),k\} - 1) + r_d, \qquad (5.16)$$

$$Q_s = \sqrt{[(r_4 - r_2)(r_3 - r_1)a/(24b)]},$$

$$\alpha_s^2 = (r_b - r_c)/(r_b - r_d),$$

$$k^2 = (r_b - r_c)(r_a - r_c)/((r_4 - r_2)(r_3 - r_1))$$

$$= \alpha_s^2(r_a - r_d)/(r_a - r_c).$$

(f8) - inside *right* loop:

$$r_a = r_1, \quad r_b = r_4, \quad r_c = r_3, \quad r_d = r_2. \qquad (5.17)$$

58

(f8) – inside *left* loop:

$$r_a = r_3, \quad r_b = r_2, \quad r_c = r_1, \quad r_d = r_4. \qquad (5.18)$$

(2s) – inside loop on *right* saddle:

$$r_a = r_1, \quad r_b = r_2, \quad r_c = r_3, \quad r_d = r_4. \qquad (5.19)$$

(2s) – inside loop on *left* saddle:

$$r_a = r_4, \quad r_b = r_3, \quad r_c = r_2, \quad r_d = r_1. \qquad (5.20)$$

(f8) – outside loops:

$$u(y) = (r_4 B + r_1 A + C(r_1 A - r_4 B))/(B + A + C(A - B)), \qquad (5.21)$$

$$A^2 = (r_4 - (r_2 + r_3)/2)^2 - (r_2 - r_3)^2/4,$$

$$B^2 = (r_1 - (r_2 + r_3)/2)^2 - (r_2 - r_3)^2/4,$$

$$C^2 = cn\{(y - y_o)\sqrt{[aAB/(6b)]}, k\},$$

$$k^2 = ((r_4 - r_1)^2 - (A - B)^2)/(4AB).$$

(2s) – between heteroclinic saddle connections:

$$u(y) = r_3 sn\{(y - y_o)r_4\sqrt{[-a/(6b)]}, k\}, \qquad (5.22)$$

$$k = r_3/r_4, \quad r_3^2 + r_4^2 = -1/a.$$

Here sn, cn, dn are Jacobi's elliptic functions and k is their modulus.

5.5   Antisoliton solutions

Clearly, the MKdV system cannot display antisolitons in (f8) mode but in (2s) and heteroclinic mode only.   Referring to section 5.2, the (2s) antisolitons are described by the solution (5.12) under the conditions:

A_+: antisoliton u(y) on *left* saddle, r_s *negative*,

$$-\infty < u(\pm\infty) < r_1 = r_s = r_2 < r_3 < r_4 < u(y_o) < \infty,$$

59

A_: antisoliton $u(y)$ on *right* saddle, r_s *positive*,

$$-\infty < u(y_o) < r_1 < r_2 < r_3 = r_s = r_4 < u(\pm\infty) < \infty.$$

Note that these antisolitons are not simply double poles as for the KdV system. In fact, they are pairs of simple poles at

$$y_P = y_o \pm \cosh^{-1}(-2r_s/A_+)/E_+ , \qquad (5.23)$$

as can be seen from (5.12). The antisolitons relating to the heteroclinic mode are given by

$$u(y) = \varepsilon\sqrt{[-3/a]} \coth(-\varepsilon(y-y_o)/\sqrt{[2b]}) , \qquad (5.24)$$

with the conditions

$\varepsilon=1$: antisoliton $u(y)$ going from *left* to *right* saddle,

$$u(-\infty) < -\sqrt{[-3/a]} = r_1 = r_2 < r_3 = r_4 = \sqrt{[-3/a]} < u(\infty),$$

$\varepsilon=-1$: antisoliton $u(y)$ going from *right* to *left* saddle,

$$u(\infty) < -\sqrt{[-3/a]} = r_1 = r_2 < r_3 = r_4 = \sqrt{[-3/a]} < u(-\infty).$$

These antisolitons represent shockwaves combined with simple poles at $y=y_o$.

5.6 The phase space of the reduced MKdV equation

It is evident that the solutions derived above are valid for the unperturbed and reduced MKdV equation

$$u_y + a u^2 u_y + b u_{yyy} = 0. \qquad (5.25)$$

As in the case of the KdV equation, we are interested in the way these solutions are embedded in the 3-dimensional phase space of the system

$$u_y = u_1$$

$$u_{1y} = u_2 \tag{5.26}$$

$$u_{2y} = (1 + au^2)u_1/b.$$

This is of course the reduced MKdV equation (5.25) represented as a first order system. Since this system exhibits the same problems as its corresponding system for the KdV equation, namely only degenerate fixed points occupying the entire u-axis, we again reduce to a two-dimensional system:

$$u_y = u_1 \tag{5.27}$$

$$u_{1y} = (- k_1 + u + au^3/3)/b \quad .$$

This system is equivalent to equation (5.1) and has the three fixed points

$$(0,r_1), \quad (0,r_2), \quad (0,r_3). \tag{5.28}$$

$r_1 < r_2 < r_3$ are the roots of

$$- k_1 + u + au^3/3 = 0. \tag{5.29}$$

Therefore, for $a > 0$, there exists only one real fixed point and we investigate only the cases for $a < 0$, consistent with our analysis of saddle connections in sections 5.1 and 5.2. We distinguish the three different cases:

case 1: $k_1{}^2 > -4/9a.$

One real fixed point exists. Depending on the signs of k_1 and b, it is either $(0,r_1)$ or $(0,r_3)$ of varying type:

$k_1, b < 0$: $(0,r_3)$ = center,

$k_1, b > 0$: $(0,r_3)$ = saddle,

$k_1 < 0 < b$: $(0,r_1)$ = saddle,

61

$k_1 > 0 > b$: $(0, r_1)$ = center.

case 2: $k_1{}^2 < -4/9a$.

Three real fixed points exist. Their type depends on sign(b);

$b < 0$: $(0, r_1)$, $(0, r_3)$ = center; $(0, r_2)$ = saddle;

$b > 0$: $(0, r_1)$, $(0, r_3)$ = saddle; $(0, r_2)$ = center.

case 3: $k_1{}^2 = -4/9a$.

Two real fixed points exist. Their type depends on sign(b);

k_1, $b < 0$: $(0, r_1)$, $(0, r_2)$ coalesce; $(0, r_3)$ = center;

k_1, $b > 0$: $(0, r_1)$, $(0, r_2)$ coalesce; $(0, r_3)$ = saddle;

$k_1 < 0 < b$: $(0, r_3)$, $(0, r_2)$ coalesce; $(0, r_1)$ = saddle;

$k_1 > 0 > b$: $(0, r_3)$, $(0, r_2)$ coalesce; $(0, r_1)$ = center.

To construct the phase space for the 3-dimensional system (5.26) we add - as before - the dimension $u_2 = u_{yy}$ to the phase diagram of the 2-dimensional system (5.27). The situation is similar to the KdV case except that the invariant surfaces P containing the 2-dimensional phase portraits are defined by (5.1). The correspondence between the three described cases, their geometry in 3-dimensional phase space and the calculated saddle connections is now easily established.

case 1: P is penetrated by the u-axis only once. The penetration point is a center for $b < 0$ and a saddle for $b > 0$.

case 2: P is penetrated three times by the u-axis. The case $b < 0$ corresponds to the (f8)-related solutions contained on P and the penetration points are the two centers and the saddle between them. The case $b > 0$ corresponds to the (2s)-related solutions and the penetration points are the two saddles and the center between them.

As already noted, this degenerates for $k_1=0$ to the heteroclinic solution (5.15).

case 3: Border case between cases 1 and 2. Two penetration points merge into one as the u-axis passes through a local extremum of P defined by (5.1). See also section 5.3.

The described geometry is illustrated in figures 5 and 6 as well as in figure 4.

5.7 Comparison with the Duffing Problem and the Forced Pendulum

The main difference between the systems under consideration here and the Duffing system as well as the pendulum is shown by the role of the integration constant k_1. Since the saddle position r_s must be on the u-axis, that is, it has the coordinates $(u=r_s, u_y=0, u_{yy}=0)$, it can be seen from eq. (5.1) or (5.29) to be a function only of a and, more important, of k_1,

$$r_s + a\, r_s{}^3/3 = k_1. \qquad\qquad (5.30)$$

k_1 therefore controls the shape of (f8) or (2s) in the phase portrait whereas k_2 determines the solution within it. Another interpretation of the role of k_1 would be the parameterization of the set of invariant two dimensional subsystems into which the phase space is foliated. Such an interpretation can be inferred from section 5.6 and is described in connection with the KdV equation.

Setting $r_s=k_1=0$ leads in the reduced and unperturbed u-u$_y$ phase diagram to symmetry with respect to both u- and u$_y$-axis. In (f8) mode this of course reduces the problem to the Duffing system studied extensively and in detail by Greenspan and Holmes [28] and

63

Guckenheimer and Holmes [29]. In (2s) mode the similarity to the forced pendulum (see e.g. Guckenheimer and Holmes) is only superficial. In the pendulum problem the two saddles can be identified, which means an inherent periodicity in the phase diagram. In other words, there is a countably infinite number of saddles and pairs of heteroclinic orbits connecting them. On the other hand the symmetric MKdV (2s) mode has only two saddles and the "outer" halves of their invariant manifolds are *unbounded*. This difference also manifests itself in the heteroclinic orbit solutions of the type

$$u(t) = \pm 2 \arctan(\sinh t), \qquad (5.31)$$

as given by Guckenheimer and Holmes, clearly different from solution (5.15). Any study of a system relating to the MKdV (2s) mode has not been found in the literature so far.

Wiggins and Holmes [65] study the Duffing oscillator with weak feedback control, and without this weak feedback perturbation their system is equivalent to the (unperturbed) (f8) mode. Their perturbation, however, relates to fluctuations of the integration constant k_1. Moreover, both the Duffing system and the pendulum are genuinely two-dimensional systems, whereas the reduced MKdV system is three-dimensional, and although its Melnikov analysis can be reduced to two dimensions, the results of this analysis were justified by reproducing them numerically in the full three-dimensional phase space.

a)

b)
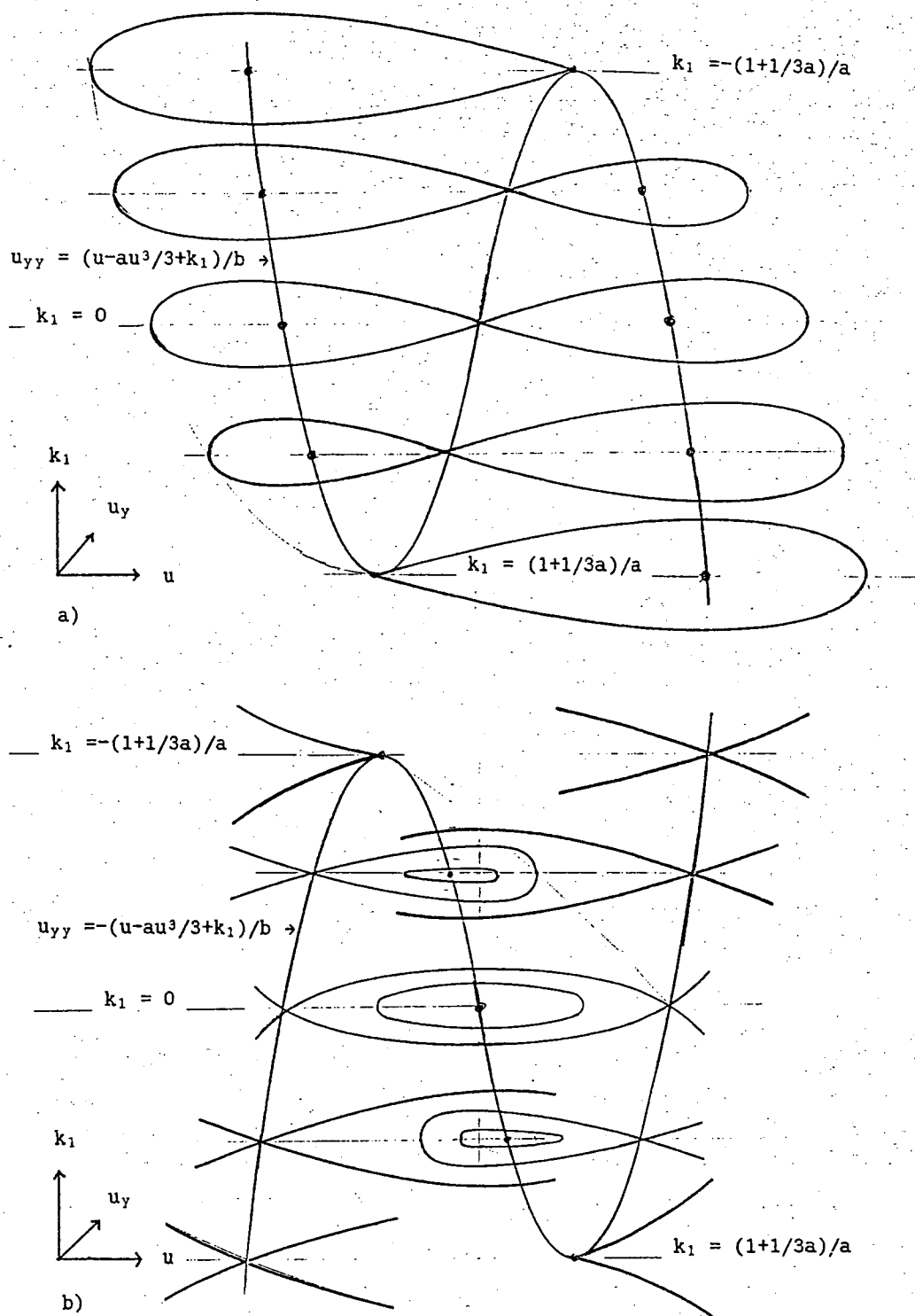
Figure 4.   (a) Figure eight phase portrait in u-u_y-k_1 space. The cubic u_{yy} is given by (5.1) and yields the set of fixed points. The figure eight is symmetric for k_1=0 and degenerates into one loop for $k_1=\pm(1+1/(3a))/a$.   (b) Analogous illustration to (4a), but for the two saddles phase portrait.

Figure 5. (a) Periodic orbits in u-u_y-u_{yy} phase space enclosed by a pair of homoclinic orbits for (f8) mode. (b) Set of homoclinic orbits for (f8) mode in u-u_y-u_{yy} phase space.

Figure 6.   (a) Periodic orbits in u-u_y-u_{yy} phase space enclosed by a
homoclinic orbit for (2s) mode.   (b) Set of homoclinic orbits for (2s)
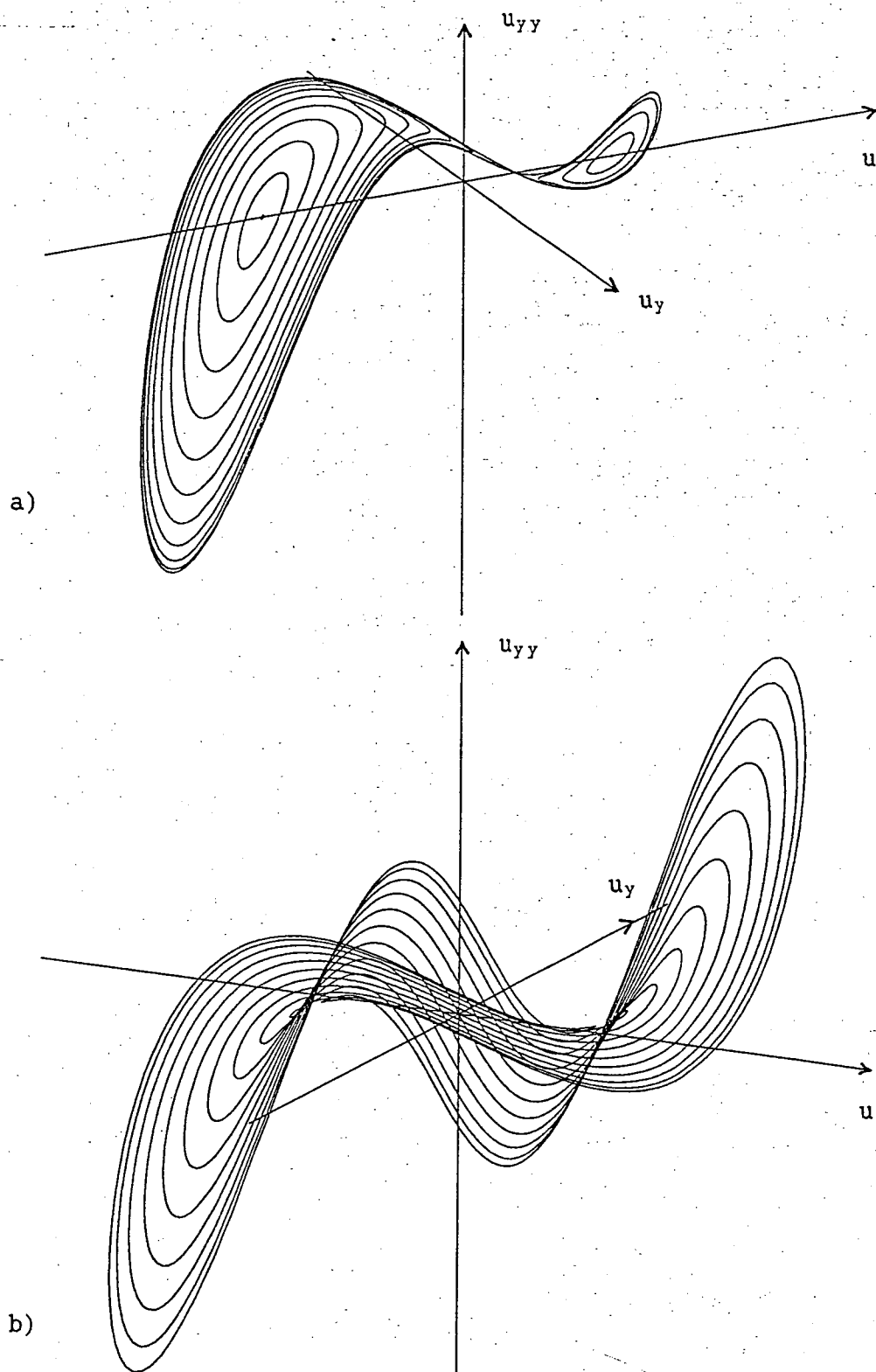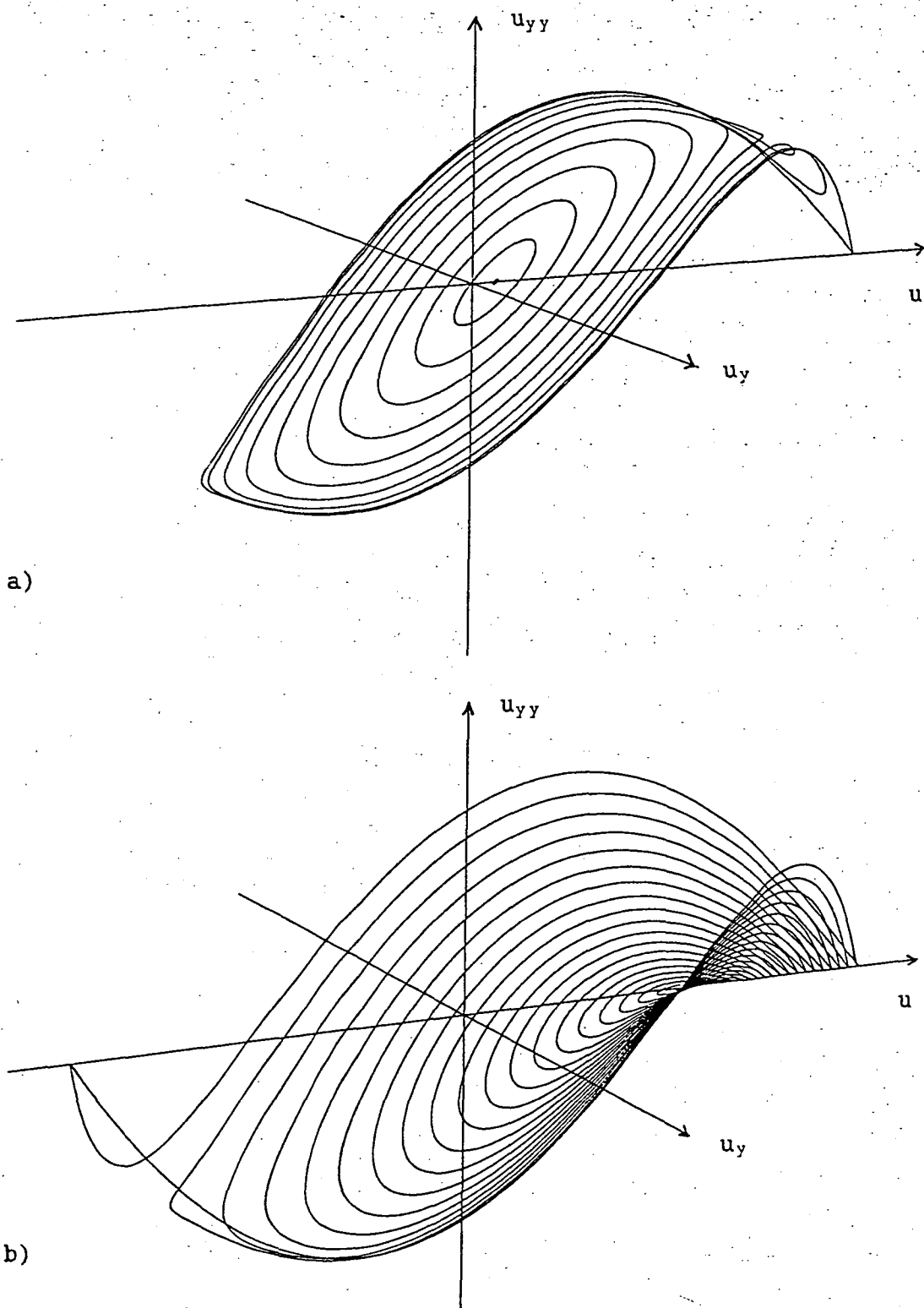mode in u-u_y-u_{yy} phase space.   Note the pair of heteroclinic orbits
representing the limit case.

6. Perturbations and the Melnikov method

Before calculating the Melnikov integrals for the 2-dimensional systems of first order ODEs corresponding to the KdV and MKdV equation, an investigation of the perturbed phase space and a short review of the Melnikov theory is needed. For a detailed introduction to the Melnikov method, see [28], [29] and [37].

6.1 Phase space of the reduced (M)KdV equation under perturbations

Now we include the dissipation term and the periodic perturbation before investigating the phase space of the reduced KdV and MKdV equation. We therefore express equation (3.8) with $c=1$ as a three-dimensional first order system:

$$u_y = u_1$$
$$u_{1y} = u_2 \qquad\qquad\qquad (6.1)$$
$$u_{2y} = (1 + au^m)u_1/b - \delta\, u_2/b - \alpha\, \cos(\omega y)/b\ ,$$

which represent KdV for $m=1$ and MKdV for $m=2$. In particular, we examine the effect of perturbations on the invariant surfaces P. The set of P is now defined by equation (3.9) and, as opposed to the unperturbed case, each surface of P has a slope of value δ in the u_1-direction, induced by the dissipation term δu_y. The periodic forcing term induces a y-periodic oscillation of the set of P with frequency ω and amplitude α/b along the u_{yy}-axis. It is important to note that, despite these perturbations, a point in phase space representing the reduced KdV or MKdV system remains on its particular surface P for all times. This indicates that the phenomenon of Arnold diffusion does not happen in such systems.

6.2   Outline of Melnikov's theory

First, we look at the homoclinic orbits. Consider a two-dimensional system like

$$u_t = f_1(u,v) + \varepsilon\, g_1(u,v,t)$$
$$v_t = f_2(u,v) + \varepsilon\, g_2(u,v,t) \;, \tag{6.2}$$

$$g_i(u,v,t) = g_i(u,v,t+T), \quad i=1,2 \tag{6.3}$$

where ε is the perturbation parameter and T is the period. The unperturbed system ($\varepsilon=0$) is assumed to be integrable and has analytic solutions u_1, v_1, u_k, v_k. In the u-v plane they define a homoclinic orbit $q_1(t-t_o)=(u_1(t-t_o),v_1(t-t_o))$ connected to a saddle s and a family of concentric periodic orbits $q_k(t-t_o)=(u_k(t-t_o),v_k(t-t_o))$, $0<k<1$, enclosed by q_1, such that $q_k \to q_1$ for $k \to 1$, as shown in Figure 1b. Introducing a small ε to the unperturbed system will cause q_1 to split into a stable and unstable invariant manifold, $W^s(t)$ and $W^u(t)$, respectively. To first order in ε the distance Δ between $W^s(t)$ and $W^u(t)$, measured perpendicular to q_1 and at time t_o, can be expressed as

$$\Delta(t_o) = \varepsilon\, M(t_o)/|f(q_1(0))| + O(\varepsilon^2) \;. \tag{6.4}$$

Here, $M(t_o)$ is the Melnikov integral defined as

$$M(t_o) = \int_{-\infty}^{\infty} \{f_1(q_1(t-t_o))g_2(q_1(t-t_o),t) - f_2(q_1(t-t_o))g_1(q_1(t-t_o),t)\}dt \tag{6.5}$$

and $|f(q_1(0))|$ is the modulus of the vector $(f_1(q_1(0)),f_2(q_1(0)))$.

Under the periodicity stated in (6.3), the distance $\Delta(t_o)$ defined in (6.4) implies the following theorem with corollary. For proofs see [28] and [29].

Theorem 6.1. If $M(t_o)$ has simple zeros and maxima and minima of order one, then, for $\varepsilon > 0$ sufficiently small, $W^s(t_o)$ and $W^u(t_o)$ intersect transversely. If $M(t_o)$ remains bounded away from zero, then $W^s(t_o) \wedge W^u(t_o) = 0$.

Corollary 6.2. Assume the perturbation (g_1, g_2) in (6.2) depends on a parameter $\mu \in R$:

$$g_i = g_i(u, v, t; \mu), \quad i = 1, 2 . \tag{6.6}$$

Suppose $M(t_o, \mu)$ has a quadratic zero:

$$M(\tau, \mu_b) = (dM/dt_o)(\tau, \mu_b) = 0 , $$
$$(d^2M/dt^2)(\tau, \mu_b) \neq 0, \quad (dM/d\mu)(\tau, \mu_b) \neq 0 . \tag{6.7}$$

Then $\mu_B = \mu_b + O(\varepsilon)$ is a bifurcation value for which quadratic homoclinic tangencies occur, i.e., there are points of tangencies between $W^s(t_o)$ and $W^u(t_o)$ for $t_o = \tau$.

What the theorem and its corollary basically say is that since $M(t_o)$ approximates $\Delta(t_o)$ up to a factor, a vanishing $M(t_o)$ means a vanishing $\Delta(t_o)$. Therefore $W^s(t_o)$ and $W^u(t_o)$ must be tangent for values of t and μ close to t_c and μ_b.

In the same way as the homoclinic orbit q_1 splits under perturbations, the periodic orbits q_k break up and may become quasiperiodic with periods T_k and T such that

$$T_k = \rho T ; \qquad \rho = \text{irrational number} \tag{6.8}$$

or may become multiply periodic

$$nT_k = mT; \qquad m,n = \text{coprime integers} \qquad\qquad (6.9)$$

where T_k is the period of the unperturbed orbit. The criterion as to whether periodic orbits according to the resonance condition (6.9) occur or whether there are quasiperiodic orbits is determined by a theorem and corollary similar to the ones above. They are based on the subharmonic Melnikov function:

$$M^{m/n}(t_o)= \int_0^{mT} [f_1(q_k(t-t_o))g_2(q_k(t-t_o),t)-f_2(q_k(t-t_o))g_1(q_k(t-t_o),t)]dt$$

$$(6.10)$$

<u>Theorem 6.3.</u> If $M^{m/n}(t_o)$ has simple zeros and maxima and minima of order one and $dT_k/dh > 0$, then, for $\epsilon(n) > \epsilon > 0$, the system (6.2) has a subharmonic orbit of period $nT_k=mT$. (h = Hamiltonian of unperturbed system)

<u>Remark</u>. It can be shown that, for periodic orbits with period T_k of Hamiltonian systems whose Hamiltonian is

$$h(u,v) = - v^2/2 + (k_1 u + u^2/2 + a\ u^j/j)/b ,$$

the requirement $dT_k/dh > 0$ is met away from their centres.

<u>Corollary 6.4.</u> Assume the perturbation (g_1,g_2) in (6.2) depends on a parameter $\mu \in R$:

$$g_i = g_i(u,v,t;\mu), \quad i=1,2 .$$

Suppose $M^{m/n}(t_o,\mu)$ has a quadratic zero:

$$M^{m/n}(\tau,\mu_b) = dM^{m/n}/dt_o(\tau,\mu_b) = 0 ,$$

$$d^2M^{m/n}/dt^2(\tau,\mu_b) \neq 0, \quad dM^{m/n}/d\mu(\tau,\mu_b) \neq 0 .$$

(6.11)

Then $\mu_B = \mu_b + O(\varepsilon)$ is a bifurcation value at which saddle-node bifurcations occur.

For proofs we refer again to [28] and [29]. Theorem 6.3 is a criterion for the existence of resonance under condition (6.9) and corollary 6.4 states the conditions for transition into resonance by saddle-node bifurcations.

6.3   The Melnikov integral of the reduced and perturbed KdV equation

We begin by expressing equation (3.9) with $m=1$ as a two-dimensional first order system of ODEs:

$$u_y = u_1$$

$$u_{1y} = (a\,u^2/2 + u + k_1)/b - \delta\,u_1 - \alpha\,\sin(\omega y)/\omega ,$$

(6.12)

after rescaling $\delta \to \delta/b$, $\alpha \to \alpha/b$. From hereon we will only work with this rescaled equation. (6.12) is the system (4.9) with perturbation added, and comparison with the system (6.2) therefore shows

$$f_1 = u_1 , \qquad\qquad \varepsilon g_1 = 0 ,$$

$$f_2 = (a\,u^2/2 + u + k_1)/b , \quad \varepsilon g_2 = -\,\delta\,u_1 - \alpha\,\sin(\omega y)/\omega.$$

(6.13)

Introducing one more rescaling, $\varepsilon g_2 \to g_2$, and observing that y plays the role of time t, the homoclinic Melnikov integral becomes

$$M(y_o) = \int_{-\infty}^{\infty} u_1 g_2\ dy = \int_{-\infty}^{\infty} u_y\ [-\delta u_y - (\alpha/\omega)\sin(\omega y)]\ dy$$

$$= -\delta \int_{-\infty}^{\infty} u_y{}^2 \, dy + \alpha \int_{-\infty}^{\infty} u \cos(\omega y) \, dy - \alpha u \sin(\omega y)/\omega \Big|_{-\infty}^{\infty}$$

$$= -\delta \int_{-\infty}^{\infty} [-2\lambda A \ \text{sech}^2(\lambda(y-y_o)) \ \tanh(\lambda(y-y_o))]^2 \, dy$$

$$+ \alpha A \int_{-\infty}^{\infty} \text{sech}^2(\lambda(y-y_o)) \cos(\omega y) \, dy \ . \qquad (6.14)$$

Here we have integrated by parts and substituted the soliton solution (4.6). After shifting $y \to y + y_o$ and applying some basic trigonometric identities the two integrals can be found in Gradshteyn and Ryzhik [66] (p.96,#2.416.1; p.505,#3.982.1):

$$M(y_o) = 16 \ \delta\lambda A^2/15 - \alpha\pi\omega \ \cos(\omega y_o)/(\lambda^2 \sinh(\pi\omega/(2\lambda))) \ . \qquad (6.15)$$

For the subharmonic Melnikov integral we obtain, in similar fashion,

$$M^{m/n}(y_o) = \int_0^{mT} f_1 g_2 \, dy = - \alpha A \int_0^{mT} \text{cn}^2(\lambda y) \cos(\omega(y+y_o)) \, dy$$

$$- 4\delta\lambda^2 A^2 \int_0^{mT} \text{sn}^2(\lambda y) \ \text{cn}^2(\lambda y) \ \text{dn}^2(\lambda y) \, dy$$

$$= - \alpha A \ I_p - 4\delta\lambda^2 A^2 \ I_d \ . \qquad (6.16)$$

73

We have substituted the cnoidal wave solution (4.3) here. The integral I_p, denoting the periodic part of $M^{m/n}$, is evaluated using a Fourier expansion of $dn^2 = 1-k^2-k^2cn^2$, as given in Greenhill [67] (p.286,#49):

$$I_p = \int_0^{mT} [(k^2-1+dn^2(\lambda y)/k^2] \, [\cos(\omega y)\cos(\omega y_0)-\sin(\omega y)\sin(\omega y_0)]dy$$

$$= \int_0^{mT} [k^2-1+E(k)/K(k)+\pi^2/K^2(k).\sum_j(j\cos(j\pi\lambda y/K(k))/\sinh(j\pi K(k')/K(k))].$$

$$[\cos(\omega y)\cos(\omega y_0) - \sin(\omega y)\sin(\omega y_0)]/k^2 \, dy \quad . \quad (6.17)$$

Here K, E are the first and second elliptic integrals and $k'^2 = 1-k^2$. Due to orthogonality of circular functions the only nonzero term in the integral (6.17) is

$$j\pi^2\cos(\omega y_0)/(K^2(k)k^2\sinh(j\pi K(k')/K(k))) \int_0^{mT}\cos(j\pi\lambda y/K(k))\cos(\omega y) \, dy \quad (6.18)$$

iff the orthogonality condition

$$j\pi\lambda/K(k) = \omega \quad (6.19)$$

applies. Otherwise all terms vanish. From (6.19) and the resonance condition

$$mT = nT_k \quad \text{with} \quad T = 2\pi/\omega, \quad T_k = 2K(k)/\lambda \quad (6.20)$$

74

we find

$$j\pi\lambda/K(k) = \omega = m\pi\lambda/nK(k) \quad \text{or} \quad j = m/n. \tag{6.21}$$

In other words, for the indices j to be integer we have the condition

$$n = 1 \quad . \tag{6.22}$$

I_p therefore collapses to

$$I_p = \omega\pi \cos(\omega y_0)/(\lambda^2 k^2 \sinh(\omega K(k')/\lambda)) \quad . \tag{6.23}$$

The dissipation part I_d can be similarly evaluated using [66] (p.630,#5.134.3). The Melnikov integral then becomes

$$M^m(y_0) = A\alpha\omega\pi \cos(\omega y_0)/(\lambda^2 k^2 \sinh(\omega K(k')/\lambda)) +$$

$$16A^2\lambda\delta \; [(1-k^2)(k^2-2)2K(k) + (k^4-k^2+1)E(k)]/(15k^4). \tag{6.24}$$

Note that k is a function of m such that

$$k(m \to \infty) \to 1 \quad , \tag{6.25}$$

and the homoclinic limit is correctly reached for $k \to 1$:

$$M^m(y_0) \to M(y_0). \tag{6.26}$$

6.4   Tangencies and quadratic zeros

From (6.14) it is clear that the homoclinic Melnikov function $M(y_0)$ has quadratic zeros for $\cos(\omega y_0) = 1$. Therefore, by corollary 6.2, the invariant manifolds W^s and W^u must have tangency points, and we define the tangency ratio $R(\omega)$ for $\alpha=\alpha_c$ and $\delta=\delta_c$:

$$R(\omega) = \alpha_c/\delta_c = 16A\lambda^3\sinh(\pi\omega/2\lambda)/(15\pi\omega) \quad . \tag{6.27}$$

75

This ratio or the perturbation frequency ω play the role of the parameter μ in corollary 6.2, which can now be expressed in the form:

$$\alpha/\delta > R(\omega) \quad <=> \quad W^s \wedge W^u \neq 0 \text{ (transverse intersection)}$$
$$\alpha/\delta = R(\omega) \quad <=> \quad W^s \wedge W^u \neq 0 \text{ (tangency)} \qquad (6.28)$$
$$\alpha/\delta < R(\omega) \quad <=> \quad W^s \wedge W^u = 0 \ .$$

Using (4.5) and (4.7), A and λ can be replaced in (6.27) and $R(\omega)$ can be rewritten in terms of the coefficients a, b and the saddle position r_s (= r_1 = r_2) on the u-axis:

$$R(\omega) = 2bB^5\sinh(\pi\omega/B)/5a\pi\omega \ , \quad B = \sqrt{[(1 - ar_s)/b]} \ . \qquad (6.29)$$

The limit cases are

$$R(\omega=0) = 2bB^4/5a \ ,$$
$$r_s = 1/a \text{ (saddle and center merge)}: R(\omega\neq0) = \infty$$
$$R(\omega=0) = 0 \ . \qquad (6.30)$$

Figures 7a and 7b show the bifurcation curves of R versus ω and saddle position r_s respectively.

The critical ratio α_c/δ_c at which saddle-node bifurcations occur is determined from the subharmonic Melnikov function (6.24),

$$R^m(\omega) = 16A\lambda^3[2(1-k^2)(k^2-2)K(k)+(k^2+1)E(k)]\sinh(\omega K(k')/\lambda)/(15\pi\omega k^2) \ .$$
$$(6.31)$$

This can also be rewritten in terms of a, b and m. We find through (4.5) and the resonance condition (6.20),

$$A = 12\lambda^2k^2b/a \ , \qquad \lambda = \omega K(k)/\pi m \ , \qquad (6.32)$$

76

$$R^m(\omega) = 64\omega^4 K^5(k)b \; [(1-k^2)(k^2-2)$$
$$+ (k^4-k^2+1)E(k)] \; \sinh(\pi m K(k')/K(k))/(5\pi^6 m^5 a). \qquad (6.33)$$

Corollary 6.4 can now be expressed as

$$\alpha/\delta > R^m(\omega) \quad <=> \quad \text{resonance}$$
$$\alpha/\delta = R^m(\omega) \quad <=> \quad \text{saddle-node bifurcation} \qquad (6.34)$$
$$\alpha/\delta < R^m(\omega) \quad <=> \quad \text{quasiperiodicity}.$$

Since the functional dependence of k on m is rather complicated due to the dependence of λ on k through the roots r_1, r_2, r_3 --- as can be seen from (6.32) and (4.5) --- the critical ratio α_c/δ_c at which bifurcations occur cannot be determined by straightforward application of (6.33). To evaluate R^m we first eliminate λ from (4.5) and the resonance condition (6.32) and obtain

$$\sqrt{[a(r_3-r_1)/(3b)]} = \omega K(k)/(\pi m),$$
$$k^2 = (r_3-r_2)/(r_3-r_1). \qquad (6.34a)$$

This relation shows the dependence of the elliptic modulus k or the roots r_1, r_2, r_3 as given by (4.2) on the order of resonance m and the perturbation frequency ω. From (4.2) we can further derive by matching powers

$$3/a = r_1+r_2+r_3, \quad -6k_1/a = r_1r_2+r_2r_3+r_3r_1, \quad 6k_2/a = r_1r_2r_3. \qquad (6.34b)$$

The integration constant k_1 can be determined from (4.1) by substituting a given saddle position $(r_s,0,0)$ on the u-axis:

$$k_1 = ar_s^2/2 - r_s. \qquad (6.34c)$$

The integration constant k_2 varies within the set of periodic solutions (4.3) and therefore cannot be determined without knowing

77

which solution becomes resonant for a given ω and m. The three determining equations for r_1, r_2, r_3 are therefore (6.34a) and the first two equations of (6.34b), which can be used to express two of the roots in terms of the third one and substitute them into (6.34a), which can now be solved numerically for k. This modulus so obtained can therefore be used to evaluate R^m via (6.32) assuming the coefficients a, b, saddle position r_s, resonance order m and perturbation frequency ω given. Illustrations of R^m are provided by Figures 7c and 7d.

6.5 The Melnikov integral of the reduced and perturbed MKdV equation

As in the KdV case in section 6.3, we begin by expressing equation (3.9) — this time with m=2 — as a two-dimensional first order system of ODEs:

$$u_y = u_1$$
$$u_{1y} = (au^3/3 + u + k_1)/b - \delta u_1 - \alpha \sin(\omega y)/\omega \ , \qquad (6.35)$$

after rescaling $\delta \to \delta/b$, $\alpha \to \alpha/b$. Following the procedure in section 6.3, we express the Melnikov integral $M(y_o)$ as

$$M(y_o) = -\delta \int_{-\infty}^{\infty} u_y^2 \, dy + \alpha \int_{-\infty}^{\infty} u \cos(\omega y) \, dy$$

$$= -\delta \, M_D + \alpha \, M_A \ . \qquad (6.36)$$

We first calculate $M(y_o)$ for the homoclinic orbits by substituting the solution (5.12) or its derivative into (6.36). The dissipation part M_D becomes now

$$M_D = \int_{-\infty}^{\infty} u_y{}^2 \, dy = (AEC)^2 \int_{-\infty}^{\infty} \sinh^2 E(y-y_o)/(A \cosh E(y-y_o) \dot{+} 2r_s)^4 \, dy.$$

(6.37)

Using the substitution $x=E(y-y_o)$ and noting evenness of the integrand w.r.t. x the integral reduces to the form as in Gradshteyn and Ryzhik ([66], p.346, #3.516.4):

$$M_D = 2E(AC)^2 \int_{-\infty}^{\infty} \sinh^2 x/(A \cosh x + 2r_s)^4 \, dx$$

$$= 2E(AC)^2 K^4 \int_{-\infty}^{\infty} \sinh^2 x/(KA \cosh x + 2Kr_s)^4 \, dx$$

$$= -4E(AD)^2 K^4 \Gamma(2)\Gamma(3/2)Q^1{}_2(2Kr_s)/(\sqrt{[\pi]}KA\Gamma(4))$$

$$= -AE\sqrt{[-C]}Q^1{}_2(2r_s/\sqrt{[-C]}).$$

(6.38)

Γ is the gamma function and K is a technical constant determined by comparison of the integral above with [66], p.346, #3.516.4:

$$K = \sqrt{[-C]} = \begin{cases} \text{imaginary for (f8); } r_s{}^2 < -1/a, \\ \text{real for (2s); } -1/a < r_s{}^2 < -3/a. \end{cases}$$

(6.39)

$Q^1{}_2$ is the associated Legendre function of the second kind:

$$Q^1{}_2(z) = -3\sqrt{[z^2-1]} \tanh^{-1}(1/z) - (3z^2-2)/\sqrt{[z^2-1]}.$$

(6.40)

This reduces for imaginary argument to

$$Q^1{}_2(ix) = i\{3\sqrt{[x^2+1]} \tan^{-1}(1/x) - (3x^2+2)/\sqrt{[x^2+1]}\}.$$

(6.41)

79

Therefore M_D stays real for (f8) as well and can be expressed in terms of A, C, E and r_s (see (5.12)) for (2s) and (f8) as

$$M_{D2s\pm} = -E_\pm(2r_sA^2/\sqrt{[-C]}\ \tanh^{-1}(\sqrt{[-C]}/2r_s) + 4r_s^2 + 2C/3), \quad (6.42)$$

$$M_{Df8\pm} = -E_\pm(2r_sA^2/\sqrt{[C]}\ \tan^{-1}(-\sqrt{[C]}/2r_s) + 4r_s^2 + 2C/3). \quad (6.43)$$

Remark. The integral in (6.38) can also be evaluated without the use of special functions. Integration by parts gives

$$\int_{-\infty}^{\infty} \sinh x\ /(A\ \cosh x + 2r_s)^4\ \sinh x\ dx = 1/(3A) \int_{-\infty}^{\infty} \cosh x\ /(A\ \cosh x + 2r_s)^3 dx$$

$$= 8/(3A) \int_0^{\infty} (u^3+u)/(A\ u^2 + 4r_s u + A)^3\ du\ ,$$

where the last integral is obtained using the evenness of cosh and the substitution u=exp(x). It can be found in [66] (p.69; #2.175.3, #2.175.9) and it is straightforward to verify $M_{D2s\pm}$ (6.42) for $4A^2 - 16r_s^2 < 0$ and $M_{Df8\pm}$ (6.43) for $4A^2 - 16r_s^2 > 0$.

Note that for the left loop (E_) of $M_{Df8\pm}$:

$$\lim_{r_s \to +(-)0} \tan^{-1}(-\sqrt{[C]}/2r_s) = +(-)\pi/2\ . \qquad (6.44)$$

The main branch of $\tan^{-1}(-\sqrt{[C]}/2r_s)$ is shown as a pair of solid curves in figure 8. To eliminate the discontinuity (6.44), the branch

situated below the main branch shown as dashed line in figure 8 is chosen for $r_s > 0$. Equivalently for the right loop (E_+):

$$\lim_{r_s \to +(-)0} \tan^{-1}(-\sqrt{[C]}/2r_s) = -(+)\pi/2. \qquad (6.45)$$

Therefore, for $r_s < 0$, the branch below the main branch is chosen. For the periodic part M_A note that we can substitute $U = u - r_s$ for u and shift $y \to y + y_o$:

$$M_A(y_o) = \int_{-\infty}^{\infty} U(y) \cos \omega(y + y_o) \, dy . \qquad (6.46)$$

Using the solution (5.12), the identity $\cos(\alpha + \beta) = \cos \alpha \cos \beta - \sin \alpha \sin \beta$ and symmetry properties of circular functions, $M_A(y_o)$ reduces to

$$M_A(y_o) = -2C \cos(\omega y_o) \int_0^{\infty} \cos(\omega y)/(A \cosh(Ey) + 2r_s) \, dy . \qquad (6.47)$$

This integral is shown in [66] (p.505, #3.983.1) to have two distinct evaluations:

1. $\underline{2r_s > A > 0 \implies 0 < -1/a < r_s^2 \implies (2s)}$:

$$M_{A2s\pm}(y_o) = \pm 2\sqrt{[-C]} \cos(\omega y_o) \, \pi \sin\{\omega/E \cosh^{-1}(2r_s/A)\}/\{E \sinh(\pi\omega/E)\}.$$

$$(6.48)$$

2. $|A| > |2r_s| > 0 \Rightarrow 0 < r_s^2 < -1/a \Rightarrow$ (f8):

$$M_{Af8\pm}(y_o) = \pm 2\sqrt{[C]} \cos(\omega y_o)\, \pi\, \sinh\{\omega/E\, \cos^{-1}(2r_s/A_+)\}/\{E\, \sinh(\pi\omega/E)\}.$$

(6.49)

Note that, due to symmetries of the hyperbolic and circular functions, the superscripts or signs on A and E can be omitted or pulled in front of the RHS in (6.48) and (6.49). Only in the argument of $\cos^{-1}$ in (6.49) do the different signs on A change the absolute value of M_{Af8}, corresponding to the two different loops. According to the convention of (5.12) we therefore distinguish two cases:

M_{Af8-}: left loop, M_{Af8+}: right loop.

As for the KdV case in section 6.4 we define the tangency ratios R_{2s} and R_{f8} for the critical values α_c and δ_c where the Melnikov functions have quadratic zeroes and stable and unstable manifolds become tangent. Following the considerations of section 6.4 the ratios turn out to be

$$R_{2s\pm} = -\{2r_s A^2/\sqrt{[-C]}\, \tanh^{-1}(\sqrt{[-C]}/2r_s) + 4r_s^2 + 2C/3\}$$
$$E^2\sinh(\pi\omega/E)/(2\pi\sqrt{[-C]}\, \sin\{\omega/E\, \cosh^{-1}(2r_s/A_+)\}),\quad (6.50)$$

$$R_{f8\pm} = -\{2r_s A^2/\sqrt{[C]}\, \tan^{-1}(-\sqrt{[C]}/2r_s) + 4r_s^2 + 2C/3\}$$
$$E^2\sinh(\pi\omega/E)/(2\pi\sqrt{[C]}\, \sinh\{\omega/E\, \cos^{-1}(2r_s/A_+)\}).\quad (6.51)$$

Figures 9 and 10 show R_{2s+} and R_{f8+} plotted against r_s and ω.

6.6   The Melnikov integrals in the degenerate limits

We study the Melnikov integrals of (2s) in the limits $r_s = \sqrt{[-1/a]}$ and $r_s = \sqrt{[-3/a]}$ and of (f8) in the limit $r_s = \pm\sqrt{[-1/a]}$.

82

It is easy to verify that

$$\lim_{r_s \to \pm\sqrt{[-1/a]}} M_{A2s\pm} = \lim_{r_s \to \pm\sqrt{[-3/a]}} M_{A2s\pm} = 0$$

$$\lim_{r_s \to \pm\sqrt{[-1/a]}} M_{D2s\pm} = \lim_{r_s \to \pm\sqrt{[-3/a]}} M_{D2s\pm} = 0,$$

$$\lim_{r_s \to \pm\sqrt{[-1/a]}} R_{2s\pm} = \lim_{r_s \to \pm\sqrt{[-3/a]}} R_{2s\pm} = \infty. \qquad (6.52)$$

To investigate the limits for the right loop of (f8) note that by definition of $E_\pm$ and C in (5.12) we have $E_+/\sqrt{[C]} = \sqrt{[a/6b]}$ and observing the continuity argument in connection with (6.44):

$$\lim_{r_s \to +\sqrt{[-1/a]}} \tan^{-1}(-\sqrt{[C]}/2r_s) = 0, \qquad (6.53)$$

which corresponds to the main branch of $\tan^{-1}$, and

$$\lim_{r_s \to -\sqrt{[-1/a]}} \tan^{-1}(-\sqrt{[C]}/2r_s) = -\pi, \qquad (6.54)$$

corresponding to the first negative branch of $\tan^{-1}$. Substituting these limits into (6.43) gives

$$\lim_{r_s \to +\sqrt{[-1/a]}} M_{Df8+} = 0, \qquad (6.55)$$

$$\lim_{r_s \to -\sqrt{[-1/a]}} M_{Df8+} = \sqrt{[-2/3b]} \; 4\pi/a. \qquad (6.56)$$

Equivalently, the limits corresponding to the left loop are

$$\lim_{r_s \to -\sqrt{[-1/a]}} M_{Df8-} = 0 \ , \tag{6.57}$$

$$\lim_{r_s \to +\sqrt{[-1/a]}} M_{Df8-} = \sqrt{[-2/3b]} \ 4\pi/a \ . \tag{6.58}$$

For the periodic part M_{Af8+} we obtain in a straightforward manner

$$\lim_{r_s \to +\sqrt{[-1/a]}} M_{Af8+} = 0 \ , \tag{6.59}$$

and by asymptotic analysis

$$\lim_{r_s \to -\sqrt{[-1/a]}} M_{Af8+} = 2 \cos(\omega y_o) \ \pi\sqrt{[6b/a]} \ \exp(\omega\sqrt{[-2/3b]}) \ ,$$
$$\tag{6.60}$$

as well as for the left loop:

$$\lim_{r_s \to -\sqrt{[-1/a]}} M_{Af8-} = 0 \ , \tag{6.61}$$

$$\lim_{r_s \to +\sqrt{[-1/a]}} M_{Af8-} = 2 \cos(\omega y_o) \ \pi\sqrt{[6b/a]} \ \exp(\omega\sqrt{[-2/3b]}) \ .$$
$$\tag{6.62}$$

$$\lim_{r_s \to -\sqrt{[-1/a]}} R_{f8+} = \sqrt{[-1/a]} \ 2/3b \ \exp(\omega\sqrt{[-3b/2]}) \tag{6.63}$$

is determined via M_{Df8+} (6.56) and M_{Af8+} (6.60), whereas

$$\lim_{r_s \to +\sqrt{[-1/a]}} R_{f8+} = \infty \tag{6.64}$$

is taken on R_{f8+} (6.51). For the left loop the limits reverse again

their symmetry:

$$\lim_{r_s \to +\sqrt{[-1/a]}} R_{f8-} = \sqrt{[-1/a]} \; 2/3b \; \exp(\omega\sqrt{[-3b/2]}) \; , \qquad (6.65)$$

$$\lim_{r_s \to -\sqrt{[-1/a]}} R_{f8-} = \infty \; . \qquad (6.66)$$

Besides the limits discussed we can determine the Melnikov integral M_h for the heteroclinic solution (5.15). Substituting it into (6.36), dissipative and periodic part M_{hD} and M_{hA} as well as the tangency ratio R_h become

$$M_{hD} = -3/2ab \int_{-\infty}^{\infty} \text{sech}^2(y/\sqrt{[2b]}) \; dy = \sqrt{[2/b]} \; 2/a \; , \qquad (6.67)$$

$$M_{hA} = \sqrt{[-6/2ab]} \; \cos(\omega y_o) \int_{-\infty}^{\infty} \cos(\omega y) \; \text{sech}^2(y/\sqrt{[2b]}) \; dy$$

$$= \sqrt{[-6b/a]} \; \pi\omega \; \cos(\omega y_o)/\sinh(\pi\omega\sqrt{[b/2]}) \; , \qquad (6.68)$$

$$R_h = 2/(\pi b\sqrt{[-3a]}) \; \sinh(\pi\omega\sqrt{[b/2]}) \; . \qquad (6.69)$$

Like in the homoclinic case, the integrals are evaluated after shifting $y \to y+y_o$ and observing trigonometric symmetries through use of [66] (p.99 ,#2.423.12 and p.505, #3.982.1).

85

6.7   Subharmonic Melnikov integrals

As before, we split the Melnikov integral into periodic part $M_A^{m/n}(y_o)$ and dissipative part $M_D^{m/n}$:

$$M^{m/n}(y_o) = \alpha\, M_A^{m/n}(y_o) - \delta\, M_D^{m/n} \;. \tag{6.70}$$

We begin with the periodic part $M_A^{m/n}(y_o)$. Setting $f_1 = u_y$, u being the periodic solution (5.16), and $g_1 = 0$, $g_2 = \sin(\omega y)$ for the periodic perturbation in the definition (6.10) leads to the integral

$$M_A^{m/n}(y_o) = \int_0^{mT/n} \cos(\omega y)/(\alpha^2 sn^2\{\Omega(y-y_o),k\} - 1)\; dy \;. \tag{6.71}$$

Like the subharmonic Melnikov integral for the KdV case in section 6.3, the evaluation of this integral requires a Fourier expansion of the term $1/(\alpha^2 sn^2\{\Omega(y-y_o),k\} - 1)$. This is done by logarithmic differentiation, as described in [67], and leads in the present case to a differential equation with no closed form solution. Therefore we cannot analytically evaluate (6.71). A numerical evaluation for $n=1$ would be sufficient and requires the determination of the modulus k as a function of the coefficients a, b saddle position r_s, resonance order m and perturbation frequency ω. Such a calculation depends on numerics as well and has been described in connection of the evaluation of the tangency ratio R^m (6.33) of the KdV problem (see eqs. 6.34a, 6.34b, 6.34c). The main operation in this calculation is the determination of roots of the function defined by (6.34a). Unfortunately the corresponding function in the present MKdV problem shows extremely sensitive dependence towards variation of the polynomial roots r_1, r_2, r_3, r_4 defined by (5.2) which resulted in

86

the failure of all algorithms employed despite the use of double precision numerics. This extreme sensitivity is clearly a consequence of the very dense resonance band structure close to the homoclinic orbit. However, we can make the estimate

$$M_A^{m/n}(y_0) \sim M_A(y_0) \quad \text{for m large,} \tag{6.72}$$

since

$$\lim_{m \to \infty} M_A^{m/n}(y_0) = M_A(y_0), \tag{6.73}$$

according to the theorem by Chow et.al [68]. (6.72) therefore applies for $M_A^{m/n}(y_0)$ provided m is sufficiently large. Moreover, due to orthogonality of circular functions and the resonance condition

$$mT = nT_k \quad \text{with} \quad T = 2\pi/\omega, \quad T_k = 2K(k)/\Omega^0 \tag{6.74}$$

we find, like in the KdV case ((6.18) - (6.22)), that

$$M_A^{m/n}(y_0) = 0 \quad \text{for } n \neq 1 . \tag{6.75}$$

We can therefore approximate the periodic part of the subharmonic Melnikov function of (f8) for m large enough by

$$M_{Af8}^m(y_0) \sim D_{f8} \cos(\omega y_0) , \tag{6.76}$$

and therefore

$$M_{Af8}^m(y_0) = 0 \quad \text{for } y_0 \sim \pi(2n+1)/\omega , \tag{6.77}$$

and equivalently for (2s)

$$M_{A2s}^m(y_0) \sim D_{2s} \cos(\omega y_0) \sin(\omega F) ,$$
$$M_{A2s}^m(\omega = j\omega_c, y_0) = 0 \quad \text{for } y_0 \sim 2\pi n/\omega \tag{6.78}$$

$$\text{or} \quad \omega_c = 2\pi/F,$$

where j, $n = 0$, 1, 2, ..., and D_{f8}, D_{2s} and F are functions of a, b, r_s, and m. According to theorem 6.3 and corollary 6.4 a critical ratio α_c/δ_c can mow be defined just as in the case of the KdV equation ((6.31) - (6.34)):

$$(\alpha_c/\delta_c)_{f8} = R^m{}_{f8}(\omega) = M_{Df8}{}^m/D_{f8} .$$

$$(\alpha_c/\delta_c)_{2s} = R^m{}_{2s}(\omega) = M_{D2s}{}^m/(D_{2s}\sin(\omega F)) .$$

$$(6.79)$$

The dissipation parts $M_{Df8}{}^m$ and $M_{D2s}{}^m$ can be evaluated via [64], (p.219,#362.25 and repeated use of #336.02, p.201) after substituting the derivative of the solution (5.16).

$$M^m{}_D = \int_0^{mT} v^2(y)\ dy$$

$$= Q_s(r_c - r_d)^2\{\Pi C_P/(\alpha_s{}^2 c_1) + E C_E/c_1 + K C_K/\alpha_s{}^2\}/(6c_o{}^2 c_1) ,$$

$$(6.80)$$

K, E, Π = complete elliptic integrals of first, second, and
      third kind

$$C_P = 3c_3{}^3 - 8c_3c_2 - 24c_o{}^2 c_1{}^2 k^2$$

$$C_E = 3c_3{}^2 - 8c_oc_1c_2$$

$$C_K = 3c_3{}^2 - 8c_oc_1c_2 - 2c_oc_1c_3 k^2$$

$$c_o = \alpha_s{}^2 - 1$$

$$c_1 = \alpha_s{}^2 - k^2$$

$$c_2 = 3k^2 - \alpha_s{}^2 - \alpha_s{}^2 k^2$$

$$c_3 = -3k^2 + 2\alpha_s{}^2 + 2\alpha_s{}^2 k^2 - \alpha_s{}^4$$

$$Q_s = \sqrt{[(r_4 - r_2)(r_3 - r_1)a/(24b)]},$$

$$\alpha_s{}^2 = (r_b - r_c)/(r_b - r_d),$$

$$k^2 = (r_b - r_c)(r_a - r_c)/((r_4 - r_2)(r_3 - r_1))$$

$$= \alpha_s^2 (r_a - r_d)/(r_a - r_c) = \text{elliptic modulus squared} .$$

r_a, r_1, etc. are the polynomial roots defined in connection with the solution (5.16).

As opposed to the periodic solutions enclosed by the homoclinic orbits, the periodic solutions (5.22) enclosed by the heteroclinic orbits lead to a subharmonic Melnikov integral whose periodic part can be evaluated in closed form. Setting the subharmonic boundaries 0 and mT in (6.36) and substituting (5.22) the subharmonic counterparts to (6.67), (6.68) and (6.69) become

$$M^m{}_{hD} = r_3 r_4 \sqrt{[-a/6b]} \int_0^{mT} cn^2\{(y-y_o)r_4\sqrt{[-a/6b]}\}\ dn^2\{(y-y_o)r_4\sqrt{[-a/6b]}\}\ dy$$

$$= 2(E - (1-k^2)/(1+k^2)\ K)/(ak(1+k^2)), \tag{6.81}$$

$$M^m{}_h\alpha = r_3 \int_0^{mT} cos(\omega y)\ sn((y-y_o)r_4\sqrt{[-a/6b]})\ dy$$

$$= 2r_3\omega\pi\sqrt{[-6b/a]}/r_4\ csch(\pi mK'/2K)\ cos(\omega y_o)\ , \tag{6.82}$$

$$R^m{}_h = \sqrt{[-6ab]}\ \pi\omega r_3 k(1+k^2)\ csch(\pi mK'/2K)/(r_4(E-(1-k^2)K/(1+k^2))), \tag{6.83}$$

K = first complete elliptic integral,

K' = associated first complete elliptic integral,

E = second complete elliptic integral,

$k = k(m)$ = elliptic modulus with

$$\lim_{m \to \infty} k = 1 \ .$$

The integral in (6.81) can be found in [64] (p.212, #361.03). As for the KdV case in section 6.3, (6.82) is evaluated by Fourier expanding sn (Byrd and Friedman, [64], p.304, #908.01) and observing orthogonality of circular functions. The following limits are easily verified:

$$\lim_{k \to 1, m \to \infty} M^m_A = 2M_{Ah}, \qquad \lim_{k \to 1, m \to \infty} M^m_D = 2M_{Dh}. \qquad (6.84)$$

The factor 2 accounts for the fact that M^m_A and M^m_D approach the sum of the respective Melnikov functions M_{Ah} and M_{Dh} of the *two* (i.e. upper *and* lower) heteroclinic orbits.

6.8 Consequences of the vanishing $M_{A2s\pm}$

As can be seen from (6.48), $M_{A2s\pm}$ vanishes for all y_0 if the perturbation frequency assumes multiples of a certain critical value ω_c. This behaviour is also illustrated in figures 11 and 12. Moreover, figure 11 in particular exhibits a rapid decline of the amplitude of $|M_{A2s\pm}|$ with increasing perturbation frequency ω. It is evident that this periodic part of the Melnikov integral is responsible for the transversal intersections and quadratic zeroes of the invariant manifolds required in theorem 6.1 and corollary 6.2. Since the result (6.48) is confirmed in section 8 by numerically generated Poincare maps of invariant manifolds, it therefore means the

absence of these intersections and tangencies, and the Smale-Birkhoff Homoclinic Theorem becomes inapplicable at the critical perturbation frequencies ω_c and for all practical purposes at higher perturbation frequencies as well. As a consequence, horseshoes and hyperbolic invariant sets with the related chaotic behaviour are nonexistent, which has been verified numerically (see section 8).

a)
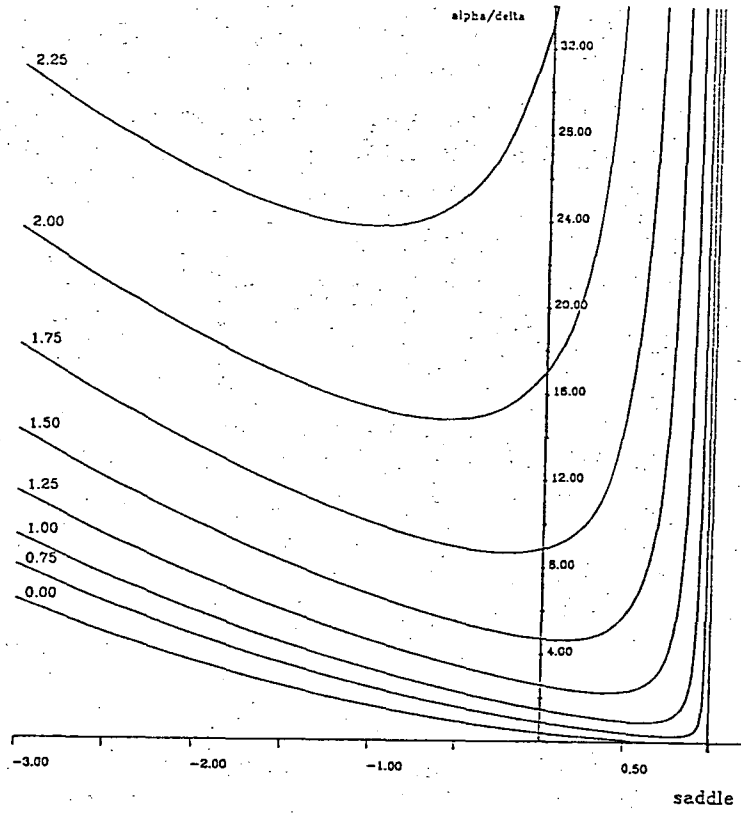
b)
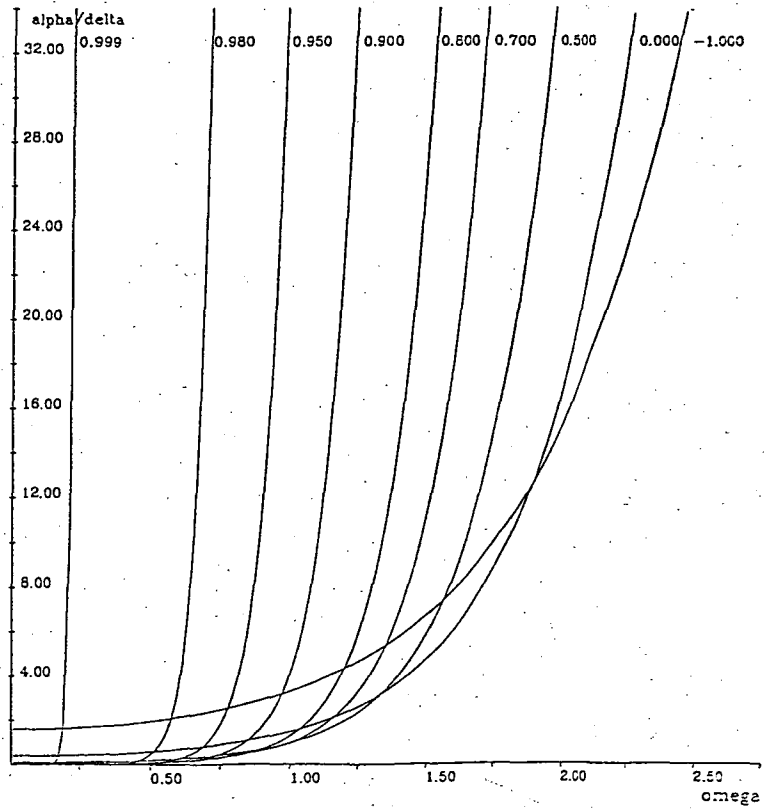
Figure 7. Bifurcation curves for KdV evaluated at a=b=1.

(a) Homoclinic curves (eq. 6.29) α_c/δ_c vs. saddle position for various

perturbation frequencies ω.

(b) as figure 7a, but α_c/δ_c vs. ω for various saddle positions.

c)

d)
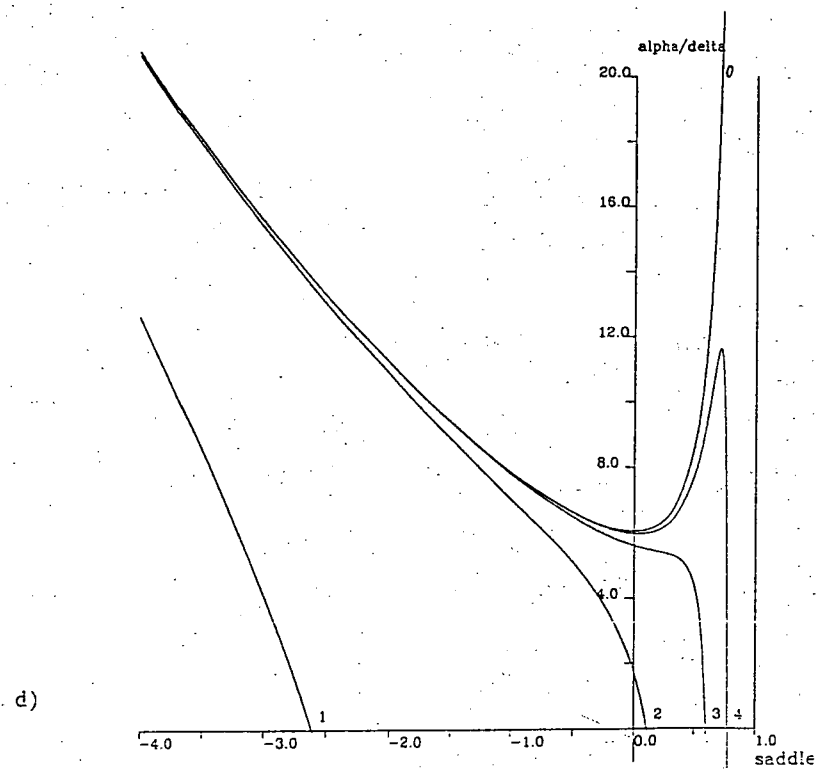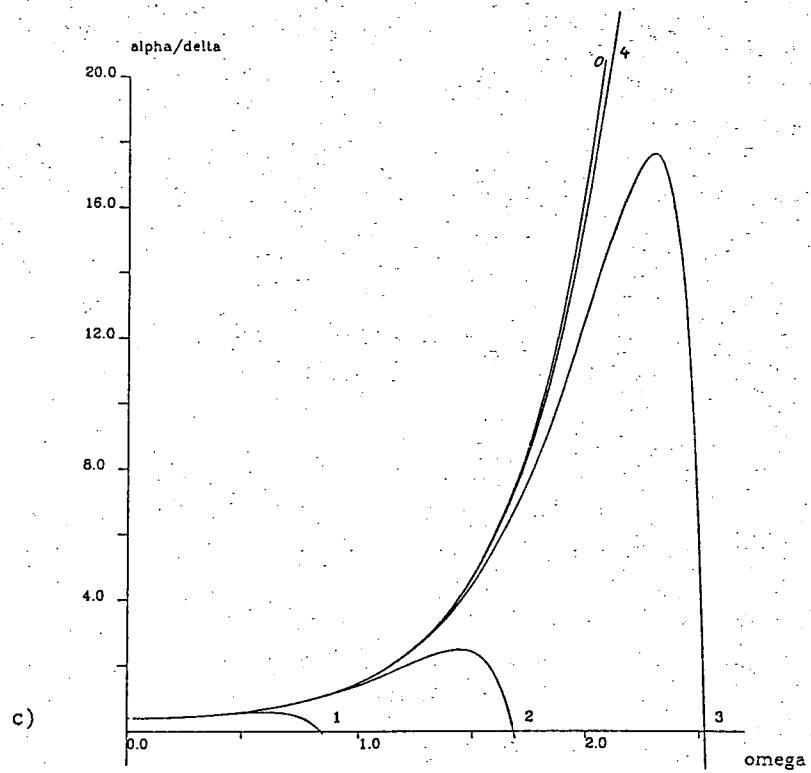
(c) Subharmonic curves (eq. 6.33) of orders as indicated and their homoclinic limit (label: 0) in α_c/δ_c vs. ω with saddle at $u=0.0$. The fourth order curve has a peak of $\alpha_c/\delta_c \sim 160$.

(d) as figure 7c, but α_c/δ_c vs. saddle position with $\omega = 1.6$.
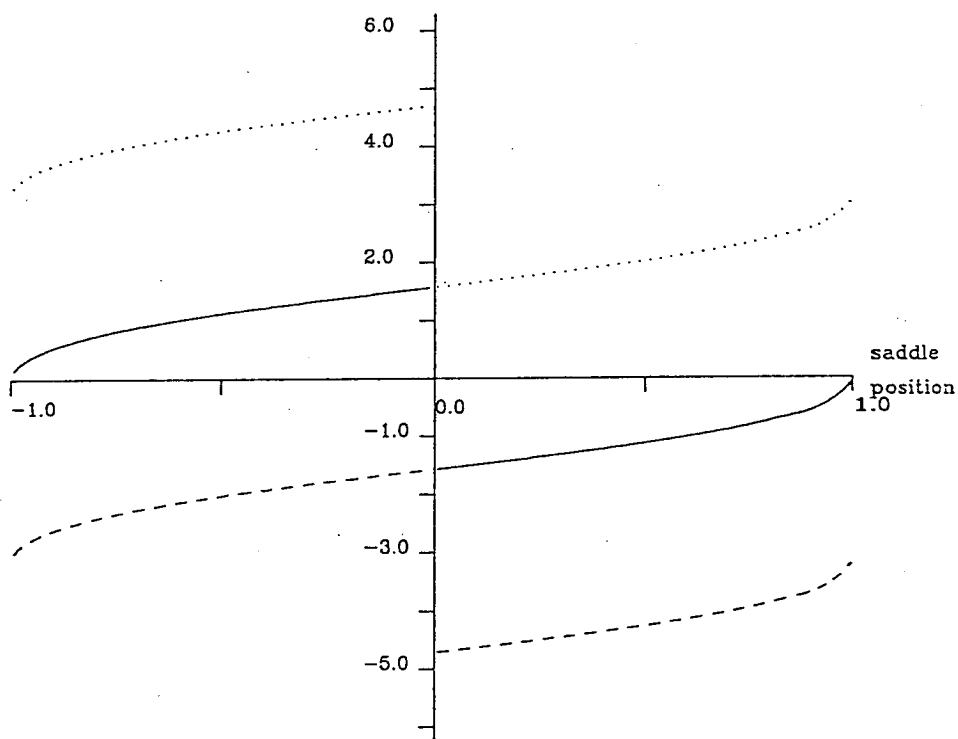
Figure 8. Three branches of the function $\tan^{-1}(-\sqrt{[C]}/2r_s)$ vs. the saddle position r_s, represented by pairs of dotted, solid, and dashed lines. See (5.12) for the form of C. The significance of the jump discontinuity is explained by (6.44).
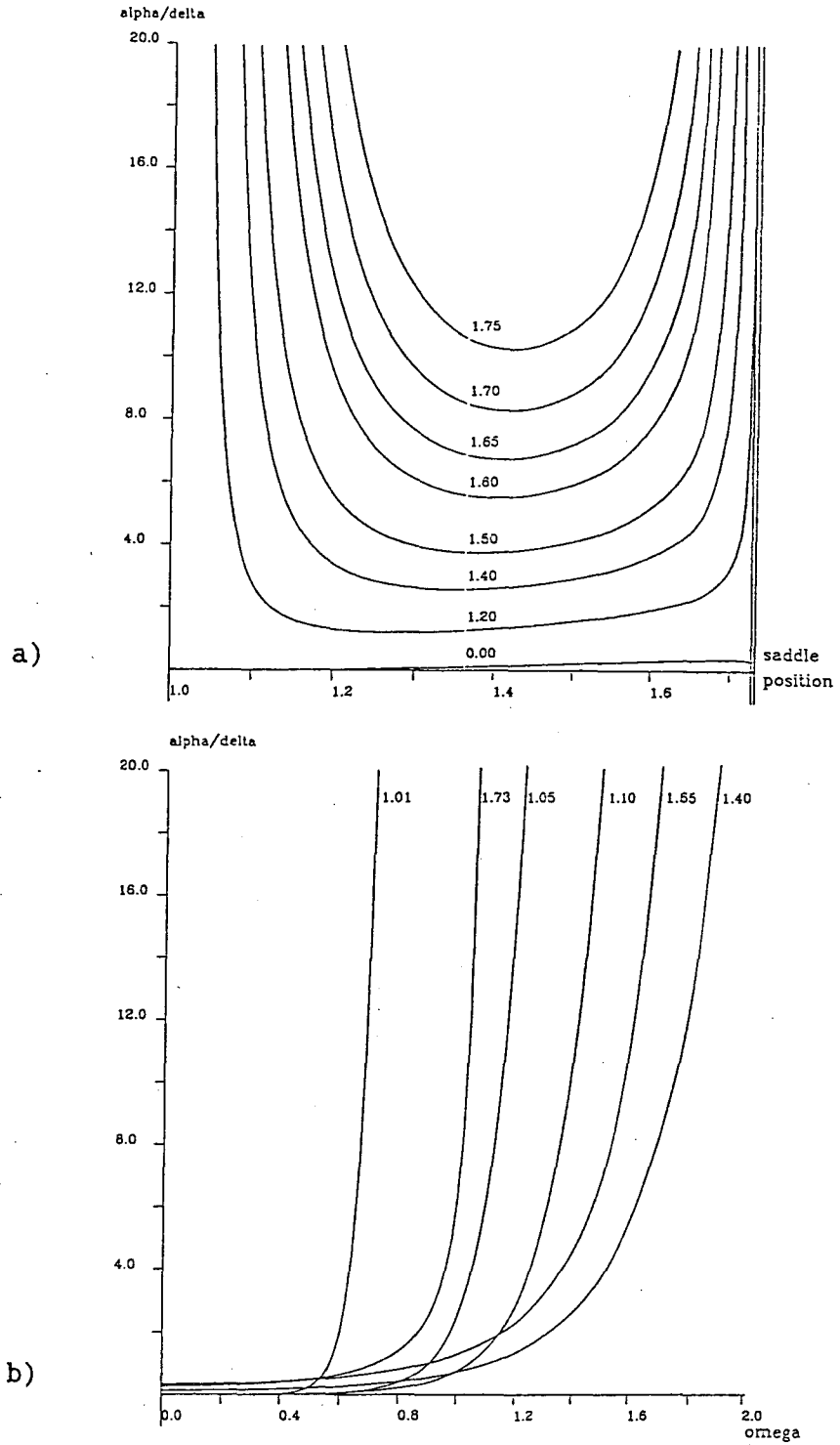
Figure 9. Bifurcation curves for the MKdV case in (2s) mode defined by (6.50) and evaluated at a=b=-1. (a) α_c/δ_c vs. saddle position for various perturbation frequencies ω. (b) α_c/δ_c vs. ω for various saddle positions.
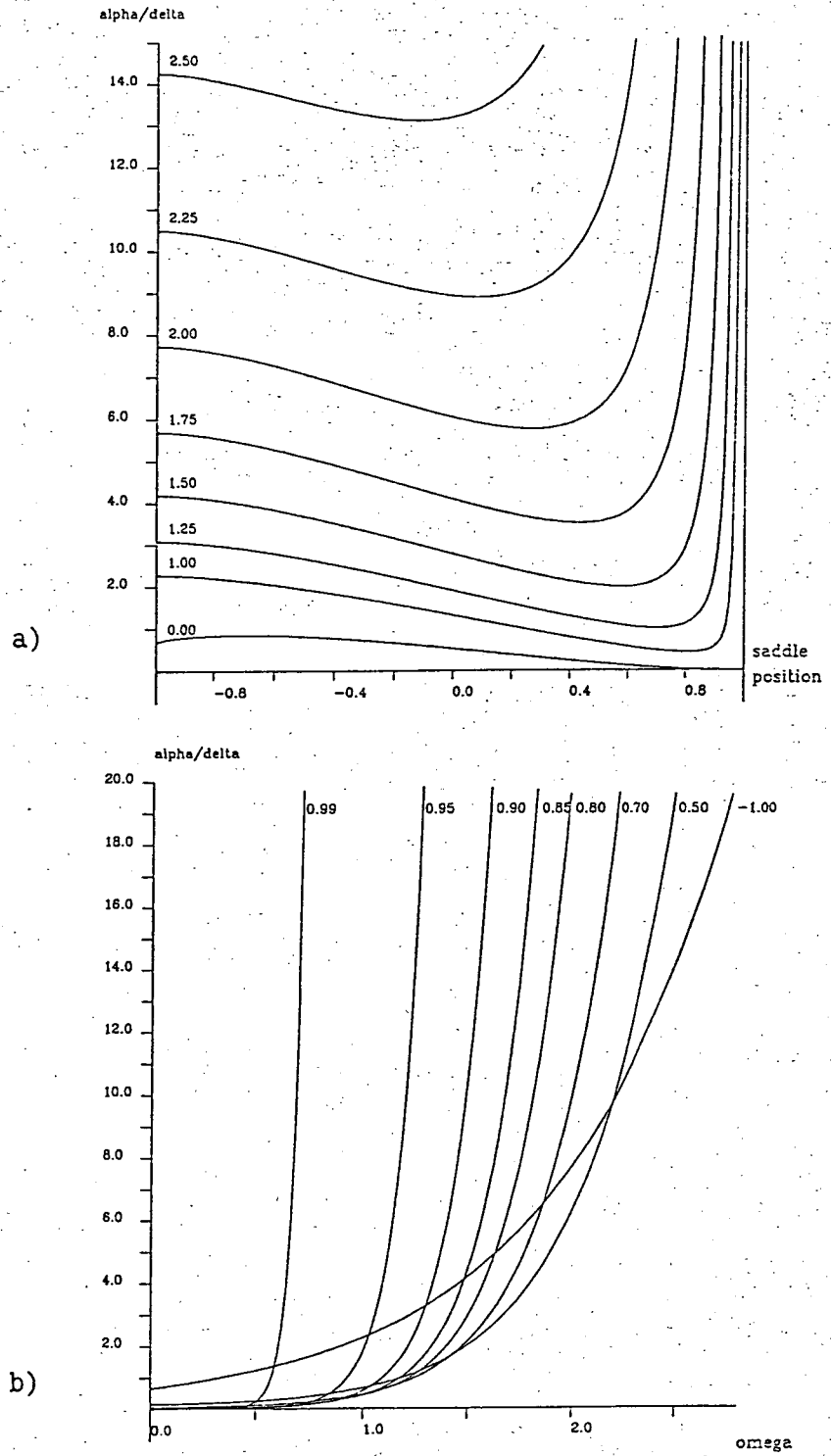
Figure 10. Bifurcation curves for the MKdV case in (f8) mode defined by (6.51) and evaluated at a=-1, b=1. (a) α_c/δ_c vs. saddle position for various perturbation frequencies ω. (b) α_c/δ_c vs. ω for various saddle positions.

a)

b)
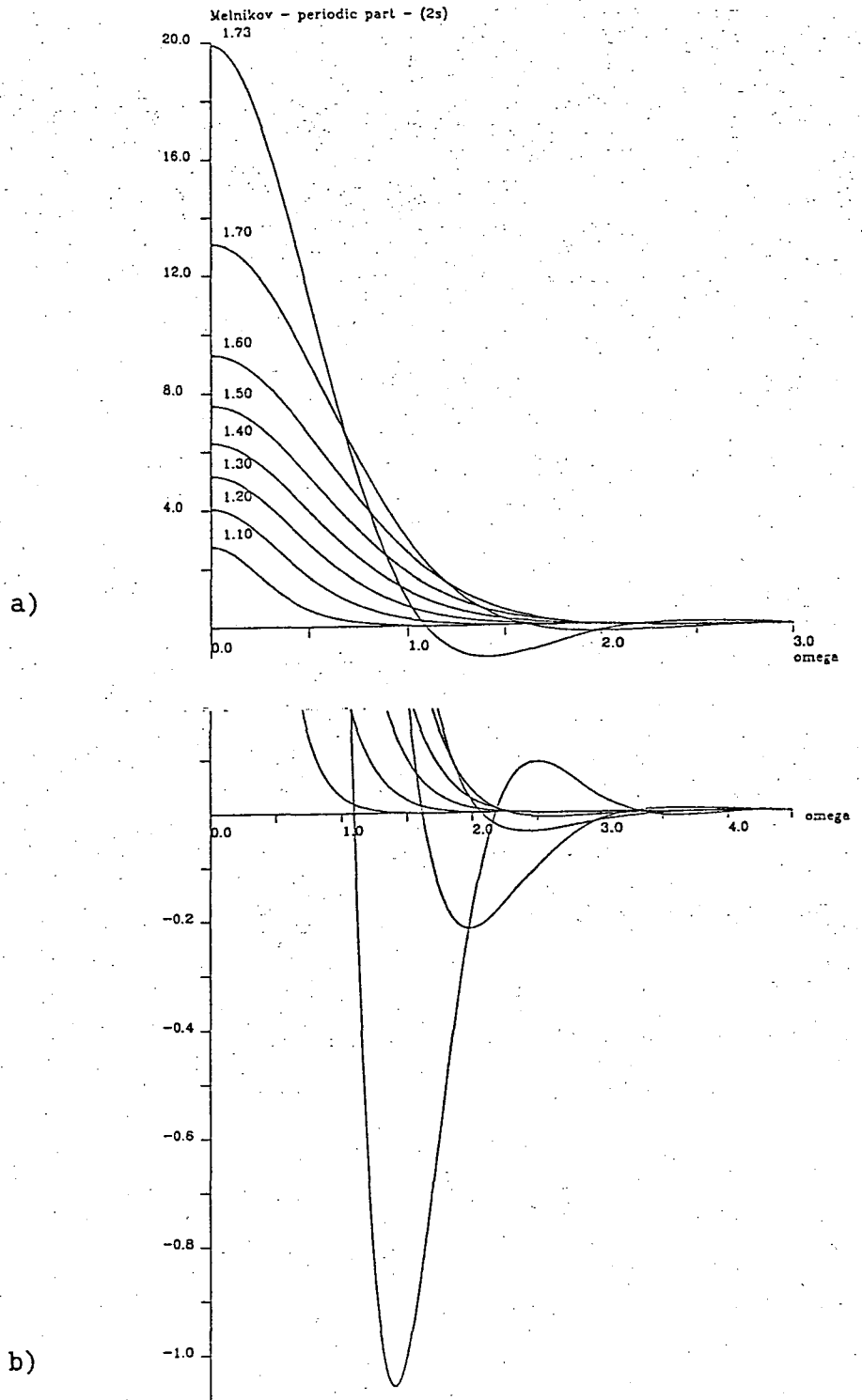
Figure 11.   Periodic perturbation contribution to the Melnikov function for the MKdV case in (2s) mode as given by (6.48) and evaluated for a=-1, b=1.   (a) Melnikov function vs. perturbation frequency ω for various saddle positions. (b) Magnification of (a) for small and negative values of the Melnikov function. Note the virtual disappearance of the function for values of ω ≥ 4.

97
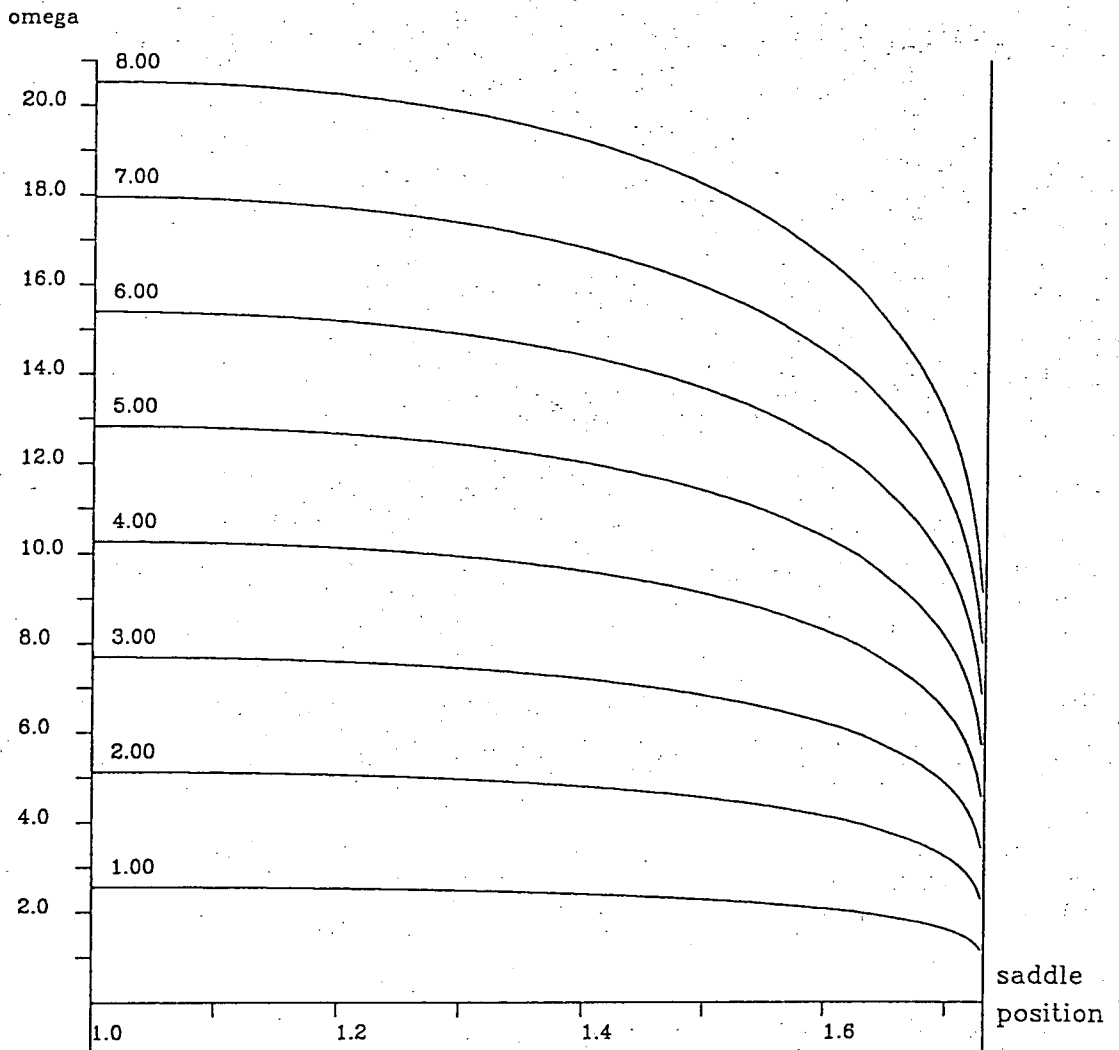
Figure 12. Zeroes of the Melnikov function for figure 11 graphed in the saddle position-ω plane.

7. Subharmonics and resonance

To study the effect of perturbations on the periodic solutions enclosed by the homoclinic or heteroclinic orbits we first discuss a method of power expansion of perturbations for determining the average flow of the Poincare map. This method is originally due to Melnikov [36] and was further adapted by Greenspan and Holmes [28]. In the present context we extend the expansion in [28] to some higher order terms as they reveal period doubling.

7.1   Structure of the subharmonic Poincare map

Our analysis follows closely Greenspan and Holmes [28], but is extended to higher orders. To take advantage of the periodicity of the unperturbed solutions considered, it is advisable to introduce the action angle variables I and θ. We begin with their definition:

$$I(u,v) = \int_0^{T_k} v \, du = \text{const.}, \quad \theta(u,v) = \Omega(I)t .\tag{7.1}$$

Here, $\Omega(I)$ is constant with respect to time and is an angular velocity defined by

$$\Omega(I) = 2\pi/T_k .\tag{7.2}$$

u and v are the dependent variables of the original system (6.2) which reduces without perturbation to

$$u^o{}_t = f_1(u^o, v^o)$$
$$v^o{}_t = f_2(u^o, v^o)\tag{7.3}$$

with T_k as period of the solution (u°, v°). The system (7.3) can now be rewritten in terms of unperturbed action angle variables θ°, I° as

$$\theta^\circ_t = \mathcal{Q}(I^\circ) = \partial\theta^\circ/\partial u^\circ \; f_1(u^\circ,v^\circ) + \partial\theta^\circ/\partial v^\circ \; f_2(u^\circ,v^\circ) = \partial H/\partial I^\circ$$

$$I^\circ_t = \partial I^\circ/\partial u^\circ \; f_1(u^\circ,v^\circ) + \partial I^\circ/\partial v^\circ \; f_2(u^\circ,v^\circ) = -\partial H/\partial\theta^\circ = 0, \tag{7.4}$$

with H as the Hamiltonian of the unperturbed system. Also observe:

$$\partial I^\circ/\partial u^\circ = (\partial I^\circ/\partial H)(\partial H/\partial u^\circ) = -f_2/\mathcal{Q}(I^\circ)$$

$$\partial I^\circ/\partial v^\circ = (\partial I^\circ/\partial H)(\partial H/\partial v^\circ) = f_1/\mathcal{Q}(I^\circ). \tag{7.5}$$

Introducing a perturbation ($\varepsilon \neq 0$), (7.4) extends to

$$\theta^E_t = \partial\theta^E/\partial u \; (f_1(u,v)+\varepsilon g_1(u,v,t)) + \partial\theta^E/\partial v \; (f_2(u,v)+\varepsilon g_2(u,v,t))$$

$$I^E_t = \partial I^E/\partial u \; (f_1(u,v)+\varepsilon g_1(u,v,t)) + \partial I^E/\partial v \; (f_2(u,v)+\varepsilon g_2(u,v,t)). \tag{7.6}$$

With the definitions

$$\mathcal{Q}(I^E) \equiv \partial\theta^E/\partial u \; f_1(u,v) + \partial\theta^E/\partial v \; f_2(u,v) \; ,$$

$$F(I^E,\theta^E,t) \equiv \partial I^E/\partial u \; g_1(u,v,t) + \partial I^E/\partial v \; g_2(u,v,t) \; , \tag{7.7}$$

$$G(I^E,\theta^E,t) \equiv \partial\theta^E/\partial u \; g_1(u,v,t) + \partial\theta^E/\partial v \; g_2(u,v,t)$$

we can express the system (7.6) as

$$\theta^E_t = \varepsilon G(I^E,\theta^E,t) + \mathcal{Q}(I^E)$$

$$I^E_t = \varepsilon F(I^E,\theta^E,t) \; . \tag{7.8}$$

We now split the perturbed solutions θ_E, I_E of (7.8) into unperturbed solutions $\mathcal{Q}(I^\circ)t$, I° with perturbation contributions φ, h with a coefficient $\sqrt{\varepsilon}$, measuring the size of perturbation:

$$\theta^E = \mathcal{Q}(I^\circ)t + \varphi \; ,$$

$$I^E = I^\circ + \sqrt{\varepsilon}\, h \; , \tag{7.9}$$

and observe that $I^o{}_t = 0$. The system (7.8) now becomes

$$\Omega(I^o) + \varphi_t = \varepsilon \, G(I^o + \sqrt{\varepsilon}\, h, \ \Omega(I^o)t + \varphi, \ t) + \Omega(I^o + \sqrt{\varepsilon}\, h) \ ,$$

$$\sqrt{\varepsilon}\, h_t = \varepsilon \, F(I^o + \sqrt{\varepsilon}\, h, \ \Omega(I^o)t + \varphi, \ t) \ . \tag{7.10}$$

A Taylor expansion about I^o w.r.t. I^E up to $O(\varepsilon^2)$, reduces (7.10) to

$$\varphi_t = \varepsilon^{1/2}\, \Omega^{o\prime}\, h + \varepsilon[\Omega^{o\prime\prime}\, h^2/2 + G^o] + \varepsilon^{3/2}[\Omega^{o\prime\prime\prime}\, h^3/6 + G^{o\prime}\, h]$$

$$+ \ \varepsilon^2[\Omega^{o\prime\prime\prime\prime}\, h^4/24 + G^{o\prime\prime}\, h^2/2] \ , \tag{7.11}$$

$$h_t = \varepsilon^{1/2}\, F^o + \varepsilon\, F^{o\prime}\, h + \varepsilon^{3/2}\, F^{o\prime\prime}\, h^2/2 + \varepsilon^2\, F^{o\prime\prime\prime}\, h^3/6 \ ,$$

with the following technical abbreviations:

$$G^o \equiv G(I^o, \ \Omega(I^o)t + \varphi, \ t), \qquad F^o \equiv F(I^o, \ \Omega(I^o)t + \varphi, \ t),$$

$$\Omega^o \equiv \Omega(I^o), \quad A' \equiv \partial A/\partial I^E(I^o), \quad A'' \equiv \partial^2 A/\partial I^{E2}(I^o), \quad \text{etc.} \tag{7.12}$$

The system (7.11) in conjunction with averaging methods according to the averaging theorem as stated by Guckenheimer and Holmes [29] is our central device for the analysis of the Poincare maps of periodic solutions under perturbation. The averaging theorem describes the approximation of a nonautonomous periodic system by this system averaged over its period plus a small periodic perturbation. As a result, fixed points in the averaged system correspond to small periodic motions in the original system. The application of this theorem will require the evaluation of the coefficients in (7.11), such as F^o, G^o, Ω^o, and their derivatives, as defined by (7.7) and (7.12). This evaluation, on the other hand, depends on the specific original system, that is, the reduced KdV or MKdV system in our case. In its lowest order (i.e. $O(\sqrt{\varepsilon})$) truncation, however, we can perform a qualitative analysis of the system (7.11) without reference to a

101

specific case.   We begin by expanding F° under use of (7.7) and the relations (7.4):

$$F^\circ = F(I^\circ, \Omega^\circ t + \varphi, t)$$

$$= \partial I^\circ/\partial u^\circ \; g_1(u^\circ, v^\circ, t) + \partial I^\circ/\partial v^\circ \; g_2(u^\circ, v^\circ, t)$$

$$= (f(u^\circ, v^\circ) \wedge g(u^\circ, v^\circ, t))/\Omega^\circ \; . \qquad (7.13)$$

Here $\wedge$ defines the wedge product: $f \wedge g = f_1 g_2 - f_2 g_1$.   Since

$$u^\circ = u^\circ(t + \varphi/\Omega^\circ), \quad v^\circ = v^\circ(t + \varphi/\Omega^\circ) \; , \qquad (7.14)$$

we introduce the shift

$$t + \varphi/\Omega^\circ \; \rightarrow \; t \qquad (7.15)$$

and rewrite F° as

$$F^\circ = F(I^\circ, \Omega^\circ t, t - \varphi/\Omega^\circ)$$

$$= \{f(u^\circ(t), v^\circ(t)) \wedge g(u^\circ(t), v^\circ(t), t - \varphi/\Omega^\circ)\}/\Omega^\circ. \qquad (7.16)$$

Truncating (7.11) after the $O(\sqrt{\varepsilon})$-term and, according to the averaging theorem, using the transformation:

$$h \rightarrow \overline{h} + \varepsilon^{1/2} V \; , \qquad \varphi \rightarrow \overline{\varphi} \; , \qquad (7.17)$$

$$V = \int F^\sim(\varphi, t) dt \; , \qquad F^\sim(\varphi, t) = \overline{F^\circ} - F^\circ \; ,$$

one gets the system

$$\overline{\varphi}_t = \sqrt{\varepsilon} \; \Omega^{\circ\prime}(\overline{h} + \sqrt{\varepsilon} \; V)$$

$$\overline{h}_t = \sqrt{\varepsilon}/\Omega^\circ \; F(I^\circ, \Omega^\circ t, t - \overline{\varphi}/\Omega^\circ) \; . \qquad (7.18)$$

We average the system (7.18) over the period $mT = T^k$ and note that $\tilde{F}$ = 0 and therefore V = 0. The resulting system

$$\overline{\varphi}_t = \sqrt{\varepsilon}\ \Omega^{o\prime}\ \overline{h}$$

(7.19)

$$\overline{h}_t = \sqrt{\varepsilon}/(mT\Omega^o) \int_0^{mT} F(I^o,\ \Omega^o t,\ t - \overline{\varphi}/\Omega^o)\ dt$$

$$= \sqrt{\varepsilon}/2\pi\ M^m(\overline{\varphi}/\Omega^o)$$

is autonomous and approximates the flow of the Poincare map up to $O(\sqrt{\varepsilon})$. Moreover, $mT\Omega_o=2\pi$, according to $mT=T^k$ and (7.2). The definition of the subharmonic Melnikov integral $M^m(\varphi/\Omega^o)$ is evident by (7.16) and can be expressed by its periodic and dissipative part:

$$M^m(\varphi/\Omega^o) = \alpha\ \cos(\varphi\omega/\Omega^o)\ M^m{}_A - \delta\ M^m{}_D\ .$$

(7.20)

The fixed points $(\varphi_s,\ h_s)$ of the system (7.19) are now

$$h_s = 0\ ,$$

$$\varphi_s = 2\pi n\Omega^o/\omega \pm \arccos(\delta M^m{}_D/(\alpha M^m{}_A)),\quad n = 0,\ 1,\ 2,\ \ldots\ ,$$

$$\alpha/\delta > R^m(\omega)\ ,$$

(7.21)

with the integer n accounting for the multiplicity of branches of arcos and $R^m(\omega)$ being the critical ratio for bifurcation as defined in (6.34). (7.19) linearizes about the fixed points to

$$\begin{bmatrix} \overline{\varphi}_t \\ \overline{h}_t \end{bmatrix} = \sqrt{\varepsilon} \begin{bmatrix} 0 & \Omega^{o\prime} \\ -\alpha/(\pi\Omega^o)\ M^m{}_A\ \sin(\varphi_s\omega/\Omega^o) & 0 \end{bmatrix} \begin{bmatrix} \overline{\varphi} \\ \overline{h} \end{bmatrix}$$

(7.22)

with the eigenvalues

$$\lambda^2 = -\ \varepsilon\alpha\omega\Omega^{o\prime}/(\pi\Omega^o)\ M^m{}_A\ \sin(\varphi_s\omega/\Omega^o)\ .$$

(7.23)

For the fixed points in (7.21) this produces for $0 \leqslant \overline{\varphi}/\Omega^\circ \leqslant mT=T_k$, m saddles $(\sin(\varphi_s\omega/\Omega^\circ)<0, +\cos^{-1}(\delta M^m{}_D/(\alpha M^m{}_A))$ in (7.21)) and m centres $(\sin(\varphi_s\omega/\Omega^\circ)>0, -\cos^{-1}(\delta M^m{}_D/(\alpha M^m{}_A))$ in (7.21)). These sinks and centres are created by a doubly degenerate Hamiltonian bifurcation at $\alpha/\delta=R^m(\omega)$ or $\sin(\varphi_s\omega/\Omega^\circ)=0$ and $\cos^{-1}(\delta M^m{}_D/(\alpha M^m{}_A))=0$ respectively. According to theorem 6.3, they correspond to a subharmonic orbit of period $mT=T_k$. Moreover, the system (7.19) has the Hamiltonian

$$H = \sqrt{\varepsilon} \left\{ \Omega^\circ{}'\overline{h}^2/2 - \int M^m(\overline{\varphi}/\Omega^\circ) \, d\overline{\varphi}/(2\pi) \right\}$$

(7.24)

$$= \sqrt{\varepsilon} \left\{ \Omega^\circ{}'\overline{h}^2/2 - \sin(\overline{\varphi}\omega/\Omega^\circ) \, \alpha\Omega^\circ/(2\pi\omega) \, M^m{}_A - \delta\overline{\varphi}/(2\pi) \, M^m{}_D + K \right\},$$

with K as integration constant. However, the system (7.19) is structurally unstable and therefore unrealistic. Note, however, that the Hamiltonian (7.24) can be used to make an $O(\sqrt{\varepsilon})$ estimate of the width of the m-th order resonance band. This width is equal to the maximal vertical diameter of the homoclinic orbit of the system (7.19). Observe that for K=0 the Hamiltonian (7.24) vanishes on this homoclinic orbit. We therefore obtain its maximal vertical diameter by setting K=H=0 in (7.24) and solving for 2h (= vertical coordinate), being the width $\Delta I(m)$ to $O(\sqrt{\varepsilon})$ accuracy of the m-th resonance band:

$$\Delta I(m) = 2\overline{h} = \sqrt{\varepsilon} \, 2(\sin(\varphi_{so}\omega/\Omega^\circ) \, \alpha\Omega^\circ/\omega \, M^m{}_A + \delta\varphi_{so} \, M^m{}_D)/(\pi\Omega^\circ{}'),$$

(7.24')

with $\varphi_{so} = -\cos^{-1}(\delta M^m{}_D/(\alpha M^m{}_A))$,

denoting a center position. In order to improve on the structural instability we apply the averaging theorem over the full system (7.11). Again employing the transformation (7.17) (without introducing a double overbar), the system becomes

104

$$\overline{\varphi}_t = \varepsilon^{1/2}\, Q_0'\, \overline{h} + \varepsilon[Q_0'V + Q_0''\,\overline{h}^2/2 + G_0]$$

$$+ \varepsilon^{3/2}\,[Q_0''V\,\overline{h} + Q_0'''\,\overline{h}^3/6 + G_0'h]$$

$$+ \varepsilon^2[Q_0''V^2/2 + Q_0'''V\,\overline{h}^2/3 + G_0'V + Q_0''''\,\overline{h}^4/24 + G_0''\,\overline{h}^2/2]$$

$$\overline{h}_t = \varepsilon^{1/2}\, F_0 + \varepsilon\, F_0'\overline{h} + \varepsilon^{3/2}\,[F_0'V + F_0''\,\overline{h}^2/2]$$

$$+ \varepsilon^2[F_0''V\,\overline{h} + F_0'''\,\overline{h}^3/6] \ . \tag{7.25}$$

Averaging over the system (7.25) (and dropping the overbars on φ, h) gives

$$\varphi_t = \varepsilon^{1/2}\, Q_0'\, h + \varepsilon[Q_0'''\, h^2/2 + \overline{G_0}] + \varepsilon^{3/2}\,[Q_0'''\, h^3/6 + \overline{G_0'}h]$$

$$+ \varepsilon^2[Q_0''\,\overline{V^2}/2 + \overline{G_0'V} + Q_0''''\, h^4/24 + \overline{G_0''}\, h^2/2] \tag{7.26}$$

$$h_t = \varepsilon^{1/2}\,\overline{F_0} + \varepsilon\overline{F_0'}\, h + \varepsilon^{3/2}\,[\overline{F_0'V} + \overline{F_0''}\, h^2/2]$$

$$+ \varepsilon^2[\overline{F_0''V}\, h + \overline{F_0'''}\, h^3/6] \ .$$

As the contributions of the $O(\varepsilon)$-, $O(\varepsilon 3/2)$-, and $O(\varepsilon^2)$ terms are small, the fixed points (φ_s, h_s) of the system (7.26) will be close to those defined in (7.21). The linearization of (7.26) about these fixed points is

$$\begin{bmatrix} \varphi_t \\ h_t \end{bmatrix} = \begin{bmatrix} a_{11} & a_{12} \\ a_{21} & a_{22} \end{bmatrix} \begin{bmatrix} \varphi \\ h \end{bmatrix}, \tag{7.27}$$

$$a_{11} = \varepsilon\overline{G_0}_f + \varepsilon^{3/2}\overline{G_0'}_f h_s + \varepsilon^2[(\overline{G_0'V})_f + \overline{G_0''}_f h_s^2/2$$

$$a_{21} = \varepsilon^{1/2}\overline{F_0}_f + \varepsilon\overline{F_0'}_f h_s + \varepsilon^{3/2}[\overline{F_0'V}_f + \overline{F_0''}_f h_s^2/2]$$

$$+ \varepsilon^2[(\overline{F_0''V})_f + \overline{F_0'''}_f h_s^3/6]$$

$$a_{12} = \varepsilon Q_0''\, h_s + \varepsilon^{3/2}\,[Q_0'''\, h_s^2/2 + \overline{G_0'}]$$

$$+ \varepsilon^2[Q_0'''''\, h_s^3/6 + \overline{G_0''}\, h_s]$$

$$a_{22} = \varepsilon\overline{F_0'} + \varepsilon 3/2\, \overline{F_0''}\, h_s + \varepsilon^2[\overline{F_0''V} + \overline{F_0'''}\, h_s^2/2] \ ,$$

$$A_f \equiv \partial A/\partial\varphi(\varphi_s) \ .$$

The actual stability type of the fixed points which appear as centres in the $O(\sqrt{\varepsilon})$-analysis is determined by the divergence of the vector field defined by (7.26) and evaluated at (φ_s, h_s). This is the trace of the matrix in (7.27):

$$\text{div}(\varphi_t(\varphi_s, h_s), h_t(\varphi_s, h_s)) = a_{11} + a_{22} . \qquad (7.28)$$

It is therefore necessary to determine $\overline{G\circ}_f$, $(\overline{G\circ'V})_f$, $\overline{F\circ'}$, $\overline{F\circ''V}$. The other terms in a_{11} and a_{22} can be ignored as $h_s = 0$.

We begin with $F\circ'$ which is, according to the definition (7.7) and the shift (7.15), before averaging

$$F\circ' = F'(I\circ, \Omega\circ t, t - \varphi/\Omega\circ)$$

$$= \partial/\partial I \ (f(u\circ(t), v\circ(t)) \wedge g(u\circ(t), v\circ(t), t - \varphi/\Omega\circ))/\Omega\circ$$

$$= (f' \wedge g + f \wedge g')/\Omega\circ - f \wedge g \ \Omega\circ'/\Omega\circ^2 . \qquad (7.29)$$

Averaging over the period mT gives

$$\overline{F\circ'} = 1/(mT\Omega\circ) \ \{\int_0^{mT} f' \wedge g \ dt + \int_0^{mT} f \wedge g' \ dt\} - M^m(\varphi/\Omega\circ)\Omega\circ'/\Omega\circ^2 . \qquad (7.30)$$

For f' we note $I \sim I\circ$ and therefore

$$f' = \partial f/\partial u\circ \ \partial u\circ/\partial I\circ + \partial f/\partial v\circ \ \partial v\circ/\partial I\circ . \qquad (7.31)$$

It is important to observe that

$$1/(\partial I\circ/\partial u\circ) \neq \partial u\circ/\partial I\circ , \quad 1/(\partial I\circ/\partial v\circ) \neq \partial v\circ/\partial I\circ , \qquad (7.32)$$

and therefore the inverses of (7.4) cannot be used at this point. $\partial u\circ/\partial I\circ$ is calculated from the differentials

$$dI^\circ = \partial I^\circ/\partial u^\circ\, du^\circ + \partial I^\circ/\partial v^\circ\, dv^\circ$$
$$d\theta^\circ = \partial\theta^\circ/\partial u^\circ\, du^\circ + \partial\theta^\circ/\partial v^\circ\, dv^\circ$$

(7.33)

Eliminating dv gives

$$\partial\theta^\circ/\partial v^\circ - \partial I^\circ/\partial v^\circ\, d\theta^\circ/dI^\circ = du^\circ/dI^\circ(\partial\theta^\circ/\partial v^\circ\, \partial I^\circ/\partial u^\circ - \partial\theta^\circ/\partial u^\circ\, \partial I^\circ/\partial v^\circ)$$

(7.34)

Since the action-angle variables θ° and I° are independent of each other we have

$$d\theta^\circ/dI^\circ = 0 ,$$

(7.35)

and therefore

$$du/dI = \partial u/\partial I + \partial u/\partial\theta\, \partial\theta/\partial I = \partial u/\partial I ,$$

(7.36)

$$\partial u^\circ/\partial I^\circ = (\partial\theta^\circ/\partial v^\circ)/(\partial\theta^\circ/\partial v^\circ\, \partial I^\circ/\partial u^\circ - \partial\theta^\circ/\partial u^\circ\, \partial I^\circ/\partial v^\circ) .$$

(7.37)

Recalling that by definition of the action angle variable θ°,

$$\partial\theta^\circ/\partial t = \varrho^\circ = \text{constant} ,$$

(7.38)

$\partial\theta^\circ/\partial u^\circ$ and $\partial\theta^\circ/\partial v^\circ$ therefore become

$$\partial\theta^\circ/\partial u^\circ = \partial\theta/\partial t\, \partial t/\partial u^\circ = \varrho^\circ/u^\circ_t = \varrho^\circ/f_1 ,$$

(7.39)

$$\partial\theta^\circ/\partial v^\circ = \partial\theta/\partial t\, \partial t/\partial v^\circ = \varrho^\circ/v^\circ_t = \varrho^\circ/f_2 ,$$

(7.40)

Substituting these and (7.4) into (7.37) gives

$$\partial u^\circ/\partial I^\circ = -\varrho^\circ/(2f_2) .$$

(7.41)

Eliminating du from the differentials leads by a similar procedure to

$$\partial v^\circ/\partial I^\circ = \varrho^\circ/(2f_1) .$$

(7.42)

f' as expressed by (7.31) finally becomes

$$f' = \partial f/\partial u^\circ \; (-\varrho^\circ/2f_2) + \partial f/\partial v^\circ \; (\varrho^\circ/2f_1)$$

$$= \varrho^\circ/2 \; (f_v/f_1 - f_u/f_2) \; , \tag{7.43}$$

Accordingly one determines for g'

$$g' = \varrho^\circ/2 \; (g_v/f_1 - g_u/f_2) \; . \tag{7.44}$$

With f' and g' the substitution of $\overline{F^{\circ\,\prime}}$ is now

$$\overline{F^{\circ\,\prime}} = 1/(2mT) \int\limits_0^{mT} ((f_{1v}/f_1 - f_{1u}/f_2)g_2 - (f_{2v}/f_1 - f_{2u}/f_2)g_1) \; dt$$

$$+ \; 1/(2mT) \int\limits_0^{mT} (g_{1u} + g_{2v} - f_1/f_2 \; g_{2u} - f_2/f_1 \; g_{1v}) \; dt$$

$$- \; M^m(\varphi/\varrho^\circ)\varrho^{\circ\,\prime}/\varrho^{\circ\,2} \; . \tag{7.45}$$

To calculate $\overline{G^\circ}_f$ we begin with the definition (7.7) expressed for $\varepsilon = 0$:

$$G(I^\circ,\theta^\circ,t) = \partial\theta^\circ/\partial u^\circ \; g_1(u^\circ,v^\circ,t) + \partial\theta^\circ/\partial v^\circ \; g_2(u^\circ,v^\circ,t) \; . \tag{7.46}$$

Substituting (7.39), (7.40), averaging over mT and taking the derivative w.r.t. φ° gives

$$\overline{G^\circ}_f = \partial\overline{G(I^\circ,\theta^\circ,t)}/\partial\varphi^\circ = \varrho^\circ/mT \int\limits_0^{mT} (\partial g_1/\partial\varphi^\circ \; 1/f_1 + \partial g_2/\partial\varphi^\circ \; 1/f_2) \; dt. \tag{7.47}$$

(7.45) and (7.47) are the two terms required for evaluation of the

108

divergence (7.28) up to $O(\varepsilon)$, as will be done specifically for the (M)KdV case in the next subsection.

7.1.1 Evaluation for (M)KdV

Below we list the nonzero terms required for the evaluation of $\overline{G^\circ}_f$, $\overline{F^\circ}'$ (and $(\overline{G^\circ V})_f$, $\overline{F^\circ{}''V}$ for later use) for the (M)KdV case. The derivatives (primed quantities) can be calculated via the expressions

$$x' = Q^\circ/2 \ (x_v/f_1 - x_u/f_2) \ , \tag{7.48}$$

$$x'' = Q^\circ/2 \ (x_v'/f_1 - x_v f_1'/f_1{}^2 - x_u'/f_2 + x_u f_2'/f_2{}^2)$$
$$+ \ Q^{\circ}{}'/2 \ (x_v/f_1 - x_u/f_2) \ , \tag{7.49}$$

which are generalizations of (7.43) or (7.44) and their second derivatives. In the expressions below n=1 applies to KdV and n=2 to MKdV

$$f_1 = u_y = v \ ,$$

$$f_2 = v_y = -u(a \ u^n/(n+1) + 1)/b - k_1/b \ ,$$

$$g_2 = - \delta \ v + \alpha \sin(\omega y) \ ,$$

$$f_{2u} = -(a \ u^n + 1)/b \ ,$$

$$f_{1v} = 1 \ ,$$

$$g_{2v} = - \delta \ ,$$

$$f_{2uu} = - na \ u^{(n-1)}/b \ ,$$

$$f_1' = Q^\circ/(2v) \ ,$$

$$f_2' = - Q^\circ/2 \ f_{2u}/f_2 \ ,$$

$$f_{2u}' = -Q^\circ/2 \ f_{2uu}/f_2 \ ,$$

$$f_1'' = Q^{\circ}{}'/(2v) - Q^{\circ 2}/(4v^3) \ ,$$

$$f_2'' = - Q^{\circ}{}'/2 \ f_{2u}/f_2 + Q^{\circ 2}/4 \ (f_{2uu}/f_2 - f_{2u}{}^2/f_2{}^3) \ ,$$

$$g_2' = - \delta \ f_1' \ ,$$

$$g_2{}'' = - \delta f_1{}'' \, ,$$

$$t \to y \qquad\qquad\qquad (7.50)$$

The average of $G°$ now becomes according to (7.46) with substitutions from (7.50) and (7.39), (7.40)

$$\overline{G°} = Q°/mT \; \{-\delta \int_0^{mT} \{v(y)/v_y(y)\}dy \; + \; \alpha \int_0^{mT} \{\sin \; \omega(y + \varphi/Q°)/v_y(y)\}dy\} \; . \qquad (7.51)$$

Note that the first integral vanishes due to periodicity of the integrand, as $v(y)$ and $v_y(y)$ are first and second derivative of the periodic cnoidal wave solution $u(y)$ for KdV given by (4.3) and for MKdV given by (5.16). (7.47) reduces to

$$\overline{G°}_f = (\alpha\omega/mT) \; \{-\sin(\omega\varphi°/Q°) \int_0^{mT} \sin(\omega y)/v_y(y) \; dy$$

$$+ \; \cos(\omega\varphi°/Q°) \int_0^{mT} \cos(\omega y)/v_y(y) \; dy\} \; . \qquad (7.52)$$

$\overline{F°'}$ reduces to

$$\overline{F°'} = - \, \delta \; - \; Q°'/Q°^2 \; M^m(\varphi/Q°)$$

$$+ \; \alpha/(2mT)\int_0^{mT} \{\sin\omega y \; \cos(\omega\varphi°/Q°) \; + \; \cos\omega y \; \sin(\omega\varphi°/Q°)\}/v(y) \; dy.$$

$$\qquad\qquad (7.53)$$

To determine the divergence (7.28) at the fixed points $\varphi_s \sim \varphi^o$ we use the decomposition (7.20) and observe from system (7.19) that $\cos(\omega\varphi_s/\mathcal{Q}^o)=0$. (7.28) now reduces within $O(\varepsilon)$ to

$$\text{div}(\varphi_t(\varphi_s,h_s),h_t(\varphi_s,h_s)) = \varepsilon(\overline{G^o}_f(\varphi_s) + \overline{F^o}'(\varphi_s))$$

$$= \varepsilon\alpha \quad \{\sin(\omega\varphi_s/\mathcal{Q}^o)/(mT) \int_0^{mT}[-\omega \, \sin(\omega y)/v_y(y) +\cos(\omega y)/(2v(y))]dy\}$$

$$+ \varepsilon\delta \, \{\mathcal{Q}^o{}'/\mathcal{Q}^{o2} \, \mathbb{M}_D{}^m - 1\}. \qquad\qquad (7.54)$$

Similar to the case of the integral (6.71), the evaluation of the integral in (7.54) would require a Fourier expansion of $1/v(y)$ and $1/v_y(y)$. This procedure is described for elliptic functions by Greenhill [67], however $v(y)$ and $v_y(y)$ represent the first and second derivative of the periodic solutions (4.3), (5.16) and (5.22) of the KdV, MKdV and heteroclinic limit of the MKdV wave quations. Such an expansion is therefore too difficult as mentioned in connection with the integral (6.71). A numerical evaluation of the integral is contingent on the knowledge of the elliptic modulus k of the periodic solutions (4.3), (5.16), (5.22) (or the roots r_1, r_2, r_3, r_4 as defined in (5.2)) and the problems with its numerical determination have been described in connection with the subharmonic Melnikov integral (6.71) too. However, the integral in (7.54) turned out to be negative for all evaluations with arbitrarily and densely selected values for the elliptic modulus k ranging between 0 and 1 and lower resonance orders m in connection with the solutions (4.3), (5.16), (5.22). (For higher m>8 precision problems in the evaluations arise) Noting that $\sin(\omega\varphi_s/\mathcal{Q}^o)>0$ if φ_3 is one of the centres in the $O(\sqrt{\varepsilon})$

analysis performed in connection with equations (7.20) - (7.23) and that $\Omega_0' < 0$, one can conclude the divergence (7.54) to be negative and the centres under the $O(\sqrt{\varepsilon})$ approximation turn out to be sinks created by a saddle-node bifurcation as described by (6.34). This $O(\varepsilon)$ approximation is therefore sufficient to determine the stability type of the fixed points between the saddles, provided one accepts numerical evaluations as mentioned above.

7.1.2 Higher orders and period doubling

The Taylor series (7.11) expands up to $O(\varepsilon^2)$ whereas the averaging techniques employed on it are based on an expansion including only $O(\sqrt{\varepsilon})$ and $O(\varepsilon)$ terms. For details we refer to the averaging theorem and its proof as stated in [29]. As a consequence, the resulting system (7.26) does not contain *all* terms of $O(\varepsilon^{3/2})$ and $O(\varepsilon^2)$. A determination of all terms of these orders would require averaging techniques derived from expansions up to $O(\varepsilon^2)$. The second order averaging used here, however, is sufficient for the analysis as performed so far, as it only includes terms up to $O(\varepsilon)$ of the expansion (7.11). Moreover, it is sufficient to show period doubling in at least one of the terms of $O(>\varepsilon)$ present in the system (7.26), as this is already enough to show its occurrence. This is the aim of this subsection and we also observe that resonance related phenomena such as period doubling can be attributed only to the periodic and not the dissipation contribution of the perturbation. We therefore take only periodic perturbation into account in the following analysis, that is, we set $\alpha \neq 0$, $\delta = 0$. We determine the $O(\varepsilon^2)$ term $G_0'V$ in (7.26) in our analysis and later it will become evident which other terms

contribute to period doubling. Beginning with the factor V, we find from (7.16), (7.17) (recall $\overline{F^{\circ}} = M^m/\mathcal{Q}^{\circ}$, $mT\mathcal{Q}^{\circ} = 2\pi$)

$$V = \int (\overline{F^{\circ}} - F^{\circ}) dy = M^m y/(2\pi) - \int F^{\circ} dy . \qquad (7.55)$$

Substituting from (7.50) into F° and using the decomposition (7.20), this reduces to

$$V = \alpha(\cos(\varphi\omega/\mathcal{Q}^{\circ}) \ M^m_A y/(2\pi) - 1/\mathcal{Q}^{\circ} \int v(y-\varphi/\mathcal{Q}^{\circ}) \ \sin(\omega y) dy . \qquad (7.56)$$

Shifting $y \to y + \varphi_s/\mathcal{Q}^{\circ}$ in the integral we finally obtain for V

$$V = - \alpha \sin(\omega\varphi/\mathcal{Q}^{\circ}) \ A(y) + \alpha \cos(\varphi\omega/\mathcal{Q}^{\circ}) \ B(y) , \qquad (7.57)$$

$$A(y) = 1/\mathcal{Q}^{\circ} \int v(y) \cos(\omega y) \ dy ,$$

$$B(y) = M^m_A y/(2\pi) - 1/\mathcal{Q}^{\circ} \int v(y) \sin(\omega y) \ dy .$$

From the definition (7.7) and the identities (7.39), (7.40) and $g_1 = 0$, G° reduces to

$$G^{\circ} = \partial\theta^{\circ}/\partial u^{\circ} \ g_1 + \partial\theta^{\circ}/\partial v^{\circ} \ g_2 = \mathcal{Q}^{\circ}/f_2 \ g_2 , \qquad (7.58)$$

with the derivative $G^{\circ}{}'$

$$G^{\circ}{}' = \{\mathcal{Q}^{\circ}{}'g_2 + \mathcal{Q}^{\circ}(g_2{}'f_2 - g_2 f_2{}')\}/f_2{}^2$$

$$= \alpha \sin(\omega y) \ C(y - \varphi/\mathcal{Q}^{\circ}) , \qquad (7.59)$$

$$C(y - \varphi/\mathcal{Q}^{\circ}) = \{\mathcal{Q}^{\circ}{}' + \mathcal{Q}^{\circ 2}/2 \ \partial v_y/\partial u(y - \varphi/\mathcal{Q}^{\circ})/v_y(y - \varphi/\mathcal{Q}^{\circ})\}/v_y{}^2(y - \varphi/\mathcal{Q}^{\circ})$$

113

$\overline{G\circ{}'V}$ now becomes

$$\overline{G\circ{}'V} = 1/(mT) \int_0^{mT} G\circ{}'V \, dy \qquad (7.60)$$

$$= \alpha^2/(mT) \int_0^{mT} \sin(\omega y) \, C(y-\varphi/\Omega\circ) \, \{\sin(\omega\varphi/\Omega\circ) \, A(y) + \cos(\varphi\omega/\Omega\circ) \, B(y)\} \, dy$$

Shifting $y \rightarrow y+\varphi/\Omega\circ$ again gives

$$\overline{G\circ{}'V} = \alpha^2/(mT) \sin(\omega\varphi/\Omega\circ) \cos(\omega\varphi/\Omega\circ) \int_0^{mT} C(y) \, [A(y+\varphi/\Omega\circ) \cos\omega(y)$$

$$+ B(y+\varphi/\Omega\circ) \sin\omega(y)] \, dy$$

$$+ \alpha^2/(mT) \sin^2(\omega\varphi/\Omega\circ) \int_0^{mT} C(y) \, A(y+\varphi/\Omega\circ) \, \sin\omega(y) \, dy$$

$$+ \alpha^2/(mT) \cos^2(\omega\varphi/\Omega\circ) \int_0^{mT} C(y) \, B(y+\varphi/\Omega\circ) \, \cos\omega(y) \, dy \,. \qquad (7.61)$$

The factors in front of the integrals clearly have half the period of $\sin(\omega\varphi/\Omega\circ)$ or $\cos(\omega\varphi/\Omega\circ)$. In other words, *two* periods of $\sin^2(\omega\varphi/\Omega\circ)$, $\cos^2(\omega\varphi/\Omega\circ)$, or $\sin(\omega\varphi/\Omega\circ)\cos(\omega\varphi/\Omega\circ)$ equal *one* period of $\sin(\omega\varphi/\Omega\circ)$ or $\cos(\omega\varphi/\Omega\circ)$. This has nontrivial implications for the $O(\varepsilon^2)$ system (7.26) as it indicates period doubling. From the construction of $G\circ{}'V$ in (7.61) we can conclude that every term consisting of a product of

114

G° or F° or derivatives thereof with V or its derivatives has products of circular functions with a factor of α^2 as in (7.61) and therefore contributes to period doubling. The other period doubling terms in (7.26) are therefore $\overline{F°'V}$ and $\overline{F°''V}$. One further observes that this is solely an effect of the sinusidal perturbations irrespective of the specific type of the underlying system. On the other hand, it depends on the underlying system whether these higher order period doubling terms are large enough compared to lower order terms in order to exhibit the effect. To investigate consecutive period doublings in higher order terms would require an extension of the averaging theorem to higher orders, a point already addressed at the beginning of this subsection. However, this would mean application of an averaging transformation of the type

$$h \rightarrow h + \varepsilon^{1/2}V + \varepsilon V_1 + \varepsilon^{3/2}V_2 + \ldots, \quad \varphi \rightarrow \varphi, \qquad (7.62)$$

with the terms V_i constructed from powers of F°. Clearly, this would make the calculations extremely tedious, although straightforward and mechanical, which raises the possibility of automating them using symbolic manipulators.

The presence of higher order period doublings would suggest a sequence of period doubling bifurcations as described in a result obtained by Gavrilov and Shil'nikov [69,70] and further elaborated upon in [28]. It is shown in [69,70] and [28] that for certain two-dimensional diffeomorphisms with a hyperbolic fixed point homoclinic tangencies or transversal intersections of the flow are created by saddle-node bifurcations depending on the value of some external parameter. That is, the two transversal intersections emerging from a tangency are a sink and a saddle with one half of its unstable

115

manifold being attracted by the sink. A further increase of the external parameter causes the sink to undergo a period-doubling or flip bifurcation where the sink degenerates into a saddle and two sinks. Each one of these sinks attracts one half of the saddle's unstable manifold.

7.2   Flow between resonance bands

Since the flow between bands must be structurally stable it suffices to use the system in $O(\sqrt{\varepsilon})$ approximation. We therefore write the system (7.22) as a linear second order ODE:

$$\varphi_{tt} = - \varepsilon \, \Omega_o{}' \, M^m/2\pi \, , \qquad (7.63)$$

which has the solution φ with derivative φ_t:

$$\varphi = - \varepsilon \, \Omega_o{}' \, M^m \, t^2/4\pi + c_1 t + c_2 \, ,$$
$$\varphi_t = - \varepsilon \, \Omega_o{}' \, M^m \, t/2\pi + c_1 \, . \qquad (7.64)$$

Expressed in terms of φ and h,

$$\varphi = - \varepsilon \, \Omega_o{}' M^m t^2/4\pi + c_1 t + c_2 \, ,$$
$$h = - \sqrt{\varepsilon} \, M^m t/2\pi + c_1/\Omega_o{}' \, . \qquad (7.65)$$

The phase portrait of (7.65) - identical to the one of (7.64) - is now clear:

For $\underline{M^m = 0}$ it is a vector field parallel to the φ-axis and with shear equal to $\Omega'(I_o)$. For $h>0$ its orientation is to the right and for $h<0$ it is to the left. $h=0$, $\varphi=c_2$ (φ-axis) are the points of orientation reversal, that is, degenerate fixed points. See figure 13a. This case is possible for the (2s) mode only and arises for $\omega = 2\pi n/F$ as in (7.26) and without dissipation.

116

For $\underline{M^m} > 0$ setting $h(t=0) = 0$ or $c_1 = 0$ and eliminating t gives for

the vector field a continuous set of parabolas parameterized by c_2:

$$\varphi = - 2\pi \, \mathcal{Q}_0'/M^m \; h^2 + c_2 \; .\qquad\qquad (7.66)$$

The set of their apices is the entire φ-axis.   See figure 13b. Note

that the case $M^m=0$ described above is the correct limit as $M^m \to 0$.

7.3   Averaged subharmonic flow for (M)KdV

We summarize the results of section 7 in combined form for the various

cases possible.

1.   (M)KdV in (f8) or heteroclinic mode.

The resonance bands exist for $\alpha/\delta > R^m(\omega)$ and consist of

saddles with sinks created by saddle-node bifurcations at

$\alpha/\delta = R^m(\omega)$. Neighbouring bands are connected by a flow with

approximate parabolic curvature as described above for the (2s)

case with $\delta > 0$. The nonvanishing periodic part of the Melnikov

function takes the place of $\delta M^m{}_D$ in (7.64) or (7.65)

respectively. See figure 13a.

2.   MKdV in (2s) mode.

(a) no dissipation; $\delta = 0$

The resonance bands consist of saddles and sinks as in case 1.

In case of a vanishing Melnikov distance neighbouring bands are

separated by a line of degenerate fixed points.   See figure

13b.

117

(b) nonzero dissipation; $\delta > 0$

The situation is the same as in case 1.

7.4 Dynamics

We look at the dissipative cases first. It is clear from figure 14 that the entire set of resonance bands, except possibly those of order $\leqslant 3$, occupies an annular region close to the saddle connections with area of less than 1 per cent of the interior. α and δ determine the size of the attracting basins around the sinks in the individual resonance bands as can be seen from (7.24'). The probability of an orbit decaying inward therefore depends on the initial conditions as well as on α and δ. It will increase with δ and decrease with α, a tendency to be expected on considerations of energy dependence. Due to the finite size of the attracting basins and their structural stability, a system will maintain its resonance under slight perturbations of α and δ as well as the coefficients a and b. A continuous variation of a or b must lead to an increase or decrease of the order of the subharmonic on which the system is locked.

For the case without damping observe that for (M)KdV in (f8) or heteroclinic mode the system drifts out of the range of the homoclinic or heteroclinic orbit. In the (f8) case this leads to chaotic oscillations with finite amplitudes whereas in the KdV or heteroclinic case the system transforms into antisolitons.

The case of MKdV in (2s) mode without dissipation is the most interesting one as it shows that external forcing (without damping) does not always mean unbounded growth. This is of course a consequence of the circle of degenerate fixed points which confines the system to the interior of the homoclinic orbit even in the absence

of dissipation. The interesting question is of course the system's behaviour on the circle of degenerate fixed points. According to the averaging theorem this means a Poincare map of infinite period and therefore no resonance. The annulus representing the outer neighbourhood of this circle is repelling whereas the annulus corresponding to the inner neighbourhood is attracting towards the circle. As a consequence machine generated Poincare maps permit a limited number of iterations since infinitesimally small perturbations are sufficient to displace the system from the circle into the outer annulus. This causes a drift outwards through the resonance bands and circles of fixed points.
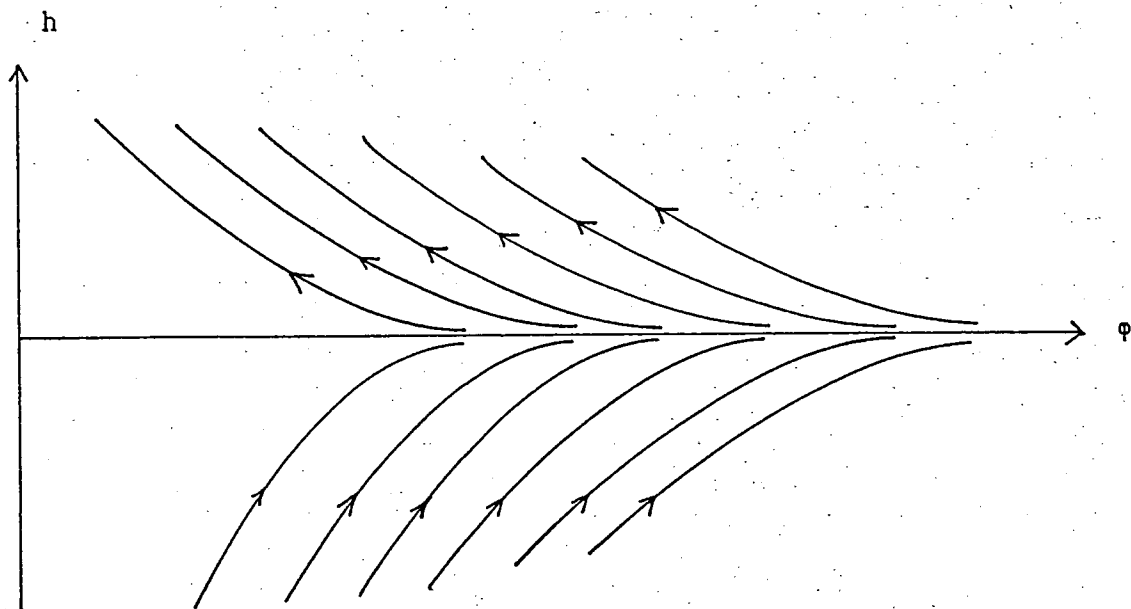
a)
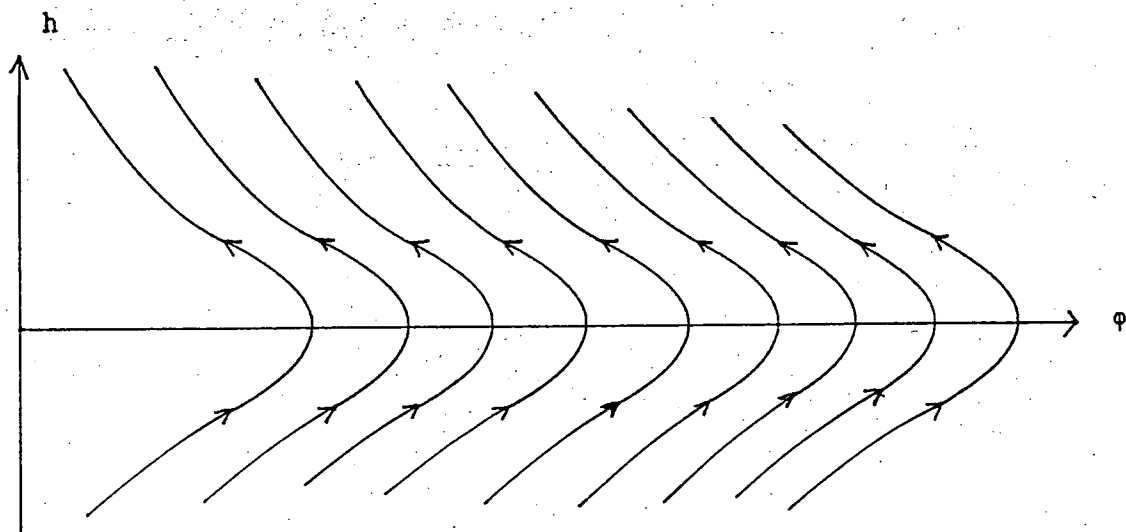
b)

Figure 13.   Structure of averaged vector fields between resonance
bands expressed in action angle variables (h, φ).   (a) Line of
degenerate fixed points at $h=0$ is approached and abandoned
asymptotically by the averaged vector field.   (b) The vector field
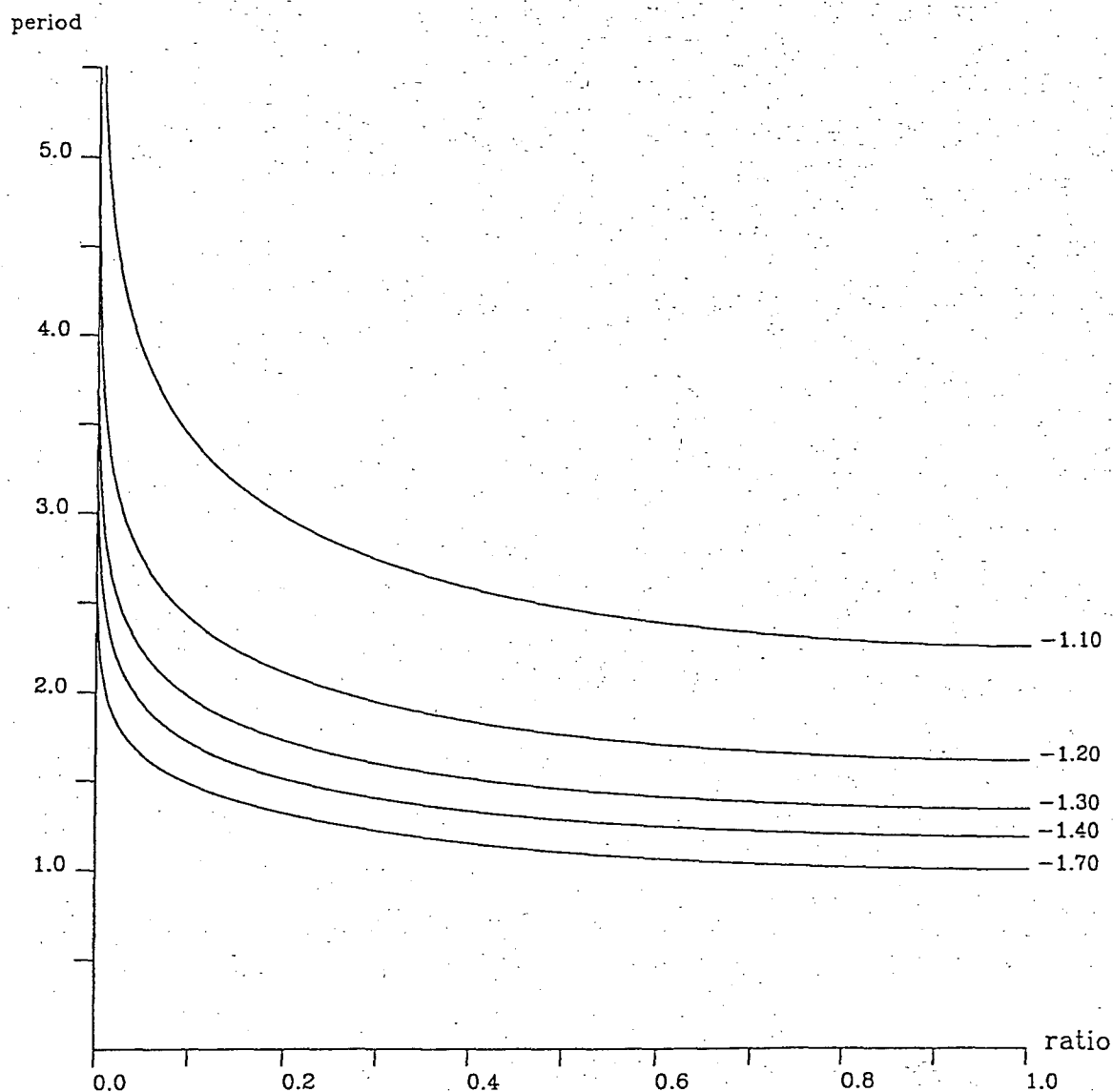assumes parabolic curvature as it crosses $h=0$.

Figure 14. Period of solutions (5.16) within the homoclinic orbit in
(2s) mode for coefficients a=-1, b=1 and graphed for various saddle
positions. The abscissa is the ratio of the distances saddle-solution
(based on u-axis) vs. saddle-center.

121

8. Numerical calculations and computer graphics

With the exception of Figures 1, 2, 4, 13, all plots are produced by use of the graphics package PLOT79 [71] and occasional application of the subroutine library NUMERICAL RECIPES [72] in combination with FORTRAN77 on a VAX780. Phase portrait trajectories (figures 3, 5, 6) and invariant manifolds (figures 15 to 19) also required application of the Runge-Kutta-Fehlberg FORTRAN ODE solver RKF45 (authors: Shampine and Watts, see [73]) on the three dimensional (M)KdV ODE systems derived from (3.8) with both $\alpha=\delta=0$ and nonzero perturbations. The invariant manifolds shown on the figures 15 to 19 show tangencies between the stable and unstable invariant manifolds for the KdV system and the MKdV system in (f8) and (2s) mode and their ratios α/δ at these tangencies are in perfect agreement with the evaluations of the formulas (6.27), (6.50) and (6.51) as determined by the Melnikov method. In general, agreement between calculated ratios and those determined from tangency graphs of manifolds was within five percent for perturbation amplitudes $\alpha \ll .2$ and perturbation frequencies $1 \ll \omega \ll 3$ and with coefficients a and b between .1 and 3. However, this good agreement breaks down for manifolds relating to relatively small unperturbed homoclinic orbits, that is, for saddles close to the saddle-center merging points, and for manifolds in the (2s) mode close to the heteroclinic limit. These cases correspond to the regions close to the poles in figures 7a, 9a and 10a. In these regions the applicability of the first order Melnikov method becomes questionable, as is evidenced by the large perturbation amplitudes α involved. Figure 18 demonstrates the existence of a surface invariant

122

with respect to perturbations in the three-dimensional phase space of the reduced KdV equation as described in section 4. An analogous invariant surface for the reduced MKdV equation as described in section 5 can be verified graphically as well. The important phenomenon of a vanishing Melnikov distance relating to the periodic perturbation for the MKdV case in (2s) mode is corroborated in figure 19 for the critical perturbation frequency $\omega=2.92$. Except for a small neighbourhood around the saddle the invariant manifolds overlay exactly within the accuracy of the graph.

In practical terms, the graphs for the invariant manifolds are generated by starting with a point p_i with coordinates $(u_i, 10^{-6}, 0)$. u_i is therefore the saddle position on the u-axis with an offset by 10^{-6} from the u-axis; the offset is needed to obtain a finite displacement of p_i under the Poincare map $p_i \rightarrow P(p_i)$, which is then performed by advancing p_i by a timestep equal to the perturbation period $T = 2\pi/\omega$. A good approximation for the initial line element on the invariant manifold W^u (or W^s respectively, by using negative time) can now be obtained by generating further points using p_i as initial condition and solving the perturbed system (3.20) for $\alpha=0$ and small timesteps. The stepsize is decreased exponentially with respect to the number of steps performed in order to compensate for the 'stretching' of the manifold under increasing time. After about 200 to 300 timesteps the set of points so generated will have reached a small enough neighbourhood of $P(p_i)$ to stop the process and readjust the resulting line of points to pass directly through $P(p_i)$. Further iterations of this line element assemble the

invariant manifold and are generated by simply Poincare mapping itsindividual points. It is evident from this method that the shorterthis initial line element is, the better the approximation of the manifold will be. As a consequence, higher frequencies ω are needed to analyse smaller homoclinic orbits.
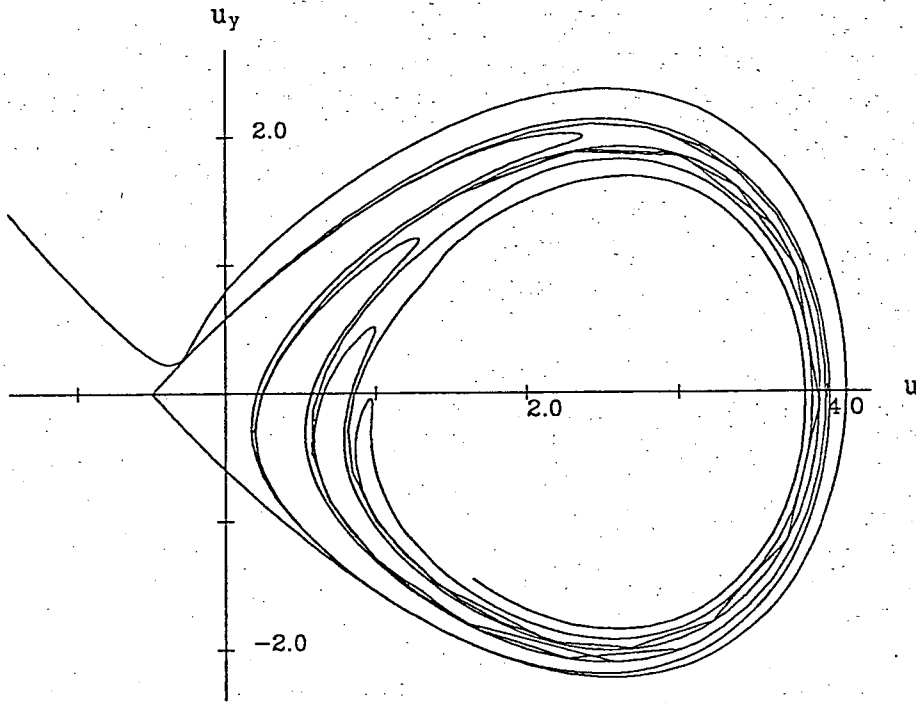
Figure 15.   Invariant manifolds at the point of tangency.   KdV with
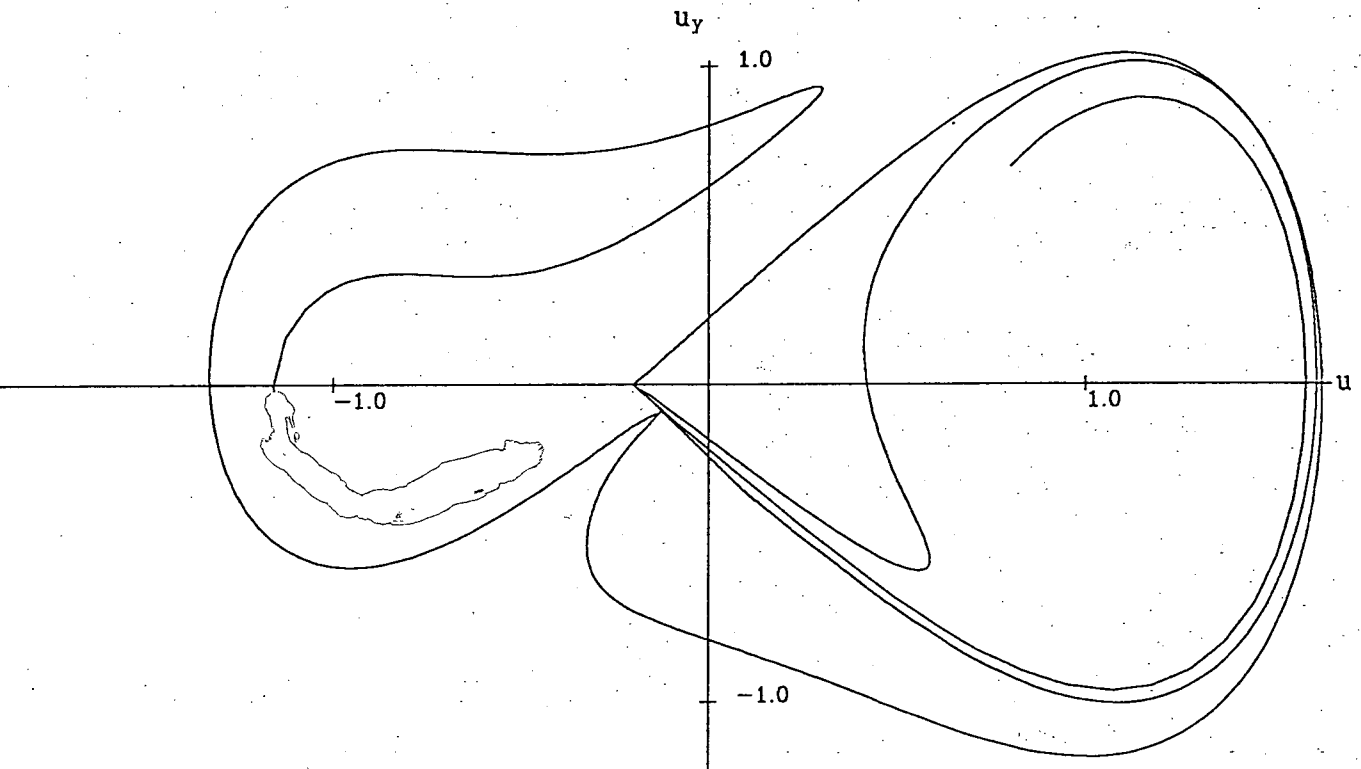
a=b=1; saddle at u=-.5; α=.064; δ=-.02; ω=1.2.

Figure 16.   Invariant   manifolds at   the point of tangency. MKdV-(f8)

with a=-3; b=-1; saddle at u=-.02; α=.064; δ=.05; ω=1.5.
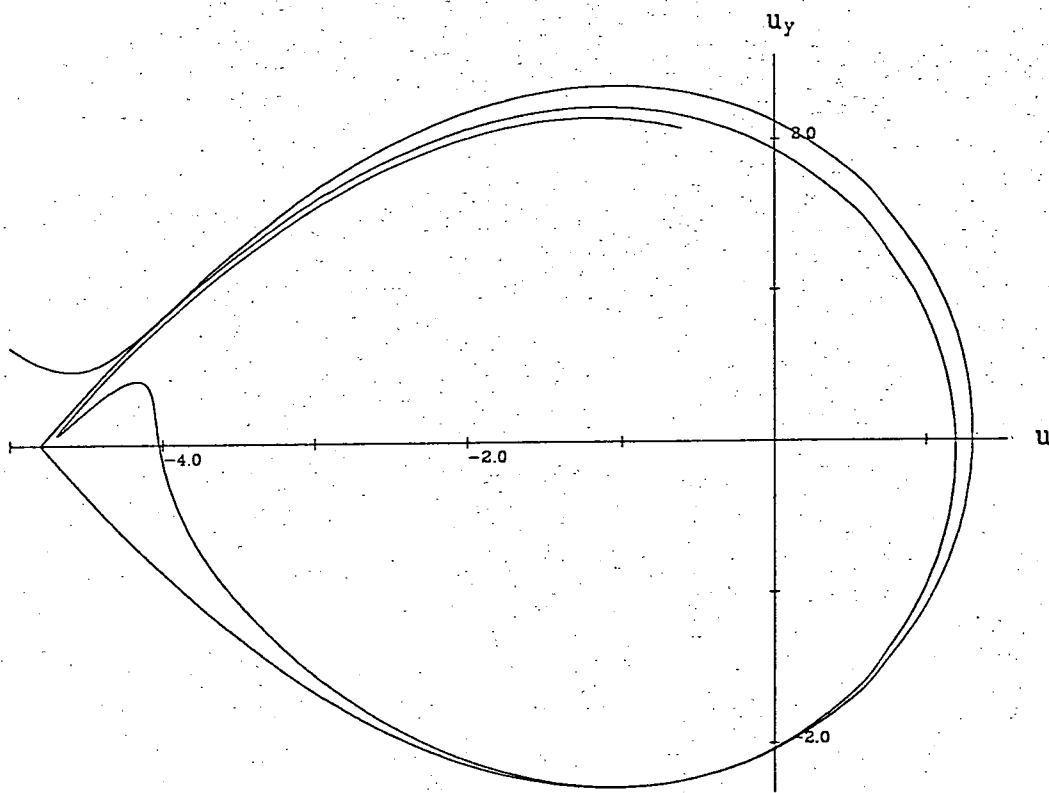
Figure 17. Invariant manifolds at the point of tangency. MKdV(2s)
with a=-.1; b=1; saddle at u=-4.8; α=.069; δ=-.01; ω=1.3.

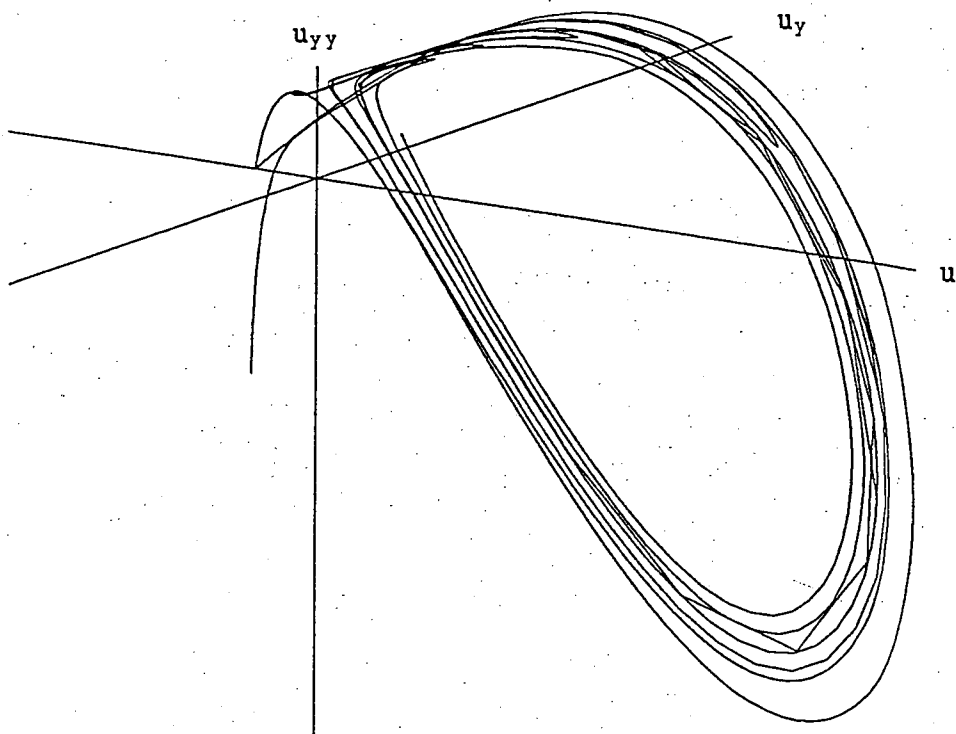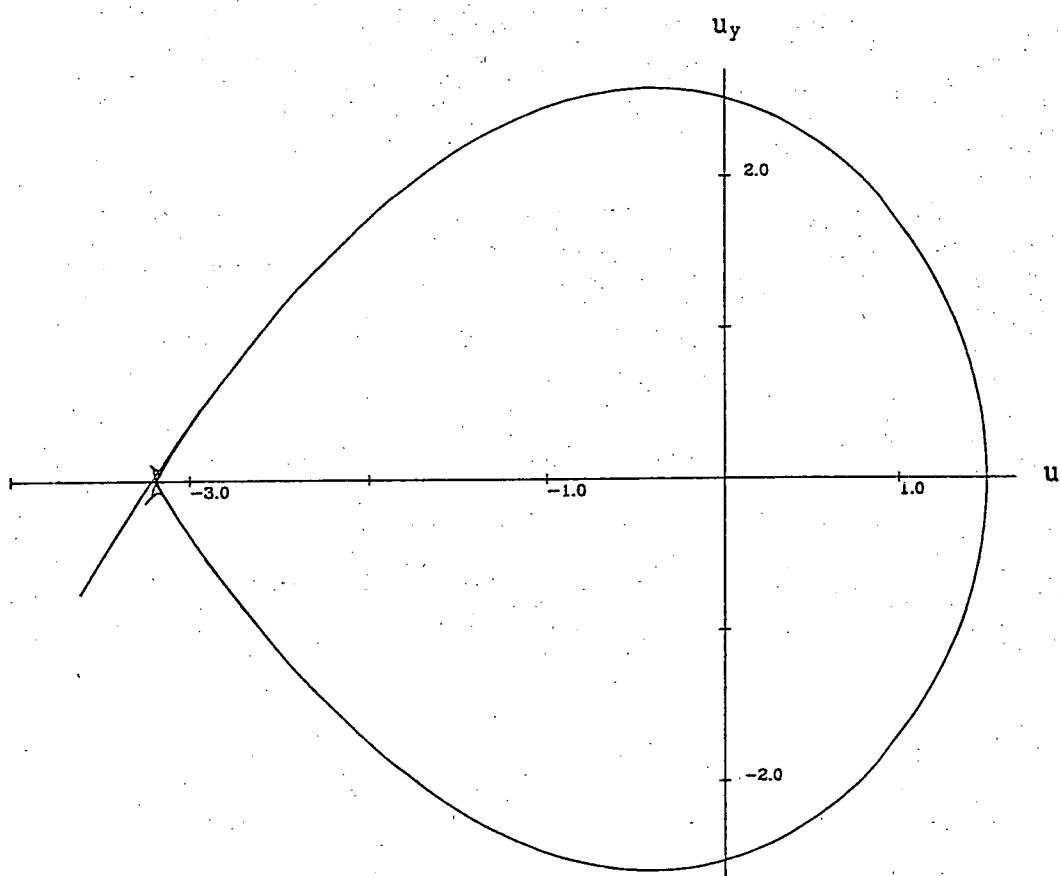Figure 18. Perspective view of Figure 15 in u-u_y-u_{yy} space.

Figure 19.   Invariant manifolds of MKdV-(2s) for a=-.25, b=.5, saddle

at u=-3.2, α=.3, δ=0 and ω=2.92, which is a critical perturbation

frequency value with vanishing periodic part of the Melnikov function.

Except for a small neighbourhood about the saddle the manifolds

overlay exactly within accuracy of the diagram.

9. Summary and conclusions

In this study, three main results can be highlighted. They are as follows:

1. Invariant two-dimensional subsystems in the three-dimensional phase space of the reduced (M)KdV systems exist.

2. Concepts of stability of solitons and structural instability of homoclinic orbits are compatible.

3. The Melnikov distance vanishes for distinct perturbation frequencies over the entire time range in the MKdV system.

These three results are obtained by direct analytic calculation within the first order perturbation approximation of the Melnikov method. However, they are supported by numerical calculations too and will now be discussed in detail.

9.1. Invariant subsystems

An important fact about the reduced (M)KdV system is that the Melnikov analysis of its degenerate three-dimensional ODE system can be relegated to a two-dimensional system obtained by integration and parameterized by one integration constant. As a result there is a set of homoclinic orbits embedded in the phase space of the 3-dimensional system as depicted in Figures 3b, 5b, 6b, corresponding to a set of solitons which are more peaked (i.e. higher and narrower in wave form) and have higher wave speed for larger homoclinic orbits. Assuming this wave speed to be held constant and subjecting the system to a perturbing periodic wave train (with the same wave speed) and to

dissipation will reduce solitons to cnoidal waves, which will change their frequency until a state of resonance with the forcing frequency is reached and the forcing energy balances dissipation. Such a balance cannot be reached in case of weak dissipation or relatively large amplitudes of the perturbing wave train. In that case an antisoliton solution is induced, which manifests itself in numerical simulations as unbounded growth. An exception is of course the MKdV system in (f8) mode, because it does not possess antisolitons but only pairs of solitons; these exchange stability and show oscillatory behaviour in random fashion. The associated dynamics take place in one and the same two-dimensional subspace. In other words, an invariant wave speed causes invariant subspaces between which no Arnold diffusion is possible.

As pointed out previously, the space coordinates of the KdV equation already have a velocity V_p with respect to the space coordinates of an underlying system describing the dynamics of the actual physical waves (e.g. in water and plasma), which have V_p as their phase velocity. That is, the KdV equation is just a further reduction of this system transformed onto a coordinate system moving with velocity V_p, and a similar rationale applies to the MKdV equation. Moreover, it has been shown that a wave ansatz with speed c on the KdV equation leaves V_p quasi invariant. As a consequence, the wave speed of the actual plasma or fluid soliton can be different to the one of the perturbing wave train. Since the requirement of invariant phase speed applies to the ansatz speed c, the plasma or fluid soliton again is not affected by this restriction.

9.2. Stability properties of solitons

Closely related to the invariance property described above is the question of soliton stability. The stability analysis of solitons and cnoidal waves, as developed by Jeffrey and Kakutani [43] and Drazin [44] and mentioned in the introduction, is based on Lyapunov stability and is restricted to perturbations *within* the solution space of the unperturbed and unreduced (M)KdV equation. Furthermore, their perturbations do not carry the restriction of invariant wave speed. As a consequence, the entire phase space of the reduced (M)KdV system corresponding to one particular wave speed may undergo a change as much as the two-dimensional subspaces are no longer invariant with respect to their structure or wave solutions. It signifies that the homoclinic orbit within a particular subspace as well as the subspace itself is deformed as the wave speed is changed or else the solution may transfer to another subspace.

In the framework of structural stability and Melnikov method the primary subject of perturbation is not the solution but the system itself. That is, the perturbation changes the system to a different one with a different phase space and solution space which contains no solitons. This indicates that even if the wave speed may not be kept invariant and may respond to the perturbation, the new solution of the perturbed system will be a soliton only if the perturbation is such that the perturbed solution space contains soliton solutions. This shows that the type of perturbation is important for the mechanism of structural instability, not necessarily the constraint to a particular invariant wave speed, although the present analysis restricts by the ansatz (3.7) to identical soliton and perturbation wave speed.

9.3   Absence of Melnikov distance

According to the Smale-Birkhoff homoclinic theorem [29] transversal intersections of invariant manifolds are crucial for the formation of Smale horseshoes and production of chaos.   As determined in section 6.5 and confirmed by numerical generation of diagrams (see figure 19), the reduced and perturbed MKdV system in (2s) mode will not always split the homoclinic orbit into stable and unstable manifold.   The homoclinic orbit will survive for certain discrete forcing frequencies and multiples thereof and for all practical intents and purposes for larger frequencies,   as illustrated by figure 11.   Transversal intersections will therefore not exist at these critical frequencies and the system cannot display chaos: the homoclinic orbit survives at these frequencies and merely oscillates with them.   This impliess structural stability for the homoclinic orbit at these frequency values but structural instability at other frequency values, i.e., almost everywhere in parameter space.   The interpretation in the soliton picture would be that of a breather or bion, or an oscillating soliton (see e.g. Drazin [44]).   The unperturbed MKdV equation is known to have breathers [44]; however, in the present case the oscillation frequency is induced by a perturbation.

As shown in section 7, the disappearance of subharmonic Melnikov functions inside the homoclinic orbit creates a set of concentric circles each of which consists of degenerate fixed points and separates two neighbouring resonance bands.   In other words, identically vanishing Melnikov functions alternate with those with a finite number of zeroes. Looking at the individual circle, one can divide its neighbourhood into an outer and inner annulus. Depending on the values of dissipation coefficient δ and perturbation amplitude

α, the circle will be attracting with respect to one annulus and repelling with respect to the other. As a consequence the system can drift through this set of circles to a resonance band which is bounded by a pair of circles which both repel into the resonance band. The resonance properties for an identically vanishing Melnikov function are therefore not very different from those with transversal intersections due to the stability properties of the circles of degenerate fixed points.

The important observation which can be made through the entire thesis is that the Melnikov analysis is clearly relevant in its applications beyond the detection of tangencies and intersections between invariant manifolds. Although it is only a first order approximation method, it has predicted in this study interesting phenomena such as invariance of subspaces, which bear on solitons and the non-splitting of manifolds. The inherent nature of these characteristics in the studied systems has been substantiated convincingly by numerical methods, which are entirely independent of the Melnikov technique.

References

[1]   T.Y. Li and J.A. Yorke, Period three implies chaos, Amer. Math. Monthly, 82 (1975), 985-992.

[2]   F.R. Marotto, Snap-back repellers imply chaos in R^n, J. Math. Anal. Appl., 63 (1978), 199-223.

[3]   K. Shiraiwa and M. Kurata, A generalization of a theorem of Marotto, Proc. Japan Acad. Ser. A Math. Sci., 55 (1979), 286-289.

[4]   The Bible, Oxford University edition, (1899), Genesis 2: 10 and 3: 1, (author not identifiable).

[5]   E. Ott, Strange attractors and chaotic motion of dynamical systems, Rev. Modern Phys., 53 (1981), 655-671.

[6]   J. Auslander and J.A. Yorke, Interval maps, factors of maps and chaos, Tohoku Math. J. (2), 32 (1980), 177-188.

[7]   D.R.J. Chillingworth, Differential topology with a view to applications, Pitman, vol.9, (1976).

[8]   J. Palis and W. de Melo, Geometric theory of dynamical systems, Springer, 1982.

[9]   H. Poincare, Memoire sur les courbes definies par les equations differentielles, Gauthier-Villar: Paris, 1880-1890.

[10]   G. Duffing, Erzwungene Schwingungen bei veraenderlicher Eigenfrequenz, Braunschweig, 1918.

[11]   B. van der Pol, Forced oscillations in a circuit with nonlinear resistance, London Phil. Mag., 3, (1927), 65-80.

[12]   E.N. Lorenz, Deterministic non-periodic flow, J. Atmos. Sci., 20 (1963), 130-141.

[13] C. Sparrow, The Lorenz equations, Springer Appl. Math. Sc., 41 (1982).

[14] D. Ruelle and F. Takens, On the nature of turbulence, Commun. Math. Phys., 20 (1971), 167-192.

[15] S. Smale, Differentiable dynamical systems, Bull. Am. Math. Soc., 73 (1976), 747-817.

[16] L.D. Landau and E. M. Lifshitz, Fluid Mechanics, Oxford: Pergamon, (1959).

[17] M.J. Feigenbaum, Quantitative universality for a class of nonlinear transformations, J. Stat. Phys., 19 (1978), 25-52.

[18] M.J. Feigenbaum, Universal behavior in nonlinear systems, Los Alamos Sci., 1 (1980), 4-27.

[19] A. C. Fowler, J. D. Gibbon and M. J. McGuinness, The complex Lorenz equations, Physica 4D, (1982), 139-163.

[20] P. Brunovsky, Notes on chaos in the cell population partial differential equation, Nonlin. Anal., 7 (1983), 167-176.

[21] A. Lasota, Stable and chaotic solutions of a first-order partial differential equation, Nonlin. Anal., 5 (1981), 1181-1193.

[22] R. Wolfe and H.C. Morris, Chaotic solutions of systems of first order partial differential equations, SIAM J. Math. Anal., 18, 4 (1987), 1040-1063.

[23] W.Y. Tseng and J. Dugundji, Nonlinear vibrations of a buckled beam under harmonic excitation, J. Appl. Math., 38 (1971), 467-476.

[24] F.C. Moon and P. J. Holmes, A magnetoelastic strange attractor, J. Sound and Vibration, 65 (1979), 275-296.

[25] P.J. Holmes, A nonlinear oscillator with a strange attractor, Phil. Trans. Roy. Soc. A, 292 (1979), 419-448.

[26] F.C. Moon, Experiments on chaotic motions of a forced nonlinear oscillator: strange attractors, Trans. ASME J. Appl. Mech., 47 (1980), 638-644.

[27] P.J. Holmes and J.E. Marsden, A partial differential equation with infinitely many periodic orbits: chaotic oscillations of a forced beam, Arch. Rat. Mech. Anal., 76 (1981), 135-166.

[28] B.D. Greenspan and P. Holmes, Homoclinic orbits, subharmonics and global bifurcations in forced oscillations. In G.I. Barenblatt, G. Iooss and D.D. Joseph, Nonlinear dynamics and turbulence, Pitman, 1983.

[29] J. Guckenheimer and P. Holmes, Nonlinear oscillations, dynamical systems and bifurcations of vector fields, Springer, 1984.

[30] C.A.J. Fletcher, Computational Galerkin methods, New York: Springer, 1984.

[31] C.A.J. Fletcher, Computational techniques for fluid dynamics, Berlin: Springer, 1988.

[32] R. Temam, Navier-Stokes equations, North-Holland Publishing Co., 1979.

[33] P. Olver, Applications of Lie groups to differential equations, Springer, 1986.

[34] G.B. Whitham, Linear and nonlinear waves, Wiley-Interscience, 1974.

[35] J.P. Eckmann, Roads to turbulence in dissipative dynamical systems, Rev. Mod. Phys. 53 (1981), 4, I, 643-654.

[36] V.K. Melnikov, On the stability of the center for periodic perturbations, Trans. Moscow Math. Soc., 12 (1963), 1-57.

[37] S. Wiggins, Global Bifurcations and chaos, Springer: Appl. Math. Sc., 73 (1988).

[38] H. Poincare, Les methodes nouvelles de la mechanique celeste, Gauthier-Villars: Paris, (1899).

[39] P.J. Holmes, Averaging and chaotic motions in forced oscillations, SIAM J. Appl. Math., 38 (1980), 65-80, (Errata and addendum, ibid., 40 (1980), 167-168).

[40] F.M.A. Salam, The Melnikov technique for highly dissipative systems, SIAM J. Appl. Math., 47, 2 (1987), 232-243.

[41] R. Lima and M. Pettini, Suppression of chaos by resonant parametric perturbations, Preprint, CNRS, 1989.

[42] Z. Liu and G. Gu, Second order Melnikov function and its application, Phys. Lett. A, 143, 4,5 (1990), 213-216.

[43] P.G. Drazin, Solitons, London Math. Soc., Lect. Notes, 85 (1983).

[44] A. Jeffrey and T. Kakutani, Weak nonlinear dispersive waves: a discussion centered around the Korteweg-de Vries equation, SIAM Rev., 14, 3 (1972), 582-643.

[45] T.B. Benjamin, On the stability of solitary waves, Proc. Roy. Soc. London A, 328 (1972), 153-183.

[46] T.B. Benjamin, Nonlinear wave motion, Lectures in applied mathematics 15 (ed. A.C. Newell), 3-47, Amer. Math. Soc., (1974).

[47] P.G. Drazin, On the stability of cnoidal waves, Quart. J. Mech. Appl. Math., 30 (1977), 91-105.

[48] B. Birnir, Chaotic perturbations of KdV, Physica, 19D (1988), 238-254.

[49] D.J. Korteweg and G. de Vries, On the change of long waves advancing in a rectangular channel,and on a new type of long stationary waves, Philos. Mag., 39 (1895), 422-443.

[50] R.S. Johnson, A nonlinear equation incorporating damping and dispersion, J. Fluid Mech., 42 (1970), 49-60.

[51] T. Kawahara, Weak nonlinear magneto-acoustic waves in a cold plasma in the presence of effective electron-ion collisions, J. Phys. Soc. Japan, 28 (1970), 1321-1329.

[52] N.J. Zabusky, A synergetic approach to problems of nonlinear dispersive wave propagation and interaction, Proc. Symp. Nonlinear Partial Differential Equations , W. Ames, ed., Academic Press, New York, 1967, 223-258.

[53] J. Boussinesq, J. Math. pures appl. (2), 17 (1872), 55-108.

[54] F. Ursell, The long-wave paradox in the theory of gravity waves, Proc. Camb. Philos. Soc., 49 (1953), 685-694.

[55] V.S. Manoranjan, T. Ortega, and J.M. Sanz-Serna, Soliton and antisoliton interactions in the "good" Boussinesq equation, J. Math. Phys., 29, 9 (1988), 1964-1968.

[56] R. Hirota, Exact N-soliton solutions of the wave equation of long waves in shallow-water and in nonlinear lattices, J.Math.Phys., 14, 7 (1973), 810-814.

[57] H.P. McKean, Boussinesq's Equation on the circle, Comm. Pure Appl. Math., 34 (1981), 599-691.

[58] T.B. Benjamin, J.L. Bona, and J.J. Mahoney, Model equations for long waves in nonlinear dispersive systems, Phil. Trans. Roy. Soc., A 272 (1972), 47-78.

[59] D.H. Peregrine, Calculations of the development of an undular
      bore, J. Fl. Mech., 25 (1966), 321-330.

[60] M. Toda, Vibration of a chain with nonlinear interaction, J.
      Phys. Soc. Japan., 22 (1967), 431-436.

[61] J. Grindlay and A.H. Opie, The nonlinear and dispersive elastic
      solid: standing waves, J. Phys. C: Solid State Phys., 10
      (1977), 947-955.

[62] A. Kumar, Soliton dynamics in a monodrome optical fibre, Phys.
      reports, 187, 2 (1990), 63-108.

[63] G.B. Whitham, Linear and nonlinear waves, Wiley-Interscience,
      1974.

[64] P.F. Byrd and M.D. Friedman, Handbook of elliptic integrals for
      Engineers and Scientists, Springer, 1971.

[65] S. Wiggins and P.J. Holmes, Homoclinic orbits in slowly varying
      oscillators, SIAM J. Math. Anal., 18 (1987), 612-629.

[66] I.S. Gradshteyn and I.M. Ryzhik, Table of integrals, series and
      products, Academic Press, 1965.

[67] A.G. Greenhill, The applications of elliptic functions,
      Macmillan/Co., 1892.

[68] S.N. Chow, J.K. Hale and J. Mallet-Paret, An example of
      bifurcation to homoclinic orbits, J. Diff. Eq., 37 (1980), 351-
      373.

[69] N.K. Gavrilov and L.P. Shil'nikov, On three-dimensional
      dynamical systems close to systems with a structurally unstable
      homoclinic curve, I, Mathematics of the USSR - Sbornik, 88(4)
      (1972), 467-485.

[70] N.K. Gavrilov and L.P. Shil'nikov, On three-dimensional dynamical systems close to systems with a structurally unstable homoclinic curve, II, Mathematics of the USSR - Sbornik, 90(1) (1973), 139-156.

[71] N.H.F. Beebe, A user's guide to PLOT79, Univ. of Utah, 1981.

[72] W.H. Press, B.P. Flannery, S.A. Teukolsky and W.T. Vetterling, Numerical recipes -- the art of scientific computing, Cambridge Univ. Press, 1988.

[73] L.F. Shampine, H.A. Watts and S.M. Davenport, Solving nonstiff ordinary differential equations -- the state of the art, SIAM Rev., 18, 3 (1976).